The impact of stimulus modality on the EEG-correlates of associative learning and the connected memory processes

Doctoral Thesis

Puszta András, MD

Supervisor: Dr. habil. Nagy Attila

Department of Physiology, Faculty of Medicine, University of Szeged Szeged, 2019

List of publications connected to the thesis

I. Puszta, A., Pertich, Á., Katona, X., Bodosi, B., Nyujtó, D., Giricz, Z., ... & Nagy, A. (2019). Power-spectra and cross-frequency coupling changes in visual and Audio-visual acquired equivalence learning. *Scientific reports*, *9*(1), 9444.

II. Puszta, A., Katona, X., Bodosi, B., Pertich, Á., Nyujtó, D., Braunitzer, G., & Nagy, A. (2018). Cortical power-density changes of different frequency bands during a visually guided associative learning test: a human EEG-study. *Frontiers in human neuroscience*, *12*, 188.

Other publications

I. Eördegh, G., Őze, A., Bodosi, B., Puszta, A., Pertich, Á., Rosu, A., ... & Nagy, A. (2019). Multisensory guided associative learning in healthy humans. *PloS one*, *14*(3), e0213094.

II. Őze, A., Puszta, A., Buzás, P., Kóbor, P., Braunitzer, G., & Nagy, A. (2018). Extrafoveally applied flashing light affects contrast thresholds of achromatic and S-cone isolating, but not LM cone modulated stimuli. *Neuroscience letters*, *678*, 99-103.

III. Braunitzer, G., Őze, A., Nagy, T., Eördegh, G., Puszta, A., Benedek, G., ... & Nagy, A. (2014). The effect of simultaneous flickering light stimulation on global form and motion perception thresholds. *Neuroscience letters*, *583*, 87-91..

Contents

List of abbreviations

CS – conditioned stimulus

CMW – Continous Morlet wavelet convolution

CR – conditioned reaction

DA - dopamine

EEG – Electroencephalogram

fMRI – Functional magnetic resonance imaging

GS – generalizing stimulus

HPC - hippocampus

MEG – magnetoencephalograph

MSN – medium spiny neuron

OCD – Obsessive-compulsive-disorder

P-A – phase-amplitude

PD – Parkinson's Disease

PF - prefrontal

RAET – Rutgers acquired equivalence test

SI – synchronization index

US – Unconditioned stimulus

Introduction

The study of basic learning and memory processes has a venerable and rich history, starting from the early 1900 when Pavlov[1] and Thorndike[2] first made public their systematic methods for studying the development of conditioned behaviors.

Whereas all types of learning involve an impact of regularities in the environment on behavior, associative learning refers to that subclass of learning in which the change in behavior is due to a regularity in the presence of multiple events[3]. In case of nonassociative forms of learning (such as habituation) takes place based on regularities in the presence of one stimulus.

In the following I will expand the different psychological properties of associative learning.

Associative learning and memory

In psychology, associative memory is defined as the ability to remember the relationship between unrelated items[4]. Associative learning is an important capability in animals, in which two or more stimulus reinforce each other and can be linked to one another.

Associative learning itself encompasses different subclasses, most importantly classical conditioning (i.e., changes in behavior that are due to the pairing of stimuli) and operant conditioning (i.e., changes in behavior that are due to the pairing of stimuli and behavior). Learning can occur both implicitly, without conscious awareness and intention to learn, and explicitly under conscious control. While there are some cases in which classical conditioning can occur implicitly[5], the operant conditioning by its definition can only occur explicitly[6,7].

During associative learning novel information is first acquired, and stored first in the working memory and, if strengthened through a process called consolidation, is eventually stored in the long-term memory. This form of memory is called declarative memory in humans.

There are a number of observations that described the different features of associative learning and memory, whose most notable features are the so-called genearlization and extinction.

During generalization, the stimuli sharing characteristics with the original conditioned stimuli (CS), the so called generalizing stimuli (GS), may become capable of eliciting similar conditioned reaction (CR), following a gradient dependent on the perceptual or functional proximity between CS and GS. Thus, individuals transfer knowledge from one experience to other situations. Most studies of rule-based behavior assume that the cues indicative of the context, and hence the valid GS rule, are explicit. However, in many real-world circumstances,

individuals have to learn simultaneously which features indicate the rule, and which features don't.

During extinction, the unconditioned stimulus (or its mental representation) ceases to follow the CS, the latter loses its predictive value and, consequently, the CR extinguishes.

Convergent findings from neuropsychological studies in humans, together with experimental lesion studies and neuroanatomical studies in animals have shown that the prefrontal cortex together with the medial temporal lobe-hippocampal system and the basal ganglia system play a pivotal role in the normal performance of this task[8-11]. In the following, the most important cortical and subcortical stuctures will be introduced, which were considered essential in several studies during associative learning.

The role of different cortical and subcortical structures in associative learning

Prefrontal cortex

A number of evidence supports the idea that the prefrontal (PF) cortex is particularly important for linking environmental contexts to rule representations, which can be used to guide appropriate behavior (i.e., which actions to select given the rule and sensory features)[12,13].

The role of prefrontal cortex in diverse, behaviorally relevant stimulus integration has also been well-described. PF cells in primates are activated more strongly by novel, reversing cues than by familiar, nonreversing cues[14]. The basis of this mechanism could be due to the fact, that the PF cortex is strongly connected with the dopaminergic system, and the number of studies described a phasic DA-release upon unpredicted stimuli[15]. Human functional imaging studies have also reported that the level of PF activation can be modulated by over-training[16,17]

Human fMRI and PET studies provided evidence on the critical role of the ventral PF cortex in the maintance of working memory[18]. The cellular activity in primates also supports the idea that the PF neurons contribute significantly sustaining representations of objects and/or cued locations[19,20]. Furthermore, removal of the ventral prefrontal cortex in monkeys severely impairs the acquisition of visuo-motor conditional tasks[10] and impairs the ability of monkeys to relearn visual matching task, even though there were no demands on working memory maintenance[18]. Rushworth et al. however found that monkeys with ventral PF lesions can recall an object over a brief delay[21].

Computational models denoted that the generalization strategies arise from hierarchically nested frontostriatal circuits[13,22] and that prefrontal cortex facilitates the association of

generalizing stimuli. Human electrophysiological findings confirmed model predictions, specificly, that with a more anterior, earlier switching signal corresponds to stimulus selection followed by a more posterior, later signal associated with stimulus controlled action selection[23].

Medial temporal lobe (MTL)

The medial temporal lobe includes anatomically related structures, which seem to be essential for declarative memory. It includes cortical areas adjacent to the hippocampal system, such as perirhinal, entorhinal, and parahippocampal cortices[24]. Previous studies have shown that primates learned associations by changing their response of the single neurons (either with sustained activity upon adaptation, or sustained activity for novel cues) in their MTL[25-29]. These learned responses are observed both when the animal had to learn a new rule, as well as when learning is incidental.

MTL is also found to signal the formation of new associations between visual scenes and spatial locations[29], and the retrieval of well-learned associations between visual stimuli[30]

In human fMRI studies, the impact of rapid sequential associative learning has also been observed in the MTL. In detail, MTL structures respond more strongly to structured versus unstructured sequences of visual stimuli[31], and their activity depends on the statistical regularities of the sequence[32-34]. Human extracellular recordings also enhanced the role of MTL-neurons in sequence learning[35].

The latter findings can be biased by the fact that neurons in the MTL are strongly modulated by attention[36] and are also activated when subjects imagine a stimulus in the absence of any bottom–up visual input[37]. It seems likely that the predictive responses in the MTL during sequence learning may contribute to the neuronal mechanisms of remembering associations, causing predictive mental images of upcoming stimuli.

Hippocampus

The hippocampus (HPC) was first described over four centuries ago by Arantius[38], but its function remained unclear until the beginning of the modern neurosciences era. HPC damage causes deficits in non-spatial associative learning[39].

In rodents, there is theta synchrony between the PFC and HPC during spatial memory performance[39] and high-frequency ripple synchrony during subsequent sleep[40], that is thought to reflect the role of HPC acquiring spatial information and then integrating it into cortical

networks for long-term storage. A similar relationship is assumed for non-spatial memories, and tested in primates[41].

Human functional imaging studies have also shown the activation of both hippocampus and PFC during associative memory[42,43] indicating that the PFC together with the HPC contributes to long-term and working memory.

The nigro-striatal DA-system

For a long time, the basal ganglia were considered strictly motor structures. However, the basal ganglia are also involved in cognitive and emotional functions, as well as in multisensory integration, in line with their anatomical connections with several areas of the cortex[44].

Dopamine (DA) is the major neurotransmitter required for reinforcement learning, and reward-related learning. According to the DA reward prediction error hypothesis, unexpected rewards strongly activate midbrain DA neurons, and this phasic activity drives reinforcement learning[45,46]. DA is also important for motivation (i.e reward-seeking behavior required for learning)[47]. Disruptions in DA signaling may therefore contribute to learning deficits associated with different neurologic and psychiatric disorders, such as the Parkinson disease or the Obsessive-compulsive-disorder (OCD)[48,49].

In PD, the ventral regions are usually less depleted in early symptoms of the disease than dorsal regions[50]. These could explain the different effects of dopamine remedication in different Parkinson's patients. Indeed, dopamine remedication was found to be beneficial to cognitive functions related to this structure i.e spatial working memory[51], task-switching, but it is less effective in tasks i.e reversal probabilistic learning and decision making[52,53] in which the ventral striatum has a critical role. These studies revealed that ventral striatum underlies general learning of stimulus associations, whereas the dorsal striatum promotes integration of various influences on selecting them[54].

The - direct and - indirect pathways of the basal ganglia are thought to mediate reward- and punishment-associative learning, respectively. Striatal D1 receptors expressed in medium spiny neurons (MSNs) signal the direct pathway of the basal ganglia, whereas D2Rs expressed in MSNs signal the indirect pathway[55]. Previous studies in rodents have shown that the direct pathway and D1Rs are associated with reward, whereas D2Rs are associated with punishment-associative learning[56]. Kravitz et al[57] used optogenetic techniques to stimulate striatal D1R- or D2R-expressing neurons during a simple reinforcement learning task. They found that D1R-expressing MSNs in the direct pathway mediate persistent reinforcement, whereas D2R-

expressing MSNs in the indirect pathway mediate transient punishment. Taken together, the suppression of striatal D1Rs selectively impairs reward-related associative learning whereas the punishment-associative learning remains unchanged[58].

In summary, it can be concluded that the PFC along with the MTL-hippocampal system and the basal ganglia system play critical role mainly in associative memory and learning, respectively. With the help of the recent clinical and fMRI findings during different associative learning paradigms we can more clearly dissociate the hippocampal versus basal ganglia system contributions to learning, memory and rule transfer. In the following a specific psycophyicical test, the visually-guided acquired equivalence learning test will be introduced, which can be applied to test the different phases of the associative memory.

Acquired equivalence task

Catherine E. Myers and co-workers have developed a learning paradigm (Rutgers Acquired Equivalence Test or also known as the fish-face paradigm), which can be applied to investigate a specific kind of associative learning, the visually guided equivalence learning [59]

The acquired equivalence test is a psychophysical test, which consists of three different parts. During the first, acquisition part, subjects learn to pair different sets of stimuli through trial-and-error. After the associations were successfully formed, the second block (that can be divided into two different parts) starts. During the second part (test part), subjects are asked to recall the already learnt associations (retrieval part), and to form new associations based on the rule that has been learnt during the acquisition part (generalisation part).

The first acquisition part of the acquired equivalence task can also be interpreted as a probabilisitic learning task, or reinforcement learning task, in which subjects learn the stimulus pairs from feedback. As predicted, Parkinson's patients were slower in this part, along with with subjects with basal-ganglia dysfunction, implicating that the basal ganglia-PFC system plays critical role in this part of the paradigm[59]. The retrieval part of the test phase can also be interpreted as working-memory maintenance task, and the generalization phase as a rule-transfer task. Patients with mediotemporal-lobe and/or hippocampal dysfunction showed significant impairment in their performance during this part of the test[60].

The impact of the stimulus modality on associative learning and memory

Although numerous studies revealed the processing of cue with different modalities, as well as the learning strategies and their neural correlates[61-63], the impcact of the stimulus modality on associative learning is not well-described. Stimulus representations, and associations, are stored and (re)activated in stimulus-relevant cortical areas [64-67]. Thus, associative learning requires cooperation between the learning circuit and other task-specific brain areas. Empirical evidence from perceptual and temporal processing experiments supports such a distinction between visual an auditory stimulus processing.[68,69]

Christopher M. Conway and Morten H. Christiansen[70] found during an implicit sequential learning paradigm, that the auditory modality displayed a quantitative learning advantage compared with visual and tactile stimuli. Additionally, they discovered that the tactile learning appears to be sensitive to initial item chunk information, whereas auditory learning appears to be most sensitive to final item chunk information.

Not only stimulus modality can affect the learning outcomes, but inversly, the learning can also modulate sensory processing via top-down mechanisms. Indeed, fMRI research has demonstrated that perception-related activity in visual cortical areas is increased with learning in a visual sequence learning paradigm[71] .

Additionally, functional connectivity between the striatum and task-specific visual areas increases during rewards[72], and functional connectivity between the striatum, frontal cortex, motor cortex and visual processing areas changes over the course of learning[73,74].

An interesting finding of different ablation studies in primates revealed different brain areas that are primarly responsible for cross-modal and inter-modal memory. Removal of the amygdala plus subjacent cortex impairs cross-modal and stimulus-reward association memory[75-79] whereas either removal of the hippocampus plus subjacent cortex or fornix transection produces impairments in spatial associative memory[80-83].

The role of neuronal oscillations in cognitive functions

Different regions of the brain have to communicate with each other to provide the basis for the integration of sensory information, sensory-motor coordination and many other functions that are critical for learning, memory, and perception. Hebb suggested that this is accomplished by the formation of assemblies of cells whose synaptic linkages are strengthened whenever the cells are activated synchronously[84]. Neuronal oscillations are natural consequences of forming

such cell assemblies via summation of hundreds of EPSPs and IPSPs, and the cerebral cortex generates multitudes of oscillations at different frequencies through mainly inhibiting spike-trains at a specific frequency. Each frequency band contributes in a different way to the brain's function[85]. In the following, the role of each frequency band in different cognitive tasks will be summarized briefly.

Delta band (0.5-3 Hz)

Sources of delta oscillations are often found in the frontal and cingulate cortices, and in line with their low frequency these oscillations span a rather wide region of neural networks – possibly in an inhibitory manner[86]. Moreover, delta-beta synchrony is reduced during lower attentional control [87,88].

Theta band (4-7 Hz)

It has been assumed that the cortical theta oscillations reflect the communication with hippocampus – a region that is known to serve memory functions and to exhibit oscillations in the theta range[89]. In addition, human EEG theta activity is observed during functional inhibition subserving executive functions[90], and reward-related learning[91]. Frontal midline theta activity has been widely investigated (for review see [92]). A more general interpretation of the increased theta power in the frontal cortex could be the coordinated reactivation of information represented in different task-specific areas. This latter assumption is in line with the results of single unit recordings in V4[93] and the LFP-synchronisation between prefrontal cortex and V4[94] in primates.

Alpha band (8-13 Hz)

EEG alpha oscillations are modulated during sensory stimulation[95]. In addition, they reflect attentional processes[96], indicating that alfa oscillations are critical for the conscious sensory processing. Alpha oscillations' power also exhibit an inverse correlation with cognitive performance, thus suggesting its gating mechanism for task-relevant cortical structures[97].

Beta band (14-30 Hz)

A number of evidence show that beta oscillations are increased in PD patients, and it correlated with the severity of the motor symptoms indicating the role of beta oscillations in the basal ganglia system[98]. Modulation of healthy human EEG beta oscillations have mainly been observed when subjects perform motor tasks[99]. Beta oscillations were observed also during sensorimotor interaction[100] and after reward in probabilistic learning paradigm.

Gamma band (> 30 Hz)

While many of the low-frequency oscillations have been associated with functional inhibition, faster gamma-band oscillations are believed to reflect cortical multi-unit activation due to the action potential post-hyperpolarization[101]. Depending on the cortical region, gamma oscillations could contribute to the active maintenance of memory contents[102] and to conscious perception[103].

Cross-frequency coupling of the neuronal oscillations

Although the functional role of different frequency bands is well described, the interactions among various rhythms are not fully understood yet. A well-studied mechanism of these interactions is the analysis of cross-frequency coupling. As described first in the hippocampus, the phase of theta oscillations biases the amplitude of the gamma waves (phase-amplitude, P-A coupling or 'nested' oscillations)[104-108]. While P-A coupling reflect mainly the spatio-temporal organization of cell assemblies[109], its mechanisms are not well understood. It was hypothesized that P-A coupling between theta and gamma rhythms occurs because of perisomatic basket cells. These neurons could contribute to both rhythms by firing theta rhythmic trains of action potentials at gamma frequency[110]. Cross-frequency P-A coupling can be found between different frequency bands and in different cognitive tasks (for review see[111]). For example, phase modulation of gamma waves by alpha oscillations has been observed in multiple neocortical structures during working memory load[112,113].

Neural oscillations in associative learning

There are a number of investigation that described the EEG-features of the different phases of the associative learning and memory. Reward-related learning key features is the positive feedback elicited beta power increment, while negative feedback causes power increment in both theta and beta power [91,114]. Furthermore, studies in associative learning tasks revealed gamma coherence over parietooccipital areas[115,116]. In working memory tasks frontal midline theta power increment is a well-known phenomen [117-119]. Also theta/alpha-gamma cross frequency coupling was described earlier in working memory load [113,120].

Aims of the study

The studies referenced above investigated mainly visually guided equivalence learning and to our knowledge no study addressed the cortical contribution to multisensory guided acquired equivalence learning.

Having realized, though, that we did not have normative data about the modality-dependence of the equivalence learning in humans we have developed a multisensory (audio-visual)-guided equivalence learning paradigm in order to compare the performance of healthy volunteers in visual and multisensory tasks. The primary goal of the present study is to investigate how the multisensory information changes the cortical oscillation features, i.e power-density changes, and cross-frequency coupling in different phases (acquisition, retrieval, generalization) of the acquired equivalence learning paradigm and to compare these changes to those in the visually guided learning paradigm. We asked whether the visual and multisensory tasks could share some common, modality independent changes in the cortical activation patterns or modality dependent cortical power and oscillation patterns will be found, which could be characteristic to visually and multisensory guided acquired equivalence learning, respectively.

Materials and methods

Participants

EEG data of 23 healthy young adults were recorded (12 females, 11 males, mean age: 26 years, range=18-32). The participants were free of any ophthalmological or neurological conditions, and they were tested for parachromatism by PseudoIsochromatic Plate Color Vision Test. The participants were recruited on a voluntary basis. The potential subjects were informed about the background and goals of the study, as well as about the procedures involved. It was also emphasized that given the lack of compensation or any direct benefit, the participants were free to quit at any time without any consequence (no one did so). Those who decided to volunteer signed an informed consent form. The study protocol conformed to the tenets of the Declaration of Helsinki in all respects, and was approved by the Medical Ethics Committee of the University of Szeged, Hungary (Number: 50/2015-SZTE). The datasets generated and analysed during the current study are available from the corresponding author on reasonable request.

Visual Associative Learning Test

The testing software (described in earlier studies and originally written for iOS[59]) was adapted to Windows and translated into Hungarian in Assembly for Windows, with the written permission of the copyright holder. The paradigm was also slightly modified to make getting through its acquisition phase by mere guessing less probable (see below). The tests were run on a PC. The stimuli were displayed on a standard 17- inch CRT monitor (refresh rate 100 Hz) in a quiet room separated by a one-way mirror from the recording room. Participants sat at a 114 cm distance from the monitor. One participant was tested at a time and no time limitation was set. The test was structured as follows: in each trial of the task, the participants saw a face and a pair of fish (where each member of the pair had different color), and had to learn through trial and error learning that which fish was connected with which face (Figure 1). There were four faces (A1, A2, B1, B2) and four possible fishes (X1, X2, Y1, Y2), referred to as antecedents and consequents, respectively. In the initial, acquisition stages, the participants were expected to learn that when A1 or A2 appears, the correct answer is to choose fish X1 over fish Y1; given face B1 or B2, the correct answer is to choose fish Y1 over fish X1. If the associations are successfully learned, participants also learn that face A1 and A2 are equivalent with respect to the associated fish (faces B1 and B2 likewise). Next, participants learned a new set of pairs: Given face A1, they had to choose fish X2 over Y2, and given face B1, fish Y2 over X2. This was the end of the acquisition phase. Until this point, the computer provided feedback about

the correctness of the choices, and six of the possible eight fish-face combinations were taught to the participants. In the following phases (retrieval and generalization), no feedback was provided anymore. Beside the already acquired six pairs (retrieval phase) the hitherto not shown but, based on the previously built pairs predictable, last two pairs were also presented (generalization phase). Having learned that faces A1 and A2 are equivalent, participants may generalize from learning that if A1 goes with X2, A2 also goes with X2; the same holds for B2 (equivalent to B1) and Y2 (associated with B1). During the acquisition stages, new associations were introduced one by one, mixed with trials of previously learned associations. The subjects had to achieve a certain number of consecutive correct answers after the presentation of each new association (4 after the presentation of the first association, and 4, 6, 8, 10, 12 with the introduction of each new association, respectively) to be allowed to proceed. This resulted an elevated number of the required consecutive correct trials compared to the original paradigm, which made getting through the acquisition phase by mere guessing less probable. Similarly, in the test phase there were 48 trials (12 trials of new and 36 trials of previously learned associations), as opposed to the 16 trials of the original paradigm.

Audio-visual associative learning test

We have developed and validated an audio-visual (multisensory or bimodal) guided acquired equivalence learning test[121]. The structure of the paradigm was the same as in case of visual associative learning test, only that the four antecedents were four sounds (A1, A2, B1, B2) and the consequents were the same four faces as in the visual associative learning paradigm. The main task of the participants was to determine from trial to trial that which of the two given faces corresponds to the sound heard at the beginning of the trial. During the acquisition phase, six of the possible eight sound-face combinations were learned. During test phase, no feedback was provided anymore, but beside the already acquired six pairs (retrieval phase); the hitherto not shown last two pairs were also presented (generalization phase).

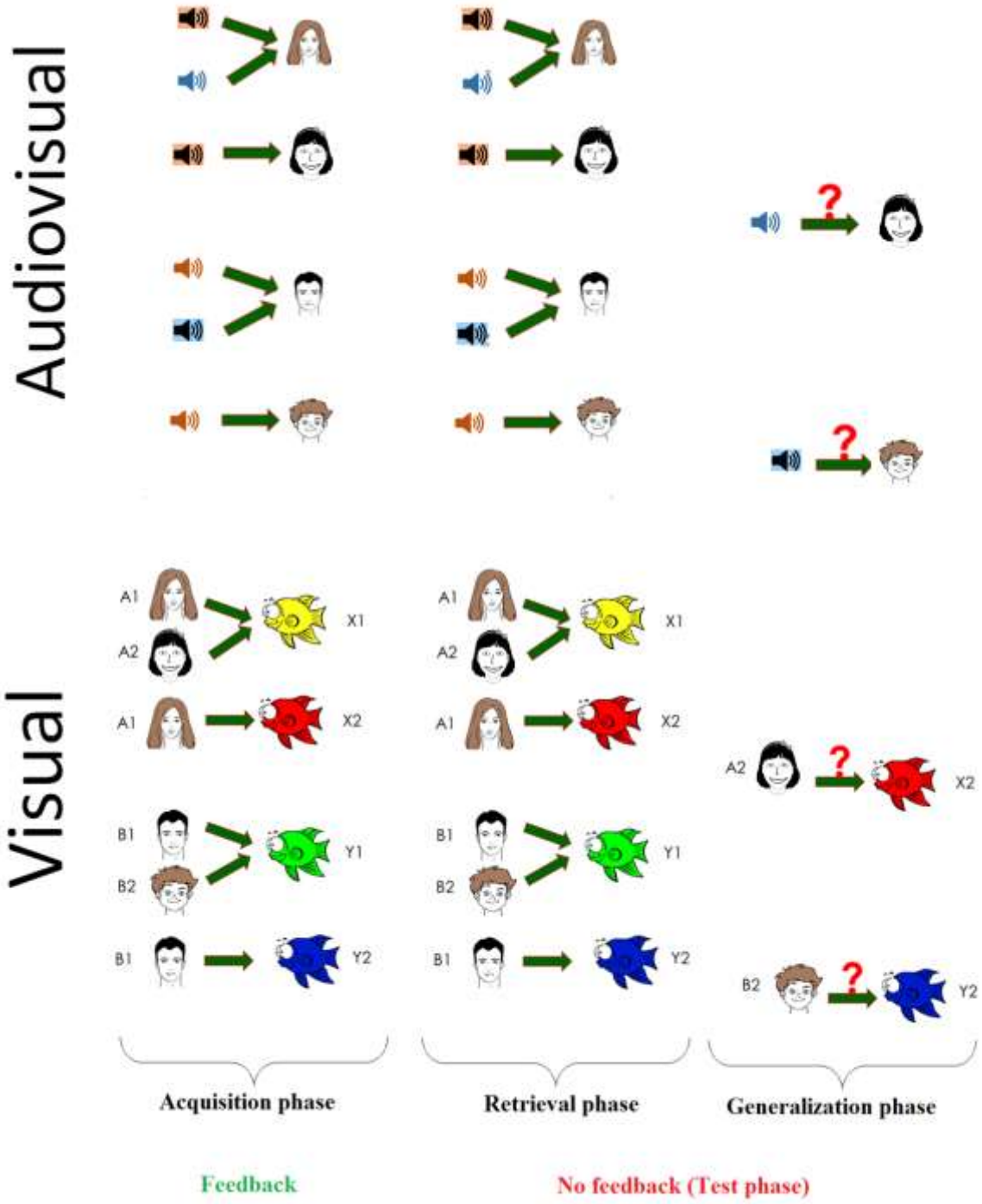

Figure 5: Graphic overview of the applied unimodal visual (lower panel) and the bimodal audio-visual (upper panel) acquired equivalence paradigms

Data acquisition

Sixty-four channel EEG recordings were performed using BiosemiActiveTwo AD-box with 64 active electrodes. Additionally, 5 extra channels were placed to the mastoids and around the eyes to record EOG and EMG. Actiview software was used for setting up the parameters and recording the EEG-data (Biosemi B.V., The Netherlands). The sampling rate was 2048 Hz. Electrode offsets were all kept within normal and acceptable ranges. Raw signals were recorded on the same computer, which controlled the psychophysical learning task. The stimulating software generated trigger signals to indicate the beginning of each trial. These trigger signals were recorded on an additional (sixty-fifth) channel. In order to obtain the baseline activity, one-minute-long resting state activities were recorded before and after testing the visual and audio-visual associative learning test. The order of the two tests (visual and audio-visual associative learning test) varied randomly across volunteers.

Pre-processing

The raw EEG data was first high-pass filtered (>2Hz, FIR filter), then we re-referenced to the average of the channels. All trials were visually inspected and those containing EMG or other artefacts not related to blinks were manually removed. Independent components analysis was computed using the eeglab toolbox for Matlab [122], and components containing blink/oculomotor artefacts or other artefacts that could be clearly distinguished from brain-driven EEG signals were subtracted from the data. Additionally, noisy channels were interpolated using eeglab toolbox. Then we used Laplacian fitting to improve the spatial resolution of the recording [123].

Data Analysis

All data analysis was performed using Matlab (MATLAB and Statistics Toolbox Release 2018a, The MathWorks, Inc., Natick, Massachusetts, United States.) and Dell Statistica for Windows v13.

Analysis of the performances in the psychophysical learning tasks

The psychophysical data were analysed in three groups: data from the acquisition phase, data from the retrieval part of the test phase (i.e. when the participant was presented an already learned association), and data from the generalization part of the test phase (i.e. previously not learned associations). The number of correct and wrong responses were calculated in all phases, as well as the ratio of these to the total number of trials during the respective phase.

Calculating normalized power spectra within subjects

Pre-processed continuous data was epoched using the TTL-signal. The trials were then sorted by the phases of the psychophysical paradigm (acquisition, retrieval and generalization phases), based on the event file generated by the stimulating software. Baseline activity was defined as the first and last approximately 60 seconds before and after the first and last TTL signal, respectively. The vast majority of the trials was somewhat longer than 1 second. In order to avoid mismatch on summation, the first second of each trial (2048 data points) was analysed. If the trial was shorter than 1 second (data points < 2048), the trial was rejected, in order to avoid zero-padding artefacts during the Fast Fourier Transform (FFT).

We computed the FFT for the remaining trials in each channel, and their power spectra were whitened. For individual results we then computed the power of each phase normalized to baseline-activity. We used logarithmic normalisation with the following equation:

$$N_{fr} = 10 * log_{10}\left(\prod_{i=1}^{n} PA_{fr_i} / \prod_{i=1}^{n} PB_{fr_i}\right)$$

Where *N* is the normalized power density of a given *fr* frequency band for a given channel, *PA* is the whitened power density in the acquisition phase's given *i* trial within the same channel and same *fr* frequency, and *PB* is the whitened power density during baseline activity.

Time-frequency analysis

Time-frequency analysis was performed using Continous Morlet wavelet convolution (CMW) via FFT algorithm [124]. FFT was firstly performed on one selected channel of the raw data. Then complex Morlet wavelets were created for each frequency (1-70 Hz) on which FFT was also executed. The cycles of the wavelets increased logarithmically as the frequency varied in a linear manner. After that, we calculated the dot product of the given channel's FFTs and the FFTs of the complex Morlet wavelets at each individual frequency, which yielded 70 complex numbers. Thereafter, the inverse Fast Fourier transform of the results of the dot product showed the alterations of the power in the time domain as follows:

$$K_x = IFFT(fft(C) \cdot fft(W_x))$$

where the *K* is the time-series of the given channel, wavelet-filtered to *x*-frequency, *C* is the time series of all trials of different phases, and *W* is the complex Morlet wavelet in a given *x* frequency. In order to avoid the edge-artefacts of the Morlet wavelet convolution, the raw data was multiplied five times before the convolution, yielding a two series-long buffer zone at the

beginning and the end of the time-series, which was cut out after the time-frequency analysis. After that, the channel's data was cut into different phases of the paradigm (baseline, acquisition, retrieval, generalization). The data set for the purposed null-hypothesis (global band) was generated by iteratively calculating the mean difference of randomized permutation of the power values of a particular channel in a given frequency band in two different phases of the paradigm. The Z-scores for each channel were then calculated between the distributions derived from the global band and the mean difference of the power values in a given frequency band between the two different analysed phases. Z-scores were corrected by the minimum and maximum point of the null hypothesis distribution (also known as cluster-mass correction [124,125].

Group-level analysis of the CMW was carried out in the same way as in the individual analysis described above, with the difference that the random permutation was performed across the mean power values of the subjects and not across the power value of each individual trial. The visualized methodological procedures of the above-described permutation-based test can be seen in Figure 2.

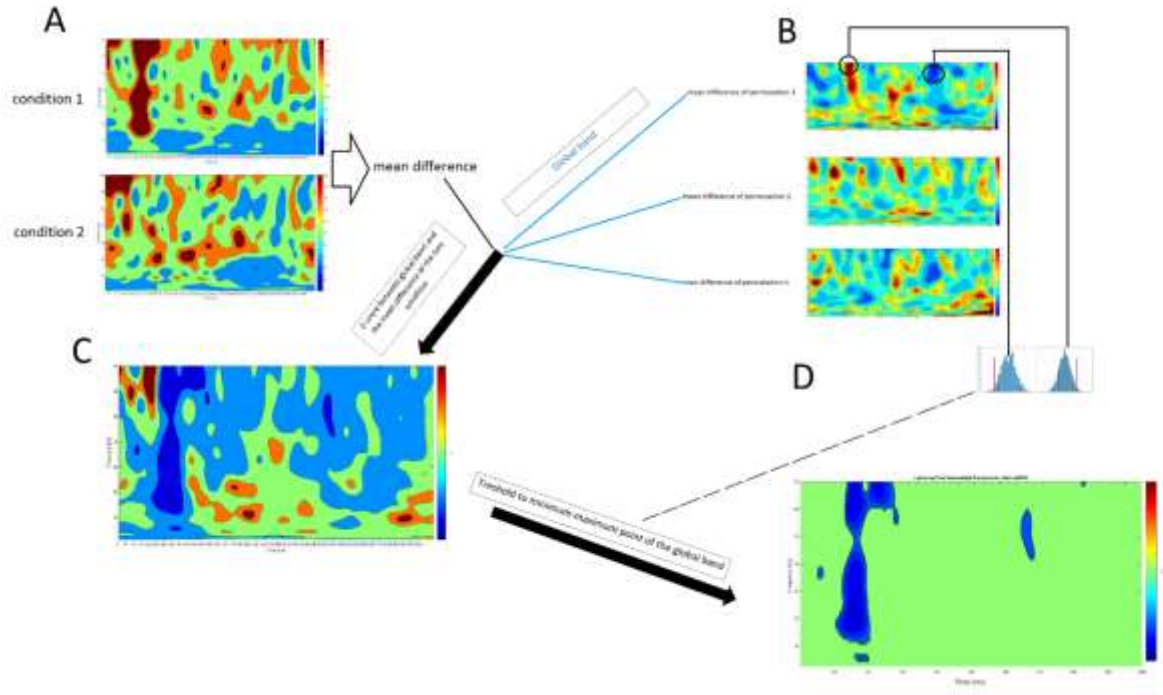

Figure 2: *Visualization of the nonparametric permutation-based analysis. Mean difference between the two comprised phases was calculated on a given channel(A). The data set for the purposed null-hypothesis (global band) was generated by iteratively calculating the mean difference of randomized permutation of the power values of a particular channel in a given*

frequency band in two different phases of the paradigm (B). The Z-scores for each channel were then calculated between the distributions derived from the global band and the mean difference of the power values in a given frequency band between the two different analyzed phases(C). Z-scores were corrected by the minimum and maximum point of the null hypothesis distribution (D).

We identified the time-windows in which we found significant difference between the visual and the audio-visual paradigm, using the interactive surface provided in one of our earlier publications. After we identified the significant time-windows and the corresponding channels in each frequency band and condition, we additionally tested if the individual normalized powers of the different frequency bands in the selected channels and time-points are significantly different in the visual and the audio-visual paradigm by using Mann-Whitney test. The individual normalized powers were obtained by normalizing each individual time-frequency power in each condition and on each channel to the mean power of the baseline activity in the same channel and same frequency using decibel-normalization. Furthermore, to see the significant differences in the time-domain in the selected channels, we performed permutation-test between the normalized power time series of the visual and audio-visual test.

Calculation of event related cross frequency coupling

Event related synchronisation index (SI) was calculated in order to examine whether the power of the high frequency oscillations are coupled to the phase of the low frequency oscillations on the same channel. The calculation was almost the same as described by Cohen [126]. We will give a detailed description of the calculation of SI in one phase of the paradigm in one channel's data referred as raw analytic signal. In the first step, the higher frequency power time series were extracted from the concatenated trials. This was done by the combination of band-pass filtering and Hilbert transformation. First, we have narrow band pass filtered the analytic signal to each frequency of beta and gamma band (15-70 Hz). The filtering method used a 4 Hz-width, two-way, least-squares FIR procedure (as implemented in the eegfilt.m script included in the eeglab package). Then we performed Hilbert transformation on the narrow bandpass-filtered epochs. The power time-series was extracted as the squared magnitude of z(t), the analytic signal obtained from the Hilbert transform (power time series: p(t) = real[z(t)]2 + imag[z(t)]2).

Then we band-pass filtered the raw analytic signal to each frequency of the low frequency range (2-20 Hz, with 4 Hz-width). The phase of the band-pass filtered low and high frequency power time series were obtained from the Hilbert transform of the two time-series, respectively.

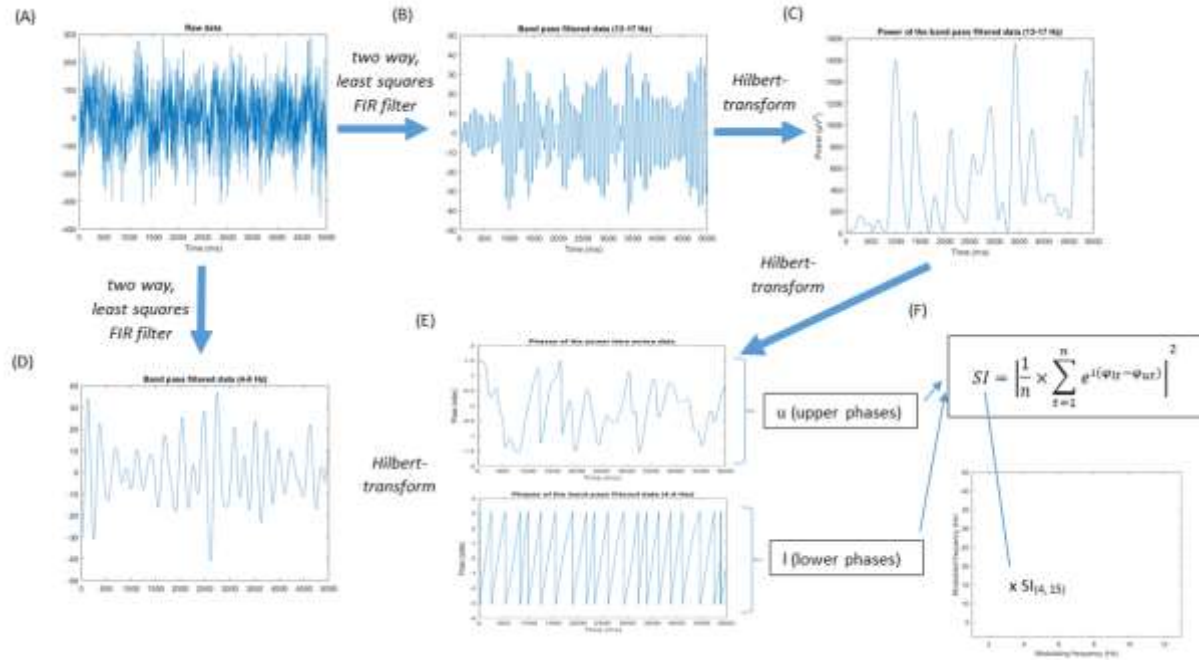

Figure 3: Graphic overview of the cross-frequency coupling analysis (based on Cohen MX, 2008). The figure demonstrates how we calculated the synchronisation index between the lower and upper frequency oscillations in a 5-sec long EEG-data of the acquisition phase of the visual acquired equivalence test. The raw analytical signal (A) was first band-pass filtered to a 4 Hz-width band centered at a high frequency (which was 15 Hz in this case). We got the power-alterations (C) of the high-frequency band pass filtered data (B) using Hilbert transformation. The phases of the power alteration of the high-frequency band-pass filtered data (E) was calculated using Hilbert transformation. For the lower frequency band phases, first we band-pass filtered the raw data to a 4 Hz-width band centered at a lower frequency band (which was 4 Hz in this case, D). The phases of lower frequency band (F) was obtained using Hilbert transformation on the lower frequency band-pass filtered data. Having obtained the phases of the higher frequency band-oscillation (E) and a lower frequency band oscillation (F), we could calculate the SI value between the two oscillations (4 Hz for modulating frequency and 15 Hz for modulated frequency in this case, F).

The synchronization between the phase of the two power time series can be calculated using the synchronization index, (SI) as follows:

$$SI = \left|\frac{1}{n} \times \sum_{t=1}^{n} e^{i(\varphi_{lt}-\varphi_{ut})}\right|^2$$

Where n is the number of time points, φut is the phase value of the fluctuations in the higher frequency power time series at time point t, and φlt is the phase value of the lower frequency band time series at the same time point. The SI varied between 0 and 1. If SI is 0 the phases are completely desynchronized, and if it is 1 the phases are perfectly synchronized.

Significant changes of the cross-frequency coupling at a population level was calculated by comparing the mean synchronisation index in a given modulating - and modulated frequency range of the baseline activity and the given phase of the paradigm. The mean SI-values in each phase of the paradigm were then compared using permutation based statistics, and the resulting Z-scores were corrected by the minimum and maximum point of the null hypothesis distribution (also known as cluster-mass correction) [124,125].

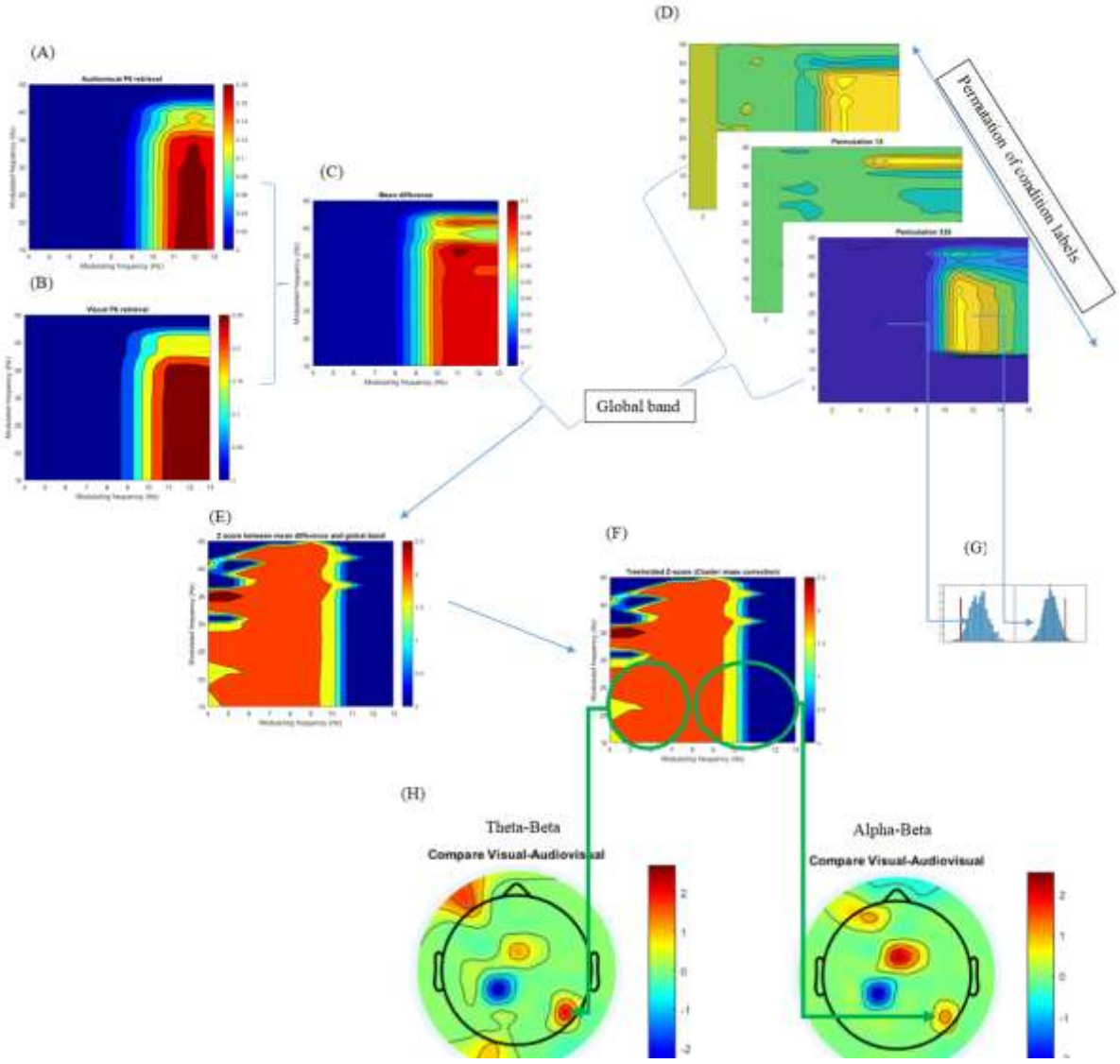

Figure 4: *Graphical overview of calculating the significant changes of the cross-frequency coupling. The figure demonstrates how the statistical difference can be in one channel (in this special case it was P6) between two conditions across subjects. First, we calculated the mean SI values of a given channel in the two conditions: in the visual (A) and audio-visual (B) paradigm. Then we calculated the mean difference (C) of them. After that, we iteratively changed the labels of the conditions, and we calculated the mean difference of each permutation (D). After 1000 iterations, we obtained the global band, a comodulogram, whose each datapoint contained 1000 values, thus giving a null-hypothesis distribution. Then we calculated*

the Z-score between the global band and the mean difference (E). The result was then thresholded to the minimum-maximum distribution of the global band (G). For the clearer interpretation we averaged the Z-scores between alpha-beta and theta-beta, and the mean Z-scores were plotted to a topographical figure (H).

Correlation between performance in the psychophysical test and the power density changes

Correlation between individual performance and power density changes in a given channel and frequency band was also calculated in each phase of the paradigm. Performance was defined as the ratio of the good trials to all trials, and the individual power changes was the individual Z-scores between the baseline activity's power density and the given phase's power density in a given channel in a given frequency band. Pearson correlation coefficient was calculated using the *'corr'* function of Matlab. Statistical analysis was performed by calculating the t-score for each correlation coefficient as follows:

$$t_{ch,fr} = r_{ch,fr} * \sqrt{\frac{n-2}{1-r_{ch,fr}^2}}$$

Where *r* is the correlation coefficient in channel (*ch*) and frequency (*fr*) band, *n* is the number of samples (in this case it was 18), and the *t* is the calculated t value in given channel and frequency band. T-values whose absolute value were smaller than 2.583 (which is the critical t-value if the degree of freedom is 16 and the significance level is 0.01) were set to 0. The corrected t-values in different frequency bands in each phase of the paradigm were plotted to a topographical map using EEGLab '*topoplot'* function.

Results

Altogether 23 healthy volunteers participated in the investigation. For the bio-mathematical analysis, the raw electrophysiological data of 18 volunteers were analysed, as in the other recordings the signal to noise ratio was low, and not even the excessive attempt to clean the data from EMG and ocular artefacts with pre-processing methods described earlier could make them acceptable.

In the following the comparison of psychophysical and electrophysiological results between the visual and audio-visual tasks in each phase of the paradigm (Acquisition, Retrieval, Generalization) will be presented.

Data visualization

The electrophysiological results in four different frequency bands (theta (4-7 Hz), alpha (8-13 Hz), beta 14-30 Hz), and gamma (31-70 Hz) will be presented below for each phase (Acquisition, Retrieval and Generalization) of the two (visual and audio-visual) paradigms.

In the time-frequency results, the group-level statistical differences between the time-frequency power spectra of the visual and audio-visual paradigm are presented in each frequency band, and in each phase of the paradigm (See **Figure 6-8**). In each case, the results are discussed in a range -500 ms – 500 ms in case of the Acquisition phase, and -500 ms-0 ms in case of the Retrieval and Generalization phases, where the 0 ms denotes the time of the answer. We will give a detailed description of the statistical differences between the visual and the audio-visual paradigm only in those cases, where we found significant difference between the visual and the audio-visual paradigms. The summary of the TF-results can be found in **Table 1**. Detailed descriptions of the changes in the time-frequency power spectra in each phase of the visual and audio-visual paradigm compared to baseline activity can be found in the supplementary material of one of our publication[127].

In the cross-frequency coupling results, the group-level statistical differences between the mean synchronization indices of the visual and audio-visual paradigm are presented in each frequency band, and in each phase of the paradigm. Detailed descriptions of the SI-value changes of each phase of the visual and audio-visual paradigm compared to the SI-value of the baseline activity are presented. Significant changes of the cross-frequency coupling in each channel in different phases of the paradigm will be presented using the *topoplot* function of EEGLab. For plotting purposes, only significant changes (i.e. where the Z-scores

were>1.69) are presented on the plots (**Figure 9**). In the smaller topographical plots, the significant difference between SI-values of the given phase and the background activity is shown. The red color indicates where the SI was significantly higher during the given phase compared to baseline-activity, and the blue color indicates where the SI in the given phase was significantly lower compared to baseline activity. On the larger topographical plots, we present the significant difference between the visual and audio-visual paradigm. Here, the red color indicates that the power of that specific frequency band in the given phase of the paradigm was significantly higher during the audio-visual task compared to the visual task, where the blue color indicates the opposite. As we found that the highest changes in the individual comodulogram occurred at the modulating frequency band 8-15 Hz and the modulated frequency band at 31-45 Hz, our results will indicate the group level results found in that frequency range.

In the power-performance-correlation results, significant correlations (i.e. where the t-values were >2.583) are presented in each phase of the visual and audio-visual paradigm. For plotting purposes, only significant correlations (i.e. Z-score >1.69) between the performance in the psychophysical test and the cortical power changes (**Figure 10**) are plotted on the topographical figures.

Performance in the psychophysical learning tests

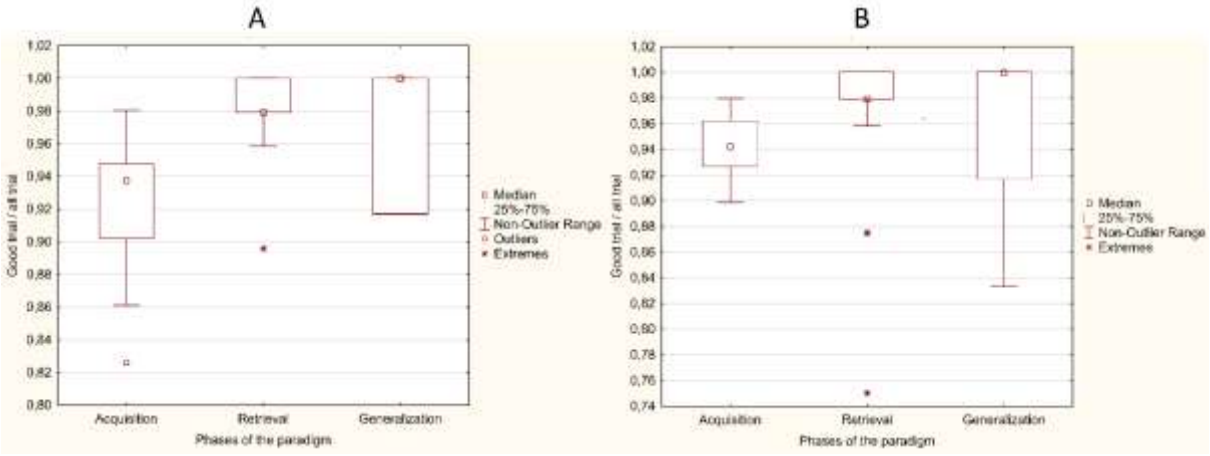

Figure 5: *Box plots of the good trial ratios in each phase of the paradigm during visual (A) and audio-visual (B) acquired equivalence test*

The median good trial ratios (good trial/all trial) during different phases of the visual acquired equivalence test were: 0.92 in the acquisition phase (range=0.83-0.98, SD±0.04), 0.96 in the retrieval phase (range = 0.9-1, SD±0.02), and 0.97 in the generalization phase (range=0.92-1, SD±0.04), see Figure 1A. Repeated measure ANOVA revealed significant difference in the good trial ratios ($F= 20.87$, $p<0.001$), and Tukey post-hoc analysis revealed that the good trial ratio in the acquisition phase was significantly lower compared to retrieval and generalization phase ($p<0.001$). The good trial ratios did not differ significantly between the generalization and retrieval phase ($p=0.992$).

The median good trial ratios during different phases of the audio-visual acquired equivalence test were: 0.94 in the acquisition phase (range=0.90-0.98, SD±0.02), 0.96 in the retrieval phase (range = 0.88-1, SD±0.03), and 0.97 in the generalization phase (range=0.83-1, SD±0.05), see Figure 1B. Repeated measure ANOVA revealed significant difference in the good trial ratios ($F= 7.49$, $p=0.002$), and Tukey post-hoc analysis revealed that the good trial ratio in the acquisition phase was significantly lower compared to retrieval ($p=0.002$) and generalization phase ($p=0.019$). The good trial ratios did not differ significantly between the generalization and retrieval phase ($p=0.709$).

Time-frequency analysis of the EEG signals recorded during the learning tests

Acquisition phase

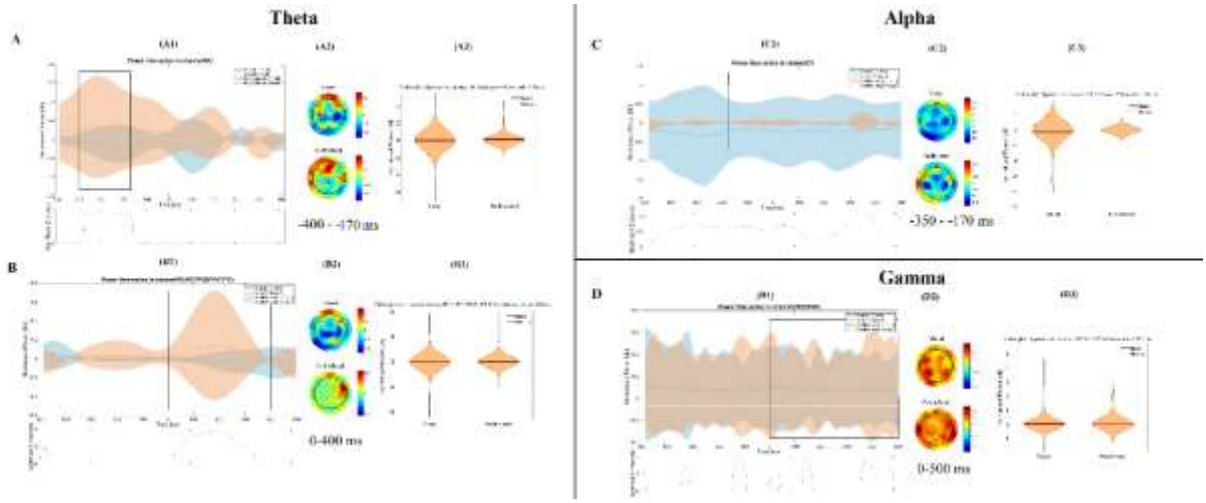

Figure 6: *Time-frequency results in the acquisition phase. The figure shows the most important differences, which were found between the visual and the audio-visual tasks. Part A and Part B represent the results in the theta band, before and after the given answer, respectively. The C and D parts show the results in the alpha and gamma bands, respectively. Within each part of the figure, there are three different subplots. The subplots with number 1 (A1, B1, C1, D1) show the normalized power-fluctuation of the given channels, and the significant Z-scores between the two time-series calculated with random permutation test before and after 500 ms of the given answer. 0 ms denotes the time point when the answer was given. The subplots with number 2 (A2, B2, C2, D2) show the topographical representation of the mean normalized power in certain time-windows. The red colour indicates power-increase, while the blue one indicates power- decrease compared to baseline-activity. The subplots with 3 (A3, B3, C3, D3) show the violin plot of the normalized powers in the selected time-window and in the selected channels.*

The Mann-Whitney test revealed that the power of the theta band was significantly higher during the audio-visual paradigm (mean=0.118 dB, STD=0.5 dB, Range=0 dB 2.814 dB) compared to the visual paradigm (mean=-0.042 dB, STD=0.459 dB, Range=-3.698 dB 2.012 dB) over the frontal channels, 400 ms to 170 ms before the answer. After the answer (from 0 ms to 400 ms after the answer), the power of the theta band was significantly higher ($p<0.001$) in the audio-visual paradigm (mean=0.078 dB, STD=0.494 dB, Range=-1.943 dB 6.794 dB) compared to the visual paradigm (mean=-0.023 dB, STD=0.655 dB, Range=-6.954 dB 5.212 dB) not only over the frontal but over the parietooccpital channels, too.

In case of the alpha frequency band we found that the power was significantly lower ($p<0.001$) during the visual paradigm (mean=-0.278 dB, STD=1.159 dB, Range=-6.664 dB 0 dB), than in the audio-visual one (mean=0.012 dB, STD=0.140 dB, Range=-1.386 dB 1.041 dB) over the

occipital channels, 350 ms to 170 ms before the answer.

We observed no significant difference in the beta power between the visual and the audio-visual paradigm.

The power of the gamma band was significantly higher (p=0.005) during the audio-visual paradigm (mean=0.093 dB, STD=0.417 dB, Range=-0.496 dB 4.472 dB) than in the visual one (mean=0.08 dB, STD=0.36 dB, Range=-0.842 dB 3.491 dB), over the parietal channels, starting from 0 ms until 500 ms after the given answer.

Retrieval part of the test phase

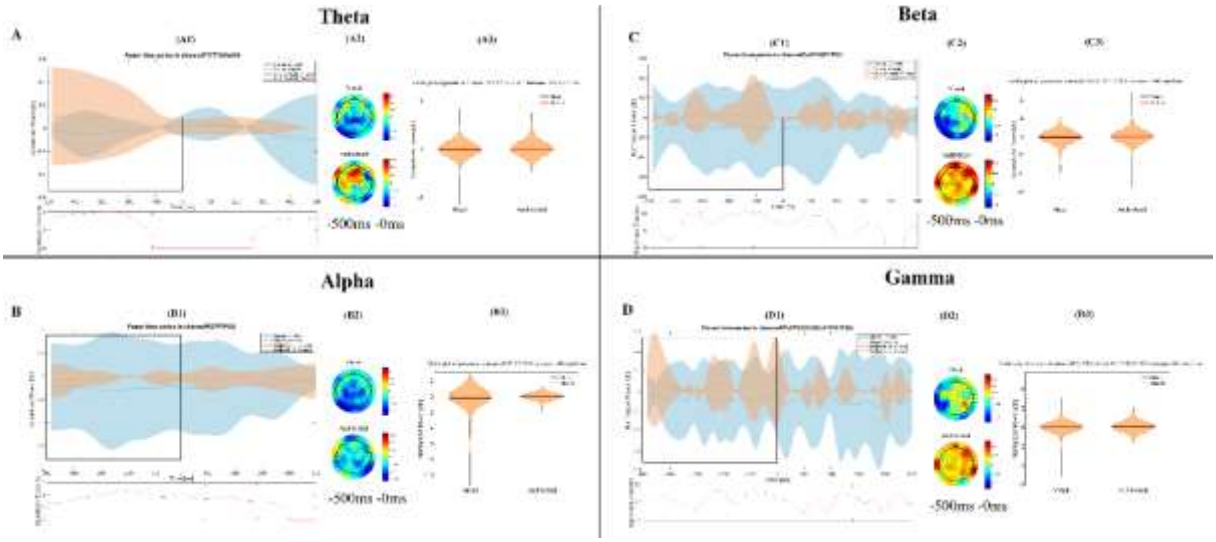

Figure 7: *Time-frequency results in the retrieval phase. The figure shows the most important differences, which were found between the visual and the audio-visual task. The A, B, C and D parts show the results in the theta, alpha, beta and gamma bands, respectively. Other conventions are same as on* ***Figure 6.***

The Mann-Whitney test revealed that the power of the theta band was significantly higher (p<0.001) in the audio-visual paradigm (mean=0.066 dB, STD=0.383 dB, Range=-1.871 dB 3.718 dB) than in the visual paradigm (mean=-0.02 dB, STD=0.276 dB, Range=-3.549 dB 2.006 dB) over the temporal and frontal channels, 500 ms to 0 ms before the answer.

In case of the power of the alpha frequency band we found that it was significantly lower (p<0.001) during the visual paradigm (mean=-0.253 dB, STD=1.058 dB, Range=-8.308 dB 0 dB) than in the audio-visual paradigm (mean=-0.036 dB, STD=0.222 dB, Range=-2.324 dB 0.971 dB) over the parietooccipital channels, from 500 ms before the answer.

The power of the beta frequency band was significantly higher (p<0.001) during the audio-visual paradigm (mean=0.027 dB, STD=0.276 dB, Range=-3.61 dB 2.994 dB) than in the visual

paradigm (mean=-0.093 dB, STD=0.47 dB, Range=-5.524 dB 1.11 dB), over the occipital and parietooccipital channels, from 500 ms before the answer.

The power of the gamma band was significantly higher ($p<0.001$) during the audio-visual paradigm (mean=0.026 dB, STD=0.27 dB, Range=-3.205 dB 4.133 dB) compared to the visual paradigm (mean=-0.041 dB, STD=0.302 dB, Range=-4.662 dB 2.088 dB), over the frontal and parietooccipital channels, starting from 500 ms before the answer.

Generalization part of the test phase

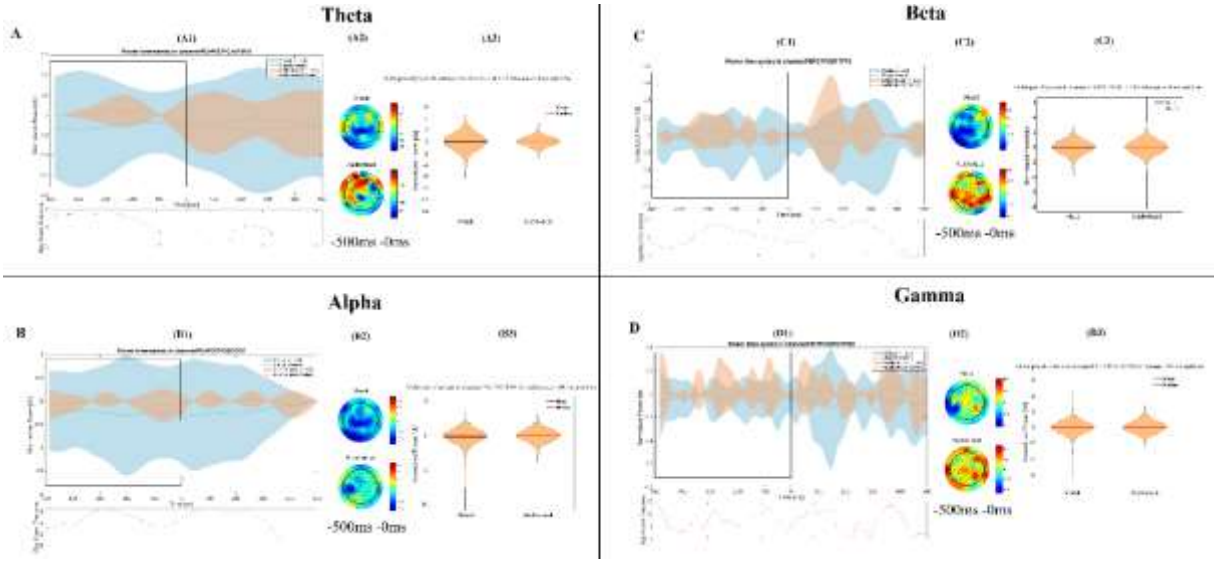

Figure 8: *Time-frequency results in the generalization phase. The figure shows the most important differences, which were found between the visual and the audio-visual task. The A, B, C and D parts show the results in the theta, alpha, beta and gamma bands, respectively. Other conventions are same as on* ***Figure 6****.*

The Mann-Whitney test revealed that the power of the theta band was significantly higher ($p<0.001$) during the audio-visual paradigm (mean=0.009 dB, STD=0.356 dB, Range=-3.022 dB 3.157 dB) than in the visual one (mean=-0.127 dB, STD=0.677 dB, Range=-8.810 dB 2.529 dB) over the frontal and parietooccipital channels, from 500 ms before the answer.

The power of the alpha frequency band was significantly lower ($p<0.001$) during the visual paradigm (mean=-0.245 dB, STD=1.065 dB, Range=-8.11 dB 0.381 dB), compared to the audio-visual paradigm (mean=-0.033 dB, STD=0.409 dB, Range=-4.785 dB 3.102 dB) over the occipital and parietooccipital channels, from 500 ms before the answer.

The power of the beta frequency band was significantly higher ($p<0.001$) during the audio-visual paradigm (mean=0.017 dB, STD=0.347 dB, Range=-5.557 dB 3.102 dB) compared to

the visual paradigm (mean=-0.066 dB, STD=0.438 dB, Range=-6.089 dB 3.068 dB), over the parietooccipital channels, starting from 500 ms before the answer.

The power of the gamma band was significantly higher in the audio-visual paradigm (mean=0.026 dB, STD=0.346 dB, Range=-4.803 dB 4.537 dB) than in the visual paradigm (mean=-0.038 dB, STD=0.376 dB, Range=-5.521 dB 3.49 dB), over the frontal and parietooccipital channels, starting from 500 ms before the answer.

Condition	Frequency band	Time bounds	Cortical region	Power in visual paradigm				p-value	Power in audio-visual paradigm			
				mean	std	min	max		mean	std	min	max
Acquisition	Theta	-400ms -170ms	Frontal	-0,042	0,459	-3,698	2,012	<0.001	0,118	0,500	0,000	2,814
Acquisition	Theta	0 ms 400 ms	Frontal Parietooccipital	-0,023	0,655	-6,954	5,212	<0.001	0,078	0,494	-1,943	6,794
Acquisition	Alpha	-350ms -170ms	Occipital	-0,278	1,159	-6,644	0,000	<0.001	0,012	0,140	-1,386	1,041
Acquisition	Gamma	0ms 500ms	Parietal	0,080	0,360	-0,842	3,491	0.005	0,093	0,417	-0,496	4,472
Retrieval	Theta	-500 ms 0 ms	Temporal Frontal	-0,020	0,276	-3,549	2,006	<0.001	0,066	0,383	-1,871	3,718
Retrieval	Alpha	-500 ms 0 ms	Parietooccipital	-0,253	1,058	-8,308	0,000	<0.001	-0,036	0,222	-2,324	0,971
Retrieval	Beta	-500 ms 0 ms	Occipital Parietooccipital	-0,093	0,470	-5,524	1,110	<0.001	0,027	0,276	-3,610	2,994
Retrieval	Gamma	-500 ms 0 ms	Frontal+Parietooccipital	-0,041	0,302	-4,662	2,088	<0.001	0,026	0,270	-3,205	4,133
Generalization	Theta	-500 ms 0 ms	Frontal+Parietooccipital	-0,107	0,677	-8,810	2,529	<0.001	0,009	0,356	-3,022	3,157
Generalization	Alpha	-500 ms 0 ms	Occipital+Parietooccipital	-0,245	1,065	-8,110	0,381	<0.001	-0,033	0,409	-4,785	3,102
Generalization	Beta	-500 ms 0 ms	Parietooccipital	-0,066	0,438	-6,089	3,068	<0.001	0,017	0,347	-5,557	3,933
Generalization	Gamma	-500 ms 0 ms	Frontal+Parietooccipital	-0,038	0,376	-5,521	3,490	<0.001	0,026	0,346	-4,803	4,537

Table 1: *Table of the statistics of the most important differences between the visual and audio-visual time-frequency results. We provide a summarizing table of the descriptive statistic of the normalized powers in different frequency band and time-window identified in the interactive surface provided in the Supplementary Data 1. The p-value between the visual and audio-visual task was calculated with Mann-Whitney test.*

Cross-frequency coupling of the EEG signals in the visual and audio-visual associative learning paradigms

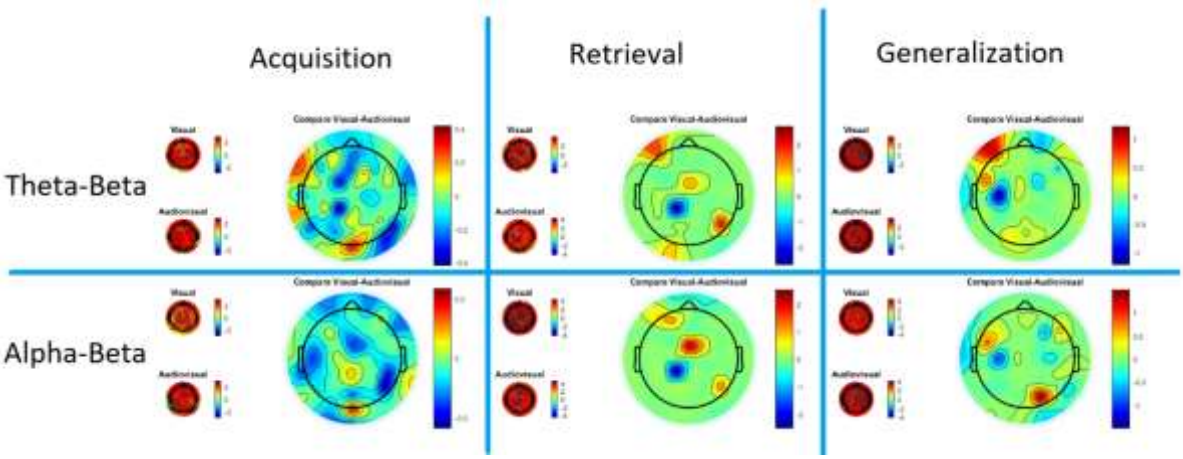

Figure 9: *Mean synchronisation indices in different phases of the paradigm. Each column represents the mean SI values in the different phases of the paradigm. The first row shows the cross frequency coupling results between theta and beta band, and the second row indicates the synchronisation between alpha and beta band. Small topographical plots represent the mean difference between the SI-values of the baseline activity and the SI values of the different phases of the visual or audio-visual stimuli. The larger plot indicates the mean difference between the visual and audio-visual paradigm. In case of the small topoplots, the red color indicates that the synchronisation was higher compared to baseline-activity. In the larger topoplots, the red color indicates that the power was significantly higher during the visual task compared to the audio-visual task, while the blue color shows the opposite*

We found significantly higher synchronization index (SI) in each phase of the paradigm compared to baseline activity both in the visual and audio-visual acquired equivalence tasks. Comparing the visual and the audio-visual task, we found that the theta-beta and alpha-beta SI was significantly higher during the acquisition phase of the audio-visual task compared to the visual task over almost every channels except the occipital visual areas.

During the retrieval phase, we found that the SI was significantly higher in the visual task compared to audio-visual task in almost every channel, except over central areas, where the synchronisation index was higher in the audio-visual task.

In the generalization phase similarly to the retrieval phase the SI was significantly higher in the visual task almost on every channel except over central areas, where the synchronisation index was higher in the audio-visual task. The most obvious differences in cross-frequency coupling between the visual and audio-visual learning task can be seen in parieto-occipital, occipital, and frontal areas.

Correlation between performance in the psychophysical test and the power density changes of the EEG signals

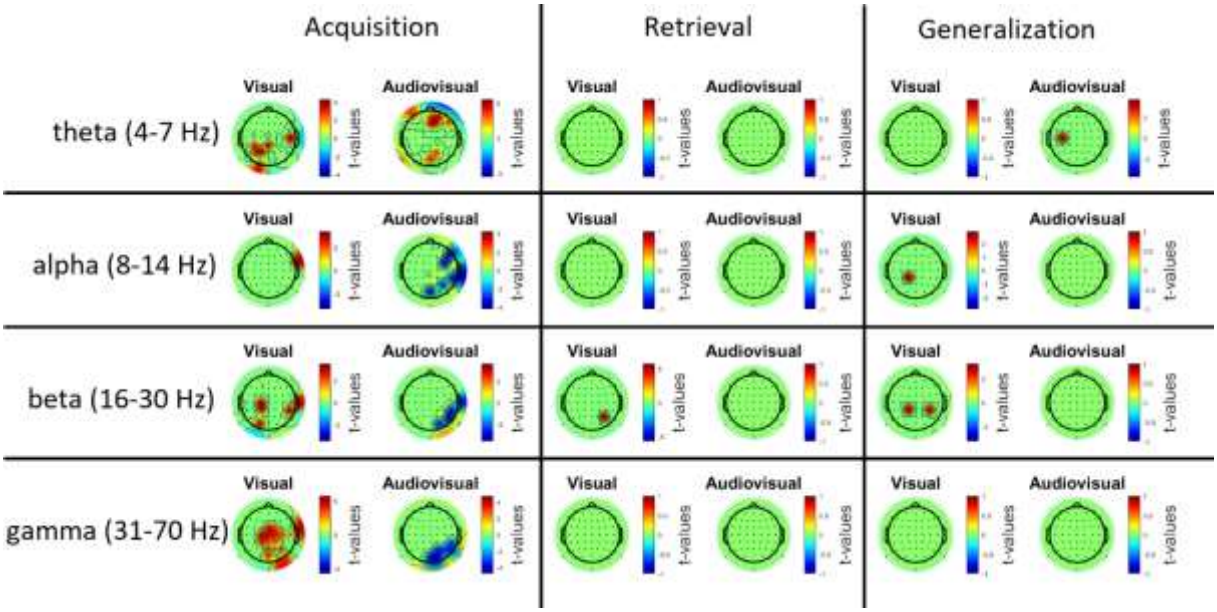

Figure 10: *Power-performance correlations in the visual and audio-visual acquired equivalence test. Each panel represents the significant correlations between the performance (good trial ratio) in the given phase of the paradigm (acquisition, retrieval, generalization), and the power in the given frequency band. The red color indicates that the power and performance were positively correlated, and the blue color indicates that they were negatively correlated.*

In general, there was strong correlation between the performance and the changes of power densities in the acquisition phase of both the visual and audio-visual paradigms but such correlation was not remarkable during retrieval and generalization phases of both visually guided and multisensory guided learning paradigms.

We found increased correlation between the theta power and the performance in the acquisition phase of the visual acquired equivalence test in parietal, parieto-occipital and temporal areas. In case of the acquisition phase of the audio-visual acquired equivalence test we found increased correlation between theta power and the performance over frontal-prefrontal areas, as well as over parieto-occipital areas.

Significant correlation was found between the power of the alpha band and the performance in the acquisition phase of the visual test in the temporal areas. In case of the acquisition phase of the audio-visual acquired equivalence test we found a negative correlation between the power

of the alpha band and the performance in the right fronto-temporal, temporal and parieto-occipital areas.

We found significant correlation between power of the beta and gamma band and the performance in the acquisition phase of the visual test in the central, parietal, parieto-occipital-occipital and temporal areas. In case of the acquisition phase of the audio-visual acquired equivalence test we found negative correlation between the power of the beta or gamma bands and the performance in the right temporal and parieto-occipital areas.

Discussion

In the present study we have analyzed the EEG correlates in a visually-guided and an audio-visually (bimodal or multisensory) guided acquired -equivalence learning tasks. However, this learning paradigm critically requires the normal function of subcortical structures, i.e. hippocampi and basal ganglia (Myers et al., Sohami et al, Moustafa et al., 2010) the cortical contribution seems to be necessary in the visually and audio-visually guided learning paradigm, too. To our knowledge, this is the first study, which addresses the comparison of the cortical power spectra and their changes in an unimodal visual and a multisensory associative learning task. The major findings of the study are that the cortical activity depends critically on the phase of the paradigm, and some changes in cortical powers are characteristic to unimodal visual and multisensory audio-visual learning tasks. In general, during the audio-visual paradigm, the power changes of the event-related low and high-oscillations were higher compared to the visual paradigm, but the psychophysical performance of the acquisition phase only correlated with the power of different frequency bands in the visual paradigm. On the other hand, while the power changes of the event-related oscillations were higher during the audio-visual paradigm, the performance did not depend on the power of different oscillations, and the strength of the cross-frequency coupling was higher. Furthermore, the performance of the acquisition phase seems to be more connected to the strength of the alpha-beta coupling during the audio-visual paradigm. We are convinced that the cortical power differences in the two paradigms cannot be the result of having previously completed the first task (precondition), as the order of the two paradigms (visual and audio-visual) varied randomly across subjects.

It is well known from earlier studies that both fundamentally involved brain structures in the visual associative learning, the basal ganglia and the hippocampi receive not only visual but multisensory information, too [128-130]

A bimodal or multimodal information could be more informative in its complexity than an unimodal stimulus from the environment. The role of multimodal cues in associative learning has been widely investigated (for review see[131]). The psychological studies provided evidence, that multisensory working memory improves recall for cross-modal objects compared to modality-specific objects[132 133] , working

memory capacity is higher for cross-modal objects under certain circumstances[134] and visual and auditory information can interfere with each other[135]. While former studies revealed that mainly cortical areas are involved in associative learning[136,137], only few electrophysiological studies showed the functional basis of the multisensory integration[138], and to our knowledge,

our study is the first that describes the role of different oscillations in multisensory guided learning and the role of multisensory integration in assocaitive learning.

The performance of the investigated population in the psychophysical test (acquisition error ratio, retrieval error ratio, generalization error ratio) was in the same range as that of the earlier investigated healthy controls of neurological and psychiatric patients[59,60,139,140]. Based on this we are strongly positive that the electrophysiological results showed here are representative.

One of the common findings both in the visual and the audio-visual paradigms is the increased theta band activity in the parietooccipital, frontal midline, and prefrontal areas during the acquisition and retrieval phases. Frontal midline theta activity has been widely investigated (for review, see[92]), and its contribution seems to be obvious to internally-guided cognitive tasks that require no external responses[141-143]. A more general interpretation of the increased theta power in the frontal cortex could be the coordinated reactivation of information represented in visual areas. This was also found in single-unit recordings in primate V4[93] as well as LFP-synchronisation between the prefrontal cortex and V4[94]. Regarding our findings, we hypothesize that the initial acquisition phase of the task requires more repeated reactivation of the cortical areas where the stimulus is processed. We also assume (based on the power-performance correlation) that the better the associations are encoded, the more enhanced theta activity can be observed in the frontal midline areas.

Earlier findings of human electrophysiological studies indicated the role of the alpha band in visual[144,145] as well as audio-visual processing[146]. Moreover, Hanslmayr and his colleagues[147] found that the performance in processing stimuli is more likely to be linked to decreased power in the alpha band. Another function that has been attributed to alpha activity is a mechanism of sensory suppression, thus functional gating of information in the task-irrelevant brain areas[148,149]. Indeed, our findings suggest that the initial parts of the trials (0-50 ms) are coupled to decreased alpha power, which were then followed by an increase of it in the visual (occipital) and audio-visual (parietooccipital) cortical areas. These together suggest that after a rapid processing of the cue image and sound, the threshold of the visual/audio-visual cortical areas for external stimuli becomes higher, allowing the information to be encoded (or retrieved).

In the case of the beta frequency range, there is a growing evidence that enhanced beta oscillations appear in patients with Parkinson's disease (PD) [150]. A number of investigations found that the power increase of the beta frequency band negatively correlates with the severity of parkinsonian motor symptoms such as akinesia and rigidity[151,152]. As a result, beta

oscillations are currently investigated as a potential biomarker tracking the effectiveness of deep brain stimulation treatment of PD patients[153]. Furthermore, deep brain stimulation of the subthalamic nucleus at beta frequencies worsens motor symptoms in PD patients[154]. One of the main functions of the basal ganglia is to contribute to associative learning by the trial-and-error method[155,156]. It is well-known that in PD (along with other deficits in which basal ganglia are affected) this learning mechanism is reduced[33,34]. Having seen in our results that a robust decrease of beta-power occurred in all phases (acquisition, retrieval and generalization phases) of both the visual and audio-visual learning tasks, one may consider that this cortical power density decrease in the beta band is a necessary cortical outcome of the normal action of the basal ganglia in visual and audio-visual associative learning tasks.

The gamma frequency band plays an important role in memory processes[157] as well as other cognitive processes, such as word learning, reading and expectancy[36,37]. We observed a power increase during the acquisition phase of the task in the frontal cortex and in associative cortical areas connected to the modality of the presented stimuli (i.e. the occipital cortex in the visual task, the parietotemporal areas in the audio-visual task). Thus, our results suggest that the acquisition phase of the learning paradigm needs strong cortical contribution. The power differences between the acquisition phase of the visual and audio-visual learning paradigm suggest stronger cortical contribution to the multisensory learning task. On the other hand, this increase in the gamma power was not obvious in the retrieval and the generalization phases of the paradigm. The explanation for this could be that the already-learned acquisitions were already transmitted to the hippocampus and the application of the earlier acquisitions does not need strong cortical activation in the gamma band. There is also evidence that a decrease in the gamma power of the local field potential correlates with performance and attention by selectively gating sensory inputs[158,159] We assume that the decrease of the gamma power we found during the task over the cortical areas where the stimulus was processed (i.e. occipital areas in the visual and parietotemporal in the audio-visual task) could be beneficial in memory encoding and retrieval by filtering irrelevant external stimuli.

Calculating the synchronization indices, we found increased coupling between theta and alpha/beta in each phase of both the visual and the audio-visual task, which are in accordance with earlier studies that emphasize the role of theta-gamma/beta coupling in memory processes[40,41] and the alpha gamma/beta coupling in visual perception[42,43]. We also found that this synchronization was significantly stronger during each phase of the audio-visual task than in the visual paradigm. Furthermore, during the retrieval and generalization phases, we found

that the synchronization between theta-beta and alpha-beta was significantly stronger in the audio-visual task. We argue that the audio-visual paradigm required stronger synchronized cortical contribution in all phases of the task because of the cross-modal integration of the visual and auditory stimuli. This indicates that the multimodal (audio-visual) associations require more synchronized activation of the cortex.

Optimal performance in the acquisition phase of the learning paradigms depends mainly on the integrity of the basal ganglia, whereas performance in the test phase (both retrieval and generalization) has been linked to the integrity of the hippocampal region[59,160,161]. It is also known that both fundamentally-involved structures, the basal ganglia and the hippocampi, are involved in attention processes (for a review, see[162]). At the behavioral level, multisensory integration could be dependent on the level of attention and is not an automatic, unconscious process[163]. A multisensory task seems to be more complex and probably needs more attention from the participants. However, our psychophysical results show no significant differences between the performances in the visual and the multisensory tasks. Although the role of attention cannot be excluded in the psychophysical learning test, the same level of performance in the unimodal visual and multimodal (audio-visual) learning paradigms contradicts the assumption that attention contributes significantly to the differences in cortical activation patterns.

Conclusion

We can conclude that the changes in the power of the different frequency-band oscillations were more enhanced during the audio-visual paradigm than in the visual one. On the other hand, we found strong correlation during the acquisition phase between the power of different frequency bands and the psychophysical performance both in the visual and the audio-visual task. In addition, the acquisition retrieval and the generalization phases of the bimodal, audio-visual task showed more synchronized cortical activity than the visual one. Our results suggest that the multisensory associative learning and the connected memory processes (retrieval, and generalization) require a prominent, and more synchronized cortical activation, while the unimodal visual associative learning and the connected memory processes require less synchronized cortical activity. These findings further emphasize the effect of multimodal integration during associative learning and memory processes.

Summary

The three phases of the applied acquired equivalence learning test, i.e. acquisition, retrieval and generalization, investigate the capabilities of humans in associative learning, working memory load and rule-transfer, respectively. Earlier findings denoted the role of different subcortical structures of the visual test. Namely, the basal-ganglia seems to be crucial for the initial, acquisition phase of the paradigm, the latter retrieval and generalization phase of the paradigm requires intact mediotemporal lobe-hippocampal system. However, there is a lack of information about how the cortical electrophysiology patterns measured with EEG are modified during the acquired equivalence task. It is also not obvious how multimodal cues would modify the EEG-patterns during acquired equivalence learning.

To test this, we have recorded EEG from 18 healthy volunteers and analyzed the power spectra and the strength of cross-frequency coupling, comparing a unimodal visual-guided and a bimodal, audio-visual-guided paradigm. Time frequency-analysis using Morlet-wavelet convolution, and cross-frequency coupling analysis with group-level permutation-based statistics were performed on each phase of the paradigm. We found that the changes in the power of the different frequency band oscillations were more enhanced during the audio-visual paradigm and they showed more synchronized activation compared to the visual paradigm. Furthermore, we found, that the performance of the acquisition phase was highly correlated with the power of the different frequency bands both in the visual and the audio-visual task. These findings indicate that multimodal acquired equivalence learning and the connected memory processes require more synchronized cortical contribution than the visual one, which might be a possible biomarker of forming multimodal associations and the multisensory integration at behavioral level.

Acknowledgments

First of all, I would like to express my deepest gratitude to Dr. Attila Nagy, who guided my path from 2nd year physiology (as my seminar teacher), through three years of scientific students' research, thesis and PhD work to writing this dissertation, helping me through in difficult situations. His scientific approach, level-headed advices, and the kindness he showed towards me is something that I would never forget.

I would also like to express my gratitude to Professor Gábor Jancsó for giving me the chance to participate in the Neuroscience PhD program and to Professor Gyula Sáry for allowing me to do my research in the Department of Physiology, as well as the teaching possibility, and the kindness they showed towards me every time I had something to discuss with them.

I would also like to thank Professor Ute Habel, and my colleagues in RWTH Uniklinik Aachen, namely Han-Gue Jo, Thilo Kellermann and Mikhail Votinov to hosted me in Aachen and guided me through the pitfalls of the fMRI.

I would also like to thank Professor Rufin Vogels for hosting me in Leuven, and Francesco Fabbrini, and all the colleagues in Leauven for teaching me the basics of the optogenetical manipulation.

I express my gratitude to Dr. Gábor Braunitzer, who helped during my earliest research carrier, and who I can always count on if I have a debate to discuss.

The life would must have been very different and difficult if I hadn't had my fellow PhD students (Attila Őze, Diána Nyujtó, Dr. Ákos Pertich, Zsófia Giricz) and postdocs (Balázs Barkóczi, Balázs Bodosi, and Eördegh Gabriella) by my side every day in the lab, and made my days better even in the worst situations. I would also like to thank all the insipration and that comes from my former master students, Xéni Katona, and Blanka Bindics as well as other master students in the Laboratory, including but not limited to Nándor Görög, Viktória Balikó, Nóra Cserháti, Anna Pihokker, Petra Rózsa, Kálmán Tót.

A deep thank goes to Péter Liszli, who did a tremendous amount of work helping me with the technical part of the research.

I would also like to thank all the collegues of the Department of Physiology, for the friendly atmosphere, specially to Péter Kaposvári, Anna Bognár, Alexandra Büki, with whom we built a relationship across Europe, that hopefully would never diminish.

I couldn’t emphasize the gratitude towards my family, my father, Lajos Puszta, my mother, Ágnes Sági, my grandparents, Mária Lakatos and Mihály Magyar, my brother, Dániel Puszta, my sister-in-law, Dr. Katalin Szabó, and the youngest member of the family, Ferenc Puszta who did much more inspiration during my PhD than they can probably imagine.

I am deeply grateful to my friends, who were always there for me: Alexis Echeff, Rita Wiesner-Deák, Péter Kátai, Dániel Boglári, Heni Tarpai, and Péter Wiesner, who are the greatest friends one can ever ask for.

And finally, I would like to thank everyone who inspired or helped me in any way: colleagues, who taught me a lot; students, who gave me inspiration, friends, who helped me through difficult situations, poets, writers, musicians, and everyone, who showed me, that life is beautiful afterall.

This work was supported by Hungarian Brain Research Program Grant KTIA_13_NAP-A-I/15, SZTE ÁOK-KKA Grant No: 2019/270-62-2, Campus Mundi Scholarship (Grant No.:CA-SMP-KA103/596/2018), IBRO PERC inEurope Short Stay Grant (Grant No.: PERCInEUROPE-2019-21)

References

1 Pavlov, I. P. Conditioned reflexes: An investigation ofthe physiological activity ofthe cerebral cortex. *Trans. and ed. GV Anrep. London: Oxford University Press* (1927).

2 Thorndike, E. L. Animal intelligence: An experimental study of the associative processes in animals. *The Psychological Review: Monograph Supplements* **2**, i (1898).

3 De Houwer, J., Hughes, S. & Barnes-Holmes, D. Associative learning as higher order cognition: Learning in human and nonhuman animals from the perspective of propositional theories and relational frame theory. *Journal of Comparative Psychology* **130**, 215 (2016).

4 Suzuki, W. A. Psychological Science Agenda| February 2005. *Psychological Science* (2005).

5 Olson, M. A. & Fazio, R. H. Implicit attitude formation through classical conditioning. *Psychological Science* **12**, 413-417 (2001).

6 Shanks, D. R. & John, M. F. S. Characteristics of dissociable human learning systems. *Behavioral and brain sciences* **17**, 367-395 (1994).

7 Brewer, W. F. There is no convincing evidence for operant or classical conditioning in adult humans. (1974).

8 Brasted, P., Bussey, T., Murray, E. & Wise, S. Role of the hippocampal system in associative learning beyond the spatial domain. *Brain* **126**, 1202-1223 (2003).

9 Brasted, P. J. & Wise, S. P. Comparison of learning-related neuronal activity in the dorsal premotor cortex and striatum. *European Journal of Neuroscience* **19**, 721-740 (2004).

10 Murray, E. A., Bussey, T. J. & Wise, S. P. in *Executive Control and the Frontal Lobe: Current Issues* 114-129 (Springer, 2000).

11 Wise, S. P. & Murray, E. A. Role of the hippocampal system in conditional motor learning: mapping antecedents to action. *Hippocampus* **9**, 101-117 (1999).

12 Miller, E. K. & Cohen, J. D. An integrative theory of prefrontal cortex function. *Annual review of neuroscience* **24**, 167-202 (2001).

13 Badre, D., Doll, B. B., Long, N. M. & Frank, M. J. Rostrolateral prefrontal cortex and individual differences in uncertainty-driven exploration. *Neuron* **73**, 595-607 (2012).

14 Asaad, W. F., Rainer, G. & Miller, E. K. Neural activity in the primate prefrontal cortex during associative learning. *Neuron* **21**, 1399-1407 (1998).

15 Schultz, W. Getting formal with dopamine and reward. *Neuron* **36**, 241-263 (2002).

16 Raichle, M. E. *et al.* Practice-related changes in human brain functional anatomy during nonmotor learning. *Cerebral cortex* **4**, 8-26 (1994).

17 Berns, G. S., Cohen, J. D. & Mintun, M. A. Brain regions responsive to novelty in the absence of awareness. *Science* **276**, 1272-1275 (1997).

18 Passingham, R. E., Toni, I. & Rushworth, M. F. in *Executive control and the frontal lobe: Current issues* 103-113 (Springer, 2000).

19 Miller, E. K., Erickson, C. A. & Desimone, R. Neural mechanisms of visual working memory in prefrontal cortex of the macaque. *Journal of neuroscience* **16**, 5154-5167 (1996).

20 Rao, S. C., Rainer, G. & Miller, E. K. Integration of what and where in the primate prefrontal cortex. *Science* **276**, 821-824 (1997).

21 Rushworth, M. F., Nixon, P. D., Eacott, M. J. & Passingham, R. E. Ventral prefrontal cortex is not essential for working memory. *Journal of Neuroscience* **17**, 4829-4838 (1997).

22 Collins, A. G. & Frank, M. J. Cognitive control over learning: Creating, clustering, and generalizing task-set structure. *Psychological review* **120**, 190 (2013).

23 Collins, A. G., Cavanagh, J. F. & Frank, M. J. Human EEG uncovers latent generalizable rule structure during learning. *Journal of Neuroscience* **34**, 4677-4685 (2014).

24 Squire, L. R., Stark, C. E. & Clark, R. E. The medial temporal lobe. *Annu. Rev. Neurosci.* **27**, 279-306 (2004).

25 Miyashita, Y. Neuronal correlate of visual associative long-term memory in the primate temporal cortex. *Nature* **335**, 817-820 (1988).

26 Sakai, K. & Miyashita, Y. Neural organization for the long-term memory of paired associates. *Nature* **354**, 152 (1991).

27 Erickson, C. A. & Desimone, R. Responses of macaque perirhinal neurons during and after visual stimulus association learning. *Journal of Neuroscience* **19**, 10404-10416 (1999).

28 Messinger, A., Squire, L. R., Zola, S. M. & Albright, T. D. Neuronal representations of stimulus associations develop in the temporal lobe during learning. *Proceedings of the National Academy of Sciences* **98**, 12239-12244 (2001).

29 Wirth, S. *et al.* Single neurons in the monkey hippocampus and learning of new associations. *Science* **300**, 1578-1581 (2003).

30 Naya, Y., Yoshida, M. & Miyashita, Y. Forward processing of long-term associative memory in monkey inferotemporal cortex. *Journal of Neuroscience* **23**, 2861-2871 (2003).

31 Turk-Browne, N. B., Scholl, B. J., Chun, M. M. & Johnson, M. K. Neural evidence of statistical learning: Efficient detection of visual regularities without awareness. *Journal of cognitive neuroscience* **21**, 1934-1945 (2009).

32 Harrison, L. M., Duggins, A. & Friston, K. J. Encoding uncertainty in the hippocampus. *Neural Networks* **19**, 535-546 (2006).

33 Bornstein, A. M. & Daw, N. D. Dissociating hippocampal and striatal contributions to sequential prediction learning. *European Journal of Neuroscience* **35**, 1011-1023 (2012).

34 Turk-Browne, N. B., Scholl, B. J., Johnson, M. K. & Chun, M. M. Implicit perceptual anticipation triggered by statistical learning. *Journal of Neuroscience* **30**, 11177-11187 (2010).

35 Reddy, L. *et al.* Learning of anticipatory responses in single neurons of the human medial temporal lobe. *Nature communications* **6**, 8556 (2015).

36 Cerf, M. *et al.* On-line, voluntary control of human temporal lobe neurons. *Nature* **467**, 1104 (2010).

37 Kreiman, G., Koch, C. & Fried, I. Imagery neurons in the human brain. *Nature* **408**, 357 (2000).

38 Bir, S. C., Ambekar, S., Kukreja, S. & Nanda, A. Julius Caesar Arantius (Giulio Cesare Aranzi, 1530–1589) and the hippocampus of the human brain: history behind the discovery. *Journal of neurosurgery* **122**, 971-975 (2015).

39 Buzsáki, G. & Moser, E. I. Memory, navigation and theta rhythm in the hippocampal-entorhinal system. *Nature neuroscience* **16**, 130 (2013).

40 Siapas, A. G. & Wilson, M. A. Coordinated interactions between hippocampal ripples and cortical spindles during slow-wave sleep. *Neuron* **21**, 1123-1128 (1998).

41 Brincat, S. L. & Miller, E. K. Frequency-specific hippocampal-prefrontal interactions during associative learning. *Nature neuroscience* **18**, 576 (2015).

42 Sperling, R. A. *et al.* Encoding novel face-name associations: A functional MRI study. *Human brain mapping* **14**, 129-139 (2001).

43 Kim, H. Neural activity that predicts subsequent memory and forgetting: a meta-analysis of 74 fMRI studies. *Neuroimage* **54**, 2446-2461 (2011).

44 Bates, S. L. & Wolbers, T. How cognitive aging affects multisensory integration of navigational cues. *Neurobiology of aging* **35**, 2761-2769 (2014).

45 Glimcher, P. W. Understanding dopamine and reinforcement learning: the dopamine reward prediction error hypothesis. *Proceedings of the National Academy of Sciences* **108**, 15647-15654 (2011).

46 Colombo, M. Deep and beautiful. The reward prediction error hypothesis of dopamine. *Studies in history and philosophy of science part C: Studies in history and philosophy of biological and biomedical sciences* **45**, 57-67 (2014).

47 Niv, Y. Cost, benefit, tonic, phasic: what do response rates tell us about dopamine and motivation? *Annals of the New York Academy of Sciences* **1104**, 357-376 (2007).

48 Frank, M. J., Seeberger, L. C. & O'reilly, R. C. By carrot or by stick: cognitive reinforcement learning in parkinsonism. *Science* **306**, 1940-1943 (2004).

49 Brambilla, P. *et al.* Increased salience of gains versus decreased associative learning differentiate bipolar disorder from schizophrenia during incentive decision making. *Psychological medicine* **43**, 571-580 (2013).

50 Gibb, W. & Lees, A. Anatomy, pigmentation, ventral and dorsal subpopulations of the substantia nigra, and differential cell death in Parkinson's disease. *Journal of Neurology, Neurosurgery & Psychiatry* **54**, 388-396 (1991).

51 Mollion, H., Ventre-Dominey, J., Dominey, P. & Broussolle, E. Dissociable effects of dopaminergic therapy on spatial versus non-spatial working memory in Parkinson's disease. *Neuropsychologia* **41**, 1442-1451 (2003).

52 Swainson, R. *et al.* Probabilistic learning and reversal deficits in patients with Parkinson's disease or frontal or temporal lobe lesions: possible adverse effects of dopaminergic medication. *Neuropsychologia* **38**, 596-612 (2000).

53 Vaillancourt, D. E., Schonfeld, D., Kwak, Y., Bohnen, N. I. & Seidler, R. Dopamine overdose hypothesis: evidence and clinical implications. *Movement Disorders* **28**, 1920-1929 (2013).

54 MacDonald, P. A. *et al.* The effect of dopamine therapy on ventral and dorsal striatum-mediated cognition in Parkinson's disease: support from functional MRI. *Brain* **134**, 1447-1463 (2011).

55 Wall, N. R., De La Parra, M., Callaway, E. M. & Kreitzer, A. C. Differential innervation of direct-and indirect-pathway striatal projection neurons. *Neuron* **79**, 347-360 (2013).

56 Nakanishi, S., Hikida, T. & Yawata, S. Distinct dopaminergic control of the direct and indirect pathways in reward-based and avoidance learning behaviors. *Neuroscience* **282**, 49-59 (2014).

57 Kravitz, A. V., Tye, L. D. & Kreitzer, A. C. Distinct roles for direct and indirect pathway striatal neurons in reinforcement. *Nature neuroscience* **15**, 816 (2012).

58 Higa, K. K. *et al.* Striatal dopamine D1 receptor suppression impairs reward-associative learning. *Behavioural brain research* **323**, 100-110 (2017).

59 Myers, C. E. *et al.* Dissociating hippocampal versus basal ganglia contributions to learning and transfer. *Journal of Cognitive Neuroscience* **15**, 185-193 (2003).

60 Bódi, N., Csibri, É., Myers, C. E., Gluck, M. A. & Kéri, S. Associative learning, acquired equivalence, and flexible generalization of knowledge in mild Alzheimer disease. *Cognitive and Behavioral Neurology* **22**, 89-94 (2009).

61 Garrison, J., Erdeniz, B. & Done, J. Prediction error in reinforcement learning: a meta-analysis of neuroimaging studies. *Neuroscience & Biobehavioral Reviews* **37**, 1297-1310 (2013).

62 Lee, D., Seo, H. & Jung, M. W. Neural basis of reinforcement learning and decision making. *Annual review of neuroscience* **35**, 287-308 (2012).

63 Maia, T. V. Reinforcement learning, conditioning, and the brain: Successes and challenges. *Cognitive, Affective, & Behavioral Neuroscience* **9**, 343-364 (2009).

64 Nyberg, L., Habib, R., McIntosh, A. R. & Tulving, E. Reactivation of encoding-related brain activity during memory retrieval. *Proceedings of the National Academy of Sciences* **97**, 11120-11124 (2000).

65 Nyberg, L. *et al.* Reactivation of motor brain areas during explicit memory for actions. *Neuroimage* **14**, 521-528 (2001).

66 Rösler, F., Heil, M. & Hennighausen, E. Distinct cortical activation patterns during long-term memory retrieval of verbal, spatial, and color information. *Journal of Cognitive Neuroscience* **7**, 51-65 (1995).

67 Slotnick, S. D. Memory for color reactivates color processing region. *NeuroReport* **20**, 1568-1571 (2009).

68 Glenberg, A. M. & Swanson, N. G. A temporal distinctiveness theory of recency and modality effects. *Journal of Experimental Psychology: Learning, Memory, and Cognition* **12**, 3 (1986).

69 Mahar, D., Mackenzie, B. & McNicol, D. Modality-specific differences in the processing of spatially, temporally, and spatiotemporally distributed information. *Perception* **23**, 1369-1386 (1994).

70 Conway, C. M. & Christiansen, M. H. Modality-constrained statistical learning of tactile, visual, and auditory sequences. *Journal of Experimental Psychology: Learning, Memory, and Cognition* **31**, 24 (2005).

71 Luft, C. D., Meeson, A., Welchman, A. E. & Kourtzi, Z. Decoding the future from past experience: learning shapes predictions in early visual cortex. *Journal of neurophysiology* **113**, 3159-3171 (2015).

72 Schiffer, A.-M., Muller, T., Yeung, N. & Waszak, F. Reward activates stimulus-specific and task-dependent representations in visual association cortices. *Journal of Neuroscience* **34**, 15610-15620 (2014).

73 den Ouden, H. E., Daunizeau, J., Roiser, J., Friston, K. J. & Stephan, K. E. Striatal prediction error modulates cortical coupling. *Journal of Neuroscience* **30**, 3210-3219 (2010).

74 Horga, G. *et al.* Changes in corticostriatal connectivity during reinforcement learning in humans. *Human brain mapping* **36**, 793-803 (2015).

75 Baylis, L. & Gaffan, D. Amygdalectomy and ventromedial prefrontal ablation produce similar deficits in food choice and in simple object discrimination learning for an unseen reward. *Experimental Brain Research* **86**, 617-622 (1991).

76 Gaffan, D. & Murray, E. A. Amygdalar interaction with the mediodorsal nucleus of the thalamus and the ventromedial prefrontal cortex in stimulus-reward associative learning in the monkey. *Journal of Neuroscience* **10**, 3479-3493 (1990).

77 Gaffan, E., Gaffan, D. & Harrison, S. Disconnection of the amygdala from visual association cortex impairs visual reward-association learning in monkeys. *Journal of Neuroscience* **8**, 3144-3150 (1988).

78 Gaffan, D. & Harrison, S. Amygdalectomy and disconnection in visual learning for auditory secondary reinforcement by monkeys. *Journal of Neuroscience* **7**, 2285-2292 (1987).

79 Murray, E. A. & Mishkin, M. Amygdalectomy impairs crossmodal association in monkeys. *Science* **228**, 604-606 (1985).

80 Gaffan, D. & Saunders, R. C. Running recognition of configural stimuli by fornix-transected monkeys. *The Quarterly Journal of Experimental Psychology Section B* **37**, 61-71 (1985).

81 Parkinson, J., Murray, E. & Mishkin, M. A selective mnemonic role for the hippocampus in monkeys: memory for the location of objects. *Journal of Neuroscience* **8**, 4159-4167 (1988).

82 Gaffan, D. & Harrison, S. A comparison of the effects of fornix transection and sulcus principalis ablation upon spatial learning by monkeys. *Behavioural brain research* **31**, 207-220 (1989).

83 Angeli, S., Murray, E. & Mishkin, M. Hippocampectomized monkeys can remember one place but not two. *Neuropsychologia* **31**, 1021-1030 (1993).

84 Hebb, D. O. (New York: Wiley, 1949).

85 Herrmann, C. S., Strüber, D., Helfrich, R. F. & Engel, A. K. EEG oscillations: from correlation to causality. *International Journal of Psychophysiology* **103**, 12-21 (2016).

86 Harmony, T. The functional significance of delta oscillations in cognitive processing. *Frontiers in integrative neuroscience* **7**, 83 (2013).

87 Putman, P. Resting state EEG delta–beta coherence in relation to anxiety, behavioral inhibition, and selective attentional processing of threatening stimuli. *International Journal of Psychophysiology* **80**, 63-68 (2011).

88 Putman, P., Arias-Garcia, E., Pantazi, I. & van Schie, C. Emotional Stroop interference for threatening words is related to reduced EEG delta–beta coupling and low attentional control. *International Journal of Psychophysiology* **84**, 194-200 (2012).

89 Mitchell, D. J., McNaughton, N., Flanagan, D. & Kirk, I. J. Frontal-midline theta from the perspective of hippocampal "theta". *Progress in neurobiology* **86**, 156-185 (2008).

90 Huster, R. J., Enriquez-Geppert, S., Lavallee, C. F., Falkenstein, M. & Herrmann, C. S. Electroencephalography of response inhibition tasks: functional networks and cognitive contributions. *International journal of psychophysiology* **87**, 217-233 (2013).

91 Cohen, M. X., Elger, C. E. & Ranganath, C. Reward expectation modulates feedback-related negativity and EEG spectra. *Neuroimage* **35**, 968-978 (2007).

92 Hsieh, L. T. & Ranganath, C. Frontal midline theta oscillations during working memory maintenance and episodic encoding and retrieval. *Neuroimage* **85 Pt 2**, 721-729, doi:10.1016/j.neuroimage.2013.08.003 (2014).

93 Liebe, S., Hoerzer, G. M., Logothetis, N. K. & Rainer, G. Theta coupling between V4 and prefrontal cortex predicts visual short-term memory performance. *Nature neuroscience* **15**, 456 (2012).

94 Lee, H., Simpson, G. V., Logothetis, N. K. & Rainer, G. Phase locking of single neuron activity to theta oscillations during working memory in monkey extrastriate visual cortex. *Neuron* **45**, 147-156 (2005).

95 Başar, E., Başar-Eroglu, C., Karakaş, S. & Schürmann, M. Gamma, alpha, delta, and theta oscillations govern cognitive processes. *International journal of psychophysiology* **39**, 241-248 (2001).

96 Hanslmayr, S., Gross, J., Klimesch, W. & Shapiro, K. L. The role of alpha oscillations in temporal attention. *Brain research reviews* **67**, 331-343 (2011).

97 Jensen, O. & Mazaheri, A. Shaping functional architecture by oscillatory alpha activity: gating by inhibition. *Frontiers in human neuroscience* **4**, 186 (2010).

98 Jenkinson, N. & Brown, P. New insights into the relationship between dopamine, beta oscillations and motor function. *Trends in neurosciences* **34**, 611-618 (2011).

99 Neuper, C. & Pfurtscheller, G. Evidence for distinct beta resonance frequencies in human EEG related to specific sensorimotor cortical areas. *Clinical neurophysiology* **112**, 2084-2097 (2001).

100 Kilavik, B. E., Zaepffel, M., Brovelli, A., MacKay, W. A. & Riehle, A. The ups and downs of beta oscillations in sensorimotor cortex. *Experimental neurology* **245**, 15-26 (2013).

101 Merker, B. Cortical gamma oscillations: the functional key is activation, not cognition. *Neuroscience & Biobehavioral Reviews* **37**, 401-417 (2013).

102 Herrmann, C. S., Munk, M. H. & Engel, A. K. Cognitive functions of gamma-band activity: memory match and utilization. *Trends in cognitive sciences* **8**, 347-355 (2004).

103 Singer, W. Consciousness and the binding problem. *Annals of the New York Academy of Sciences* **929**, 123-146 (2001).

104 Canolty, R. T. *et al.* High gamma power is phase-locked to theta oscillations in human neocortex. *science* **313**, 1626-1628 (2006).

105 Demiralp, T. *et al.* Gamma amplitudes are coupled to theta phase in human EEG during visual perception. *International journal of psychophysiology* **64**, 24-30 (2007).

106 Tort, A. B., Komorowski, R. W., Manns, J. R., Kopell, N. J. & Eichenbaum, H. Theta–gamma coupling increases during the learning of item–context associations. *Proceedings of the National Academy of Sciences* **106**, 20942-20947 (2009).

107 Tort, A. B., Komorowski, R., Eichenbaum, H. & Kopell, N. Measuring phase-amplitude coupling between neuronal oscillations of different frequencies. *Journal of neurophysiology* **104**, 1195-1210 (2010).

108 Wulff, P. *et al.* Hippocampal theta rhythm and its coupling with gamma oscillations require fast inhibition onto parvalbumin-positive interneurons. *Proceedings of the National Academy of Sciences* **106**, 3561-3566 (2009).

109 Buzsáki, G. Neural syntax: cell assemblies, synapsembles, and readers. *Neuron* **68**, 362-385 (2010).

110 Gloveli, T. *et al.* Orthogonal arrangement of rhythm-generating microcircuits in the hippocampus. *Proceedings of the National Academy of Sciences* **102**, 13295-13300 (2005).

111 Schroeder, C. E. & Lakatos, P. Low-frequency neuronal oscillations as instruments of sensory selection. *Trends in neurosciences* **32**, 9-18 (2009).

112 Palva, S. & Palva, J. M. New vistas for α-frequency band oscillations. *Trends in neurosciences* **30**, 150-158 (2007).

113 Roux, F. & Uhlhaas, P. J. Working memory and neural oscillations: alpha–gamma versus theta–gamma codes for distinct WM information? *Trends in cognitive sciences* **18**, 16-25 (2014).

114 Donamayor, N., Marco-Pallarés, J., Heldmann, M., Schoenfeld, M. A. & Münte, T. F. Temporal dynamics of reward processing revealed by magnetoencephalography. *Human brain mapping* **32**, 2228-2240 (2011).

115 Gruber, T., Keil, A. & Müller, M. M. Modulation of induced gamma band responses and phase synchrony in a paired associate learning task in the human EEG. *Neuroscience letters* **316**, 29-32 (2001).

116 Gruber, T., Müller, M. M. & Keil, A. Modulation of induced gamma band responses in a perceptual learning task in the human EEG. *Journal of cognitive neuroscience* **14**, 732-744 (2002).

117 Hsieh, L.-T. & Ranganath, C. Frontal midline theta oscillations during working memory maintenance and episodic encoding and retrieval. *Neuroimage* **85**, 721-729 (2014).

118 Jensen, O. & Tesche, C. D. Frontal theta activity in humans increases with memory load in a working memory task. *European journal of Neuroscience* **15**, 1395-1399 (2002).

119 Onton, J., Delorme, A. & Makeig, S. Frontal midline EEG dynamics during working memory. *Neuroimage* **27**, 341-356 (2005).

120 Schack, B., Vath, N., Petsche, H., Geissler, H.-G. & Möller, E. Phase-coupling of theta–gamma EEG rhythms during short-term memory processing. *International Journal of Psychophysiology* **44**, 143-163 (2002).
121 Eördegh, G. *et al.* Multisensory guided associative learning in healthy humans. *PloS one* **14**, e0213094 (2019).
122 Delorme, A. & Makeig, S. EEGLAB: an open source toolbox for analysis of single-trial EEG dynamics including independent component analysis. *Journal of neuroscience methods* **134**, 9-21 (2004).
123 Perrin, F., Pernier, J., Bertrand, O. & Echallier, J. Spherical splines for scalp potential and current density mapping. *Electroencephalography and clinical neurophysiology* **72**, 184-187 (1989).
124 Cohen, M. X. *Analyzing neural time series data: theory and practice*. (MIT press, 2014).
125 Ing, A. & Schwarzbauer, C. Cluster size statistic and cluster mass statistic: Two novel methods for identifying changes in functional connectivity between groups or conditions. *PloS one* **9**, e98697 (2014).
126 Cohen, M. X. Assessing transient cross-frequency coupling in EEG data. *Journal of neuroscience methods* **168**, 494-499 (2008).
127 Puszta, A. *et al.* Power-spectra and cross-frequency coupling changes in visual and Audio-visual acquired equivalence learning. *Scientific reports* **9**, 9444 (2019).
128 Nagy, A., Eördegh, G., Paróczy, Z., Márkus, Z. & Benedek, G. Multisensory integration in the basal ganglia. *European Journal of Neuroscience* **24**, 917-924 (2006).
129 Ravassard, P. *et al.* Multisensory control of hippocampal spatiotemporal selectivity. *Science* **340**, 1342-1346 (2013).
130 Nagy, A., Paróczy, Z., Norita, M. & Benedek, G. Multisensory responses and receptive field properties of neurons in the substantia nigra and in the caudate nucleus. *European Journal of Neuroscience* **22**, 419-424 (2005).
131 Quak, M., London, R. E. & Talsma, D. A multisensory perspective of working memory. *Frontiers in human neuroscience* **9**, 197 (2015).
132 Goolkasian, P. & Foos, P. W. Bimodal format effects in working memory. *The American journal of psychology*, 61-78 (2005).
133 Delogu, F., Raffone, A. & Belardinelli, M. O. Semantic encoding in working memory: Is there a (multi) modality effect? *Memory* **17**, 655-663 (2009).
134 Fougnie, D. & Marois, R. What limits working memory capacity? Evidence for modality-specific sources to the simultaneous storage of visual and auditory arrays. *Journal of Experimental Psychology: Learning, Memory, and Cognition* **37**, 1329 (2011).
135 Morey, C. C. & Cowan, N. When do visual and verbal memories conflict? The importance of working-memory load and retrieval. *Journal of Experimental Psychology: Learning, Memory, and Cognition* **31**, 703 (2005).
136 Calvert, G. A., Campbell, R. & Brammer, M. J. Evidence from functional magnetic resonance imaging of crossmodal binding in the human heteromodal cortex. *Current biology* **10**, 649-657 (2000).
137 Beauchamp, M. S., Lee, K. E., Argall, B. D. & Martin, A. Integration of auditory and visual information about objects in superior temporal sulcus. *Neuron* **41**, 809-823 (2004).
138 Giard, M. H. & Peronnet, F. Auditory-visual integration during multimodal object recognition in humans: a behavioral and electrophysiological study. *Journal of cognitive neuroscience* **11**, 473-490 (1999).

139 Öze, A. *et al.* Acquired equivalence and related memory processes in migraine without aura. *Cephalalgia* **37**, 532-540 (2017).

140 Myers, C. E. *et al.* Learning and generalization deficits in patients with memory impairments due to anterior communicating artery aneurysm rupture or hypoxic brain injury. *Neuropsychology* **22**, 681 (2008).

141 Hsieh, L. T., Ekstrom, A. D. & Ranganath, C. Neural oscillations associated with item and temporal order maintenance in working memory. *J Neurosci* **31**, 10803-10810, doi:10.1523/JNEUROSCI.0828-11.2011 (2011).

142 Gevins, A., Smith, M. E., McEvoy, L. & Yu, D. High-resolution EEG mapping of cortical activation related to working memory: effects of task difficulty, type of processing, and practice. *Cereb Cortex* **7**, 374-385 (1997).

143 Roberts, B. M., Hsieh, L. T. & Ranganath, C. Oscillatory activity during maintenance of spatial and temporal information in working memory. *Neuropsychologia* **51**, 349-357, doi:10.1016/j.neuropsychologia.2012.10.009 (2013).

144 Worden, M. S., Foxe, J. J., Wang, N. & Simpson, G. V. Anticipatory biasing of visuospatial attention indexed by retinotopically specific-band electroencephalography increases over occipital cortex. *J Neurosci* **20**, 1-6 (2000).

145 Ergenoglu, T. *et al.* Alpha rhythm of the EEG modulates visual detection performance in humans. *Cognitive Brain Research* **20**, 376-383 (2004).

146 Schaefer, R. S., Vlek, R. J. & Desain, P. Music perception and imagery in EEG: Alpha band effects of task and stimulus. *International Journal of Psychophysiology* **82**, 254-259 (2011).

147 Hanslmayr, S. *et al.* Prestimulus oscillations predict visual perception performance between and within subjects. *Neuroimage* **37**, 1465-1473 (2007).

148 Foxe, J. J. & Snyder, A. C. The role of alpha-band brain oscillations as a sensory suppression mechanism during selective attention. *Frontiers in psychology* **2**, 154 (2011).

149 Michels, L., Moazami-Goudarzi, M., Jeanmonod, D. & Sarnthein, J. EEG alpha distinguishes between cuneal and precuneal activation in working memory. *Neuroimage* **40**, 1296-1310 (2008).

150 Beck, M. H. *et al.* Short- and long-term dopamine depletion causes enhanced beta oscillations in the cortico-basal ganglia loop of parkinsonian rats. *Experimental neurology* **286**, 124-136, doi:10.1016/j.expneurol.2016.10.005 (2016).

151 Stein, E. & Bar-Gad, I. beta oscillations in the cortico-basal ganglia loop during parkinsonism. *Experimental neurology* **245**, 52-59, doi:10.1016/j.expneurol.2012.07.023 (2013).

152 Timmermann, L. & Fink, G. R. Pathological network activity in Parkinson's disease: from neural activity and connectivity to causality? *Brain : a journal of neurology* **134**, 332-334, doi:10.1093/brain/awq381 (2011).

153 Little, S. *et al.* Controlling Parkinson's disease with adaptive deep brain stimulation. *Journal of visualized experiments : JoVE*, doi:10.3791/51403 (2014).

154 Chen, C. C. *et al.* Stimulation of the subthalamic region at 20 Hz slows the development of grip force in Parkinson's disease. *Experimental neurology* **231**, 91-96, doi:10.1016/j.expneurol.2011.05.018 (2011).

155 Doya, K. Complementary roles of basal ganglia and cerebellum in learning and motor control. *Current opinion in neurobiology* **10**, 732-739 (2000).

156 Graybiel, A. M. The basal ganglia: learning new tricks and loving it. *Current opinion in neurobiology* **15**, 638-644 (2005).

157 Howard, M. W. *et al.* Gamma oscillations correlate with working memory load in humans. *Cerebral cortex* **13**, 1369-1374 (2003).

158 Ossandón, T. *et al.* Transient Suppression of Broadband Gamma Power in the Default-Mode Network Is Correlated with Task Complexity and Subject Performance. *The Journal of Neuroscience* **31**, 14521-14530, doi:10.1523/jneurosci.2483-11.2011 (2011).
159 Chalk, M. *et al.* Attention Reduces Stimulus-Driven Gamma Frequency Oscillations and Spike Field Coherence in V1. *Neuron* **66**, 114-125, doi:https://doi.org/10.1016/j.neuron.2010.03.013 (2010).
160 Myers, C. E. *et al.* Dissociating hippocampal versus basal ganglia contributions to learning and transfer. *J Cogn Neurosci* **15**, 185-193, doi:10.1162/089892903321208123 (2003).
161 Moustafa, A. A., Myers, C. E. & Gluck, M. A. A neurocomputational model of classical conditioning phenomena: a putative role for the hippocampal region in associative learning. *Brain Res* **1276**, 180-195, doi:10.1016/j.brainres.2009.04.020 (2009).
162 Smith, Y., Surmeier, D. J., Redgrave, P. & Kimura, M. Thalamic contributions to basal ganglia-related behavioral switching and reinforcement. *Journal of Neuroscience* **31**, 16102-16106 (2011).
163 Koelewijn, T., Bronkhorst, A. & Theeuwes, J. Attention and the multiple stages of multisensory integration: A review of audio-visual studies. *Acta Psychol (Amst)* **134**, 372-384, doi:10.1016/j.actpsy.2010.03.010 (2010).

I.

Puszta, A., Pertich, Á., Katona, X., Bodosi, B., Nyujtó, D., Giricz, Z., ... & Nagy, A. (2019). Power-spectra and cross-frequency coupling changes in visual and Audio-visual acquired equivalence learning. *Scientific reports*, *9*(1), 9444.

SCIENTIFIC REPORTS

OPEN

Power-spectra and cross-frequency coupling changes in visual and Audio-visual acquired equivalence learning

Received: 14 August 2018
Accepted: 17 June 2019
Published online: 01 July 2019

András Puszta[1], Ákos Pertich[1], Xénia Katona[1], Balázs Bodosi[1], Diána Nyujtó[1], Zsófia Giricz[1], Gabriella Eördegh[2] & Attila Nagy[1]

The three phases of the applied acquired equivalence learning test, i.e. acquisition, retrieval and generalization, investigate the capabilities of humans in associative learning, working memory load and rule-transfer, respectively. Earlier findings denoted the role of different subcortical structures and cortical regions in the visual test. However, there is a lack of information about how multimodal cues modify the EEG-patterns during acquired equivalence learning. To test this we have recorded EEG from 18 healthy volunteers and analyzed the power spectra and the strength of cross-frequency coupling, comparing a unimodal visual-guided and a bimodal, audio-visual-guided paradigm. We found that the changes in the power of the different frequency band oscillations were more critical during the visual paradigm and they showed less synchronized activation compared to the audio-visual paradigm. These findings indicate that multimodal cues require less prominent, but more synchronized cortical contribution, which might be a possible biomarker of forming multimodal associations.

Associative learning is a complex task in which rule-transfer is increased between two superficially dissimilar stimuli (or antecedents) that have previously been associated with similar outcomes (or consequents)[1]. Catherine E. Myers and co-workers developed a learning paradigm (Rutgers Acquired Equivalence Test, also known as the fish-face paradigm), which can be applied to investigate a specific kind of associative learning, visually-guided equivalence learning[2]. This complex test consists of three phases which can be interpreted as better-known tests: The initial phase can be described as an associative learning or trial-and-error learning or rule-based learning task, which primarily requires an intact basal ganglia-network[2,3]. The second part is the retrieval phase, which can be interpreted as working memory maintenance, and the third part is the generalization or rule-transfer phase, which primarily requires an intact hippocampal-mediotemporal system[4,5]. Our research group adapted and modified the Rutgers Acquired Equivalence Test to make it more sensitive, and recently investigated the development of these learning functions in healthy humans and how migraines affect them[6]. This learning paradigm critically requires the normal function of subcortical structures, i.e. hippocampi and basal ganglia[2,7]. Cortical contribution is also necessary in the visually-guided learning paradigm as stimulus representations and associations are stored and (re)activated in stimulus-relevant cortical areas[8–11]. Thus, associative learning requires cooperation between the learning circuit and other task-specific brain areas.

Different areas of the brain must interact to provide the basis for the integration of sensory information, sensory-motor coordination and many other functions that are critical for learning, memory, and perception. Hebb suggested that this is accomplished by forming assemblies of cells whose synaptic linkages are strengthened whenever the cells are activated synchronously[12]. Neuronal oscillations are a natural consequence of forming such cell assemblies via the summation of hundreds of EPSPs and IPSPs, and the cerebral cortex generates multitudes of oscillations at different frequencies mainly through inhibiting spike-trains at a specific frequency. To investigate these oscillations during associative learning, our research group used electroencephalography (EEG),

[1]Department of Physiology, Faculty of Medicine, University of Szeged, Dóm tér 10, Szeged, Hungary. [2] Department of Oral Biology and Experimental Dental Research, Faculty of Dentistry, University of Szeged, Tisza Lajos krt. 64, Szeged, Hungary. Correspondence and requests for materials should be addressed to A.P. (email: puszta.andris@gmail.com) or A.N. (email: nagy.attila.1@med.u-szeged.hu)

which is a well-known non-invasive monitoring method for investigating the electrical signals generated by large assemblies of neurons and their connections.

A number of investigations have described the EEG-features of the different phases of associative learning and memory. One key feature of the reward-related learning is that the positive feedback elicits beta power increment, while negative feedback causes power increment in both theta and beta power[13,14]. Furthermore, studies in associative learning tasks revealed gamma coherence over parietooccipital areas[15,16]. In working memory tasks, frontal midline theta power increment is a well-known phenomenon[17–19]. Theta/alpha-gamma cross frequency coupling in working memory load was described earlier[20,21]. The tasks described above mainly used unimodal stimulus-pairs to associate, and there is less information about how these patterns change if we apply multimodal stimulus-pairs.

It is well known from earlier studies that both brain structures fundamentally involved in visual associative learning, the basal ganglia and the hippocampi, receive not only visual but also multisensory information[22–25]. A bimodal or multimodal stimulus could be more informative in its complexity than a unimodal stimulus from the environment. The studies referenced above investigated visually-guided equivalence learning and to our knowledge no study has addressed the cortical contribution to multisensory-guided acquired equivalence learning.

Multimodal information could be more informative, than a unimodal stimulus from the environment[26,27]. Multisensory integration occurs at different levels of brain functions. It can be observed at the cellular level[28–31] in several brain regions, such as the superior colliculus[32], the basal ganglia[33,34] the cortex[35], and the hippocampus[36], and it can also be observed on the behavioral level[37,38]. In the present study we investigate the effect of multisensory stimuli on associative learning and we ask whether there are any specific changes in the power spectra and in the cross-frequency coupling of the human neocortex in a multisensory task compared to a unimodal visual one[39].

Results

Altogether 23 healthy volunteers participated in the investigation. For the biomathematical analysis (including the psychophysical results, time-frequency (TF) results, cross-frequency coupling results, and power - /synchronization index (SI) - performance correlation), the raw electrophysiological data of 18 volunteers were analyzed, as in the other recordings the signal to noise ratio was low, and neither the excessive attempt to clean the data from muscular and ocular artefacts with preprocessing methods described earlier could make them acceptable.

Data visualization. The electrophysiological results in four different frequency bands (theta (4–7 Hz), alpha (8–13 Hz), beta 14–30 Hz), and gamma (31–70 Hz) will be presented below for each phase (Acquisition, Retrieval and Generalization) of the two (visual and Audio-visual) paradigms.

In the time-frequency results, the group-level statistical differences between the time-frequency power spectra of the visual and audiovisual paradigm are presented in each frequency band, and in each phase of the paradigm (See Figs 1–3). In every case, the results are discussed in a range −500 ms–500 ms in case of the Acquisition phase, and −500 ms-0 ms in case of the Retrieval and Generalization phases, where the 0 ms denotes the time of the answer. We will give a detailed description of the statistical differences between the visual and the audiovisual paradigm only in those cases, where we found significant difference between the visual and the audiovisual paradigms. Detailed descriptions of the changes in the time-frequency power spectra in each phase of the visual and Audio-visual paradigm compared to baseline activity are presented in the Supplementary Data (Supplementary Data 1). Furthermore, because of the huge amount of data, our detailed results of the time-frequency analysis cannot be interpreted with one plot. Instead, we provide an interactive surface, where the significant changes are available on each of the 64 channels in 10 ms-time bins (Supplementary Data 1).

In the cross-frequency coupling results, the group-level statistical differences between the mean synchronization indices of the visual and Audio-visual paradigm are presented in each frequency band, and in each phase of the paradigm. Also, detailed descriptions of the SI-value changes of each phase of the visual and Audio-visual paradigm compared to the SI-value of the baseline activity are presented. Significant changes of the cross-frequency coupling in each channel in different phases of the paradigm will be presented using the *topoplot* function of EEGLab. For plotting purposes, only significant changes (i.e. where the Z-scores were >1.69) are presented on the plots (Fig. 4). In the smaller topographical plots, the significant difference between SI-values of the given phase and the background activity is shown. The red color indicates where the SI was significantly higher during the given phase compared to baseline-activity, and the blue color indicates where the SI in the given phase was significantly lower compared to baseline activity. On the larger topographical plots, we present the significant difference between the visual and audiovisual paradigm. Here, the red color indicates that the power of that specific frequency band in the given phase of the paradigm was significantly higher during the audiovisual task compared to the visual task, where the blue color indicates the opposite. As we found that the highest changes in the individual comodulogram occurred at the modulating frequency band 8–15 Hz and the modulated frequency band at 31–45 Hz, our results will indicate the group level results found in that frequency range.

In the power-performance-correlation results, significant correlations (i.e. where the t-values were >2.583) are presented in each phase of the visual and audiovisual paradigm. For plotting purposes, only significant correlations (i.e. Z-score >1.69) between the performance in the psychophysical test and the cortical power changes (Fig. 5) are plotted on the topographical figures.

Performance in the visual and the Audio-visual psychophysical tests. The mean correct trial ratios (correct trials/all trials) during different phases of the visual acquired equivalence test were as follows: 0.92 in the acquisition phase (range = 0.83–0.98, SD ± 0.04), 0.98 in the retrieval phase (range = 0.9–1, SD ± 0.02), and 0.98 in the generalization phase (range = 0.92–1, SD ± 0.04), (Fig. 6A). Repeated measure analysis of variance (ANOVA) revealed significant difference in the correct trial ratios ($F = 20.87$, $p < 0.001$), and Tukey post-hoc

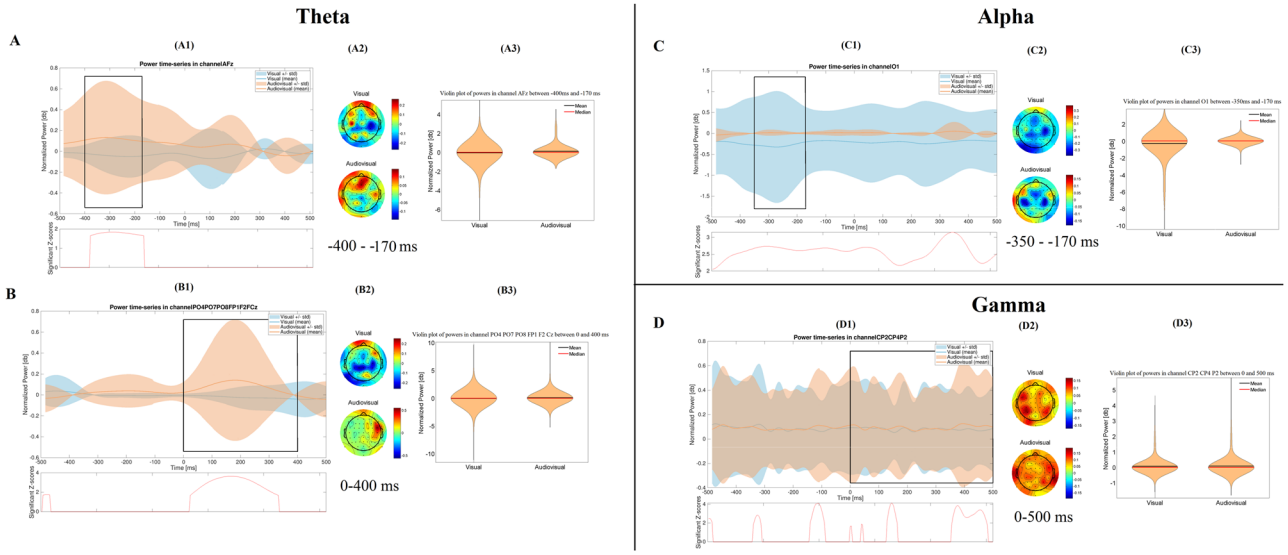

Figure 1. Time-frequency results in the acquisition phase. The figure shows the most important differences, which were found between the visual and the audiovisual tasks. Part (**A**) and Part (**B**) represent the results in the theta band, before and after the given answer, respectively. The (**C**,**D**) parts show the results in the alpha and gamma bands, respectively. Within each part of the figure, there are three different subplots. The subplots with number 1 (A1,B1,C1,D1) show the normalized power-fluctuation of the given channels, and the significant Z-scores between the two time-series calculated with random permutation test before and after 500 ms of the given answer. 0 ms denotes the time point when the answer was given. The subplots with number 2 (A2,B2,C2,D2) show the topographical representation of the mean normalized power in certain time-windows. The red colour indicates power-increase, while the blue one indicates power- decrease compared to baseline-activity. The subplots with 3 (A3,B3,C3,D3) show the violin plot of the normalized powers in the selected time-window and in the selected channels.

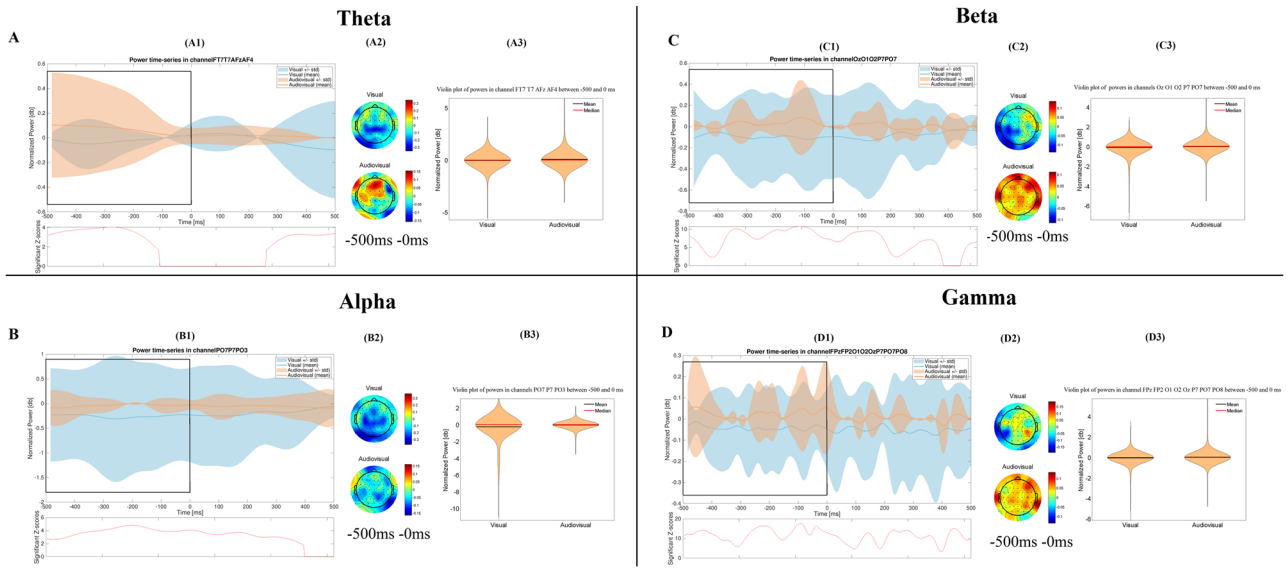

Figure 2. Time-frequency results in the retrieval phase. The figure shows the most important differences, which were found between the visual and the audiovisual task. The (**A**–**D**) parts show the results in the theta, alpha, beta and gamma bands, respectively. Other conventions are same as on Fig. 1.

analysis revealed that the correct trial ratio in the acquisition phase was significantly lower compared to the retrieval and generalization phases ($p < 0.001$). The correct trial ratios did not differ significantly between the generalization and retrieval phase ($p = 0.992$).

The mean correct trial ratios during different phases of the Audio-visual acquired equivalence test were as follows: 0.94 in the acquisition phase (range = 0.90–0.98, SD ± 0.02), 0.98 in the retrieval phase (range = 0.88–1,

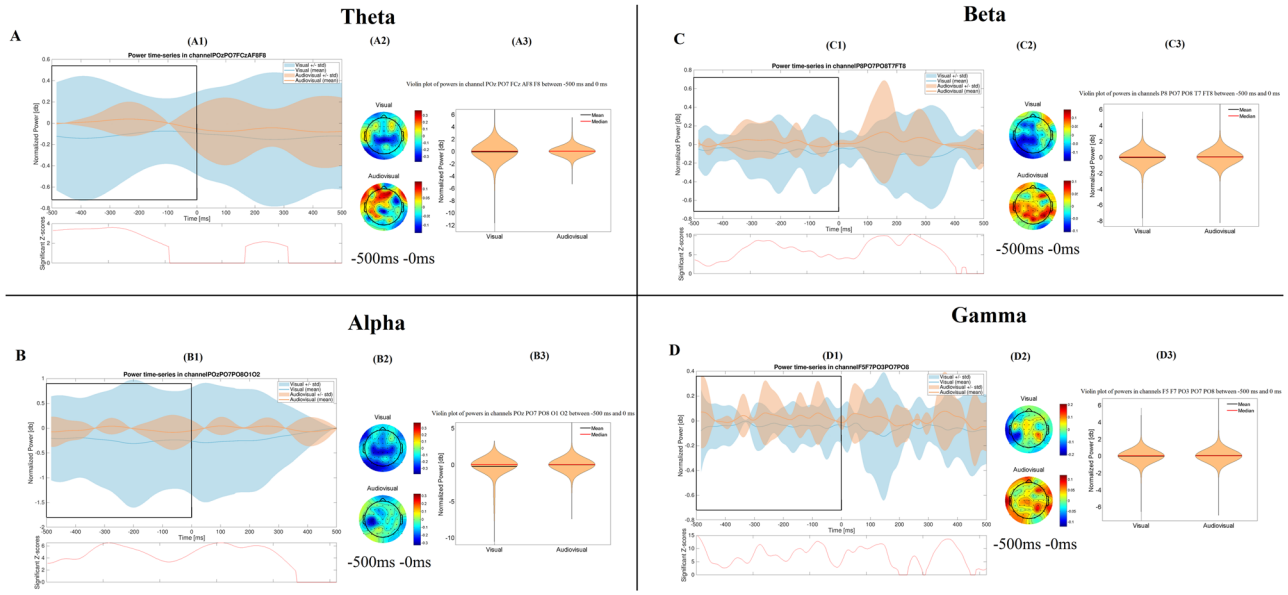

Figure 3. Time-frequency results in the generalization phase. The figure shows the most important differences, which were found between the visual and the audiovisual task. The (**A**–**D**) parts show the results in the theta, alpha, beta and gamma bands, respectively. Other conventions are same as on Fig. 1.

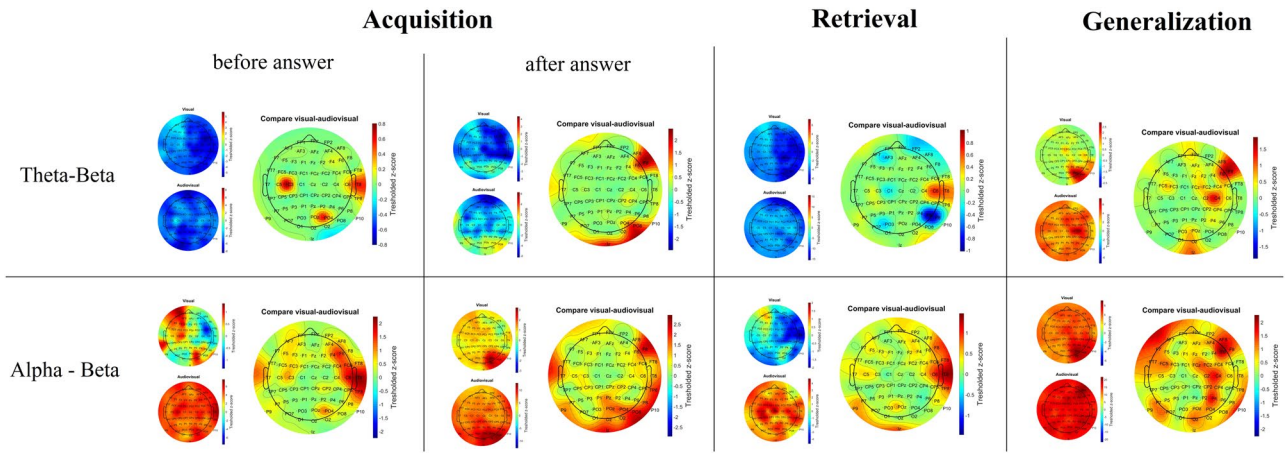

Figure 4. Topographical representation of the cross-frequency theta-beta and alpha-beta coupling results during the visual and audiovisual task. In the smaller topographical plots, the significant difference between SI-values of the given phase and the background activity is shown. The red color indicates where the SI was significantly higher during the given phase compared to baseline-activity, and the blue color indicates where the SI in the given phase was significantly lower compared to baseline activity. On the larger topographical plots, we present the significant difference between the visual and audiovisual paradigm. Here, the red color indicates that the power of that specific frequency band in the given phase of the paradigm was significantly higher during the audiovisual task compared to the visual task, where the blue color indicates the opposite.

SD ± 0.03), and 0.97 in the generalization phase (range = 0.83–1, SD ± 0.05), (Fig. 6B). Repeated measure ANOVA revealed significant difference in the correct trial ratios ($F = 7.49$, $p = 0.002$), and Tukey post-hoc analysis revealed that the correct trial ratio in the acquisition phase was significantly lower compared to the retrieval ($p = 0.002$) and generalization phases ($p = 0.019$). The correct trial ratios did not differ significantly between the generalization and retrieval phase ($p = 0.709$).

Group-level analysis of the time-frequency power spectra in the visual and Audio-visual associative learning paradigms. We interpret our EEG results in each frequency band by showing the cortical areas and the corresponding channels where we found significant differences between the power spectra of the two paradigms. Because of the huge amount of data, our detailed results cannot be interpreted with one plot. Instead, we provide an interactive surface where each significant difference is presented in all 64 channels and in

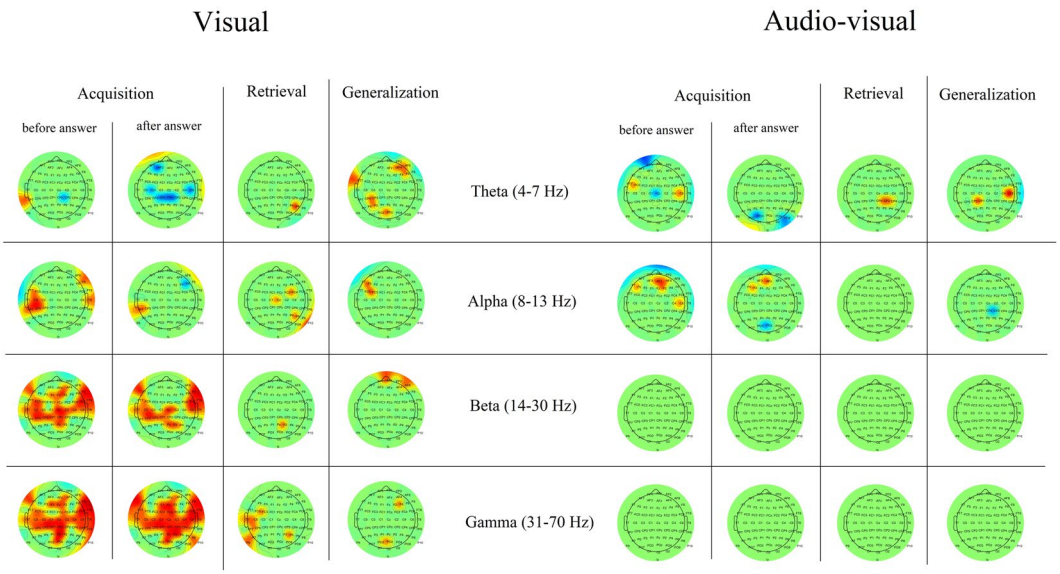

Figure 5. Topographical representation of the power-performance correlation in each phase of the paradigm, during the visual and audiovisual task. Significant correlations (i.e. where the t-values were >2.583) are presented in each phase of the visual and audiovisual paradigm. For plotting purposes, only significant correlations between the performance in the psychophysical test and the cortical power changes are plotted on the topographical figures.

each 10 ms-time section (Supplementary Data 1). Additionally, we provide summarizing pictures and a table of our results (see in Figs 1–3 for Acquisition, Retrieval, Generalization, respectively and Table 1).

Acquisition phase. For the graphical interpretation of our time-frequency results in the acquisition phase see Fig. 1.

The Mann-Whitney test revealed that the power of the theta band was significantly higher during the audiovisual paradigm (mean = 0.118 dB, STD = 0.5 dB, Range = 0 dB 2.814 dB) compared to the visual paradigm (mean = −0.042 dB, STD = 0.459 dB, Range = −3.698 dB 2.012 dB) over the frontal channels, 400 ms to 170 ms before the answer. After the answer (from 0 ms to 400 ms after the answer), the power of the theta band was significantly higher ($p < 0.001$) in the audiovisual paradigm (mean = 0.078 dB, STD = 0.494 dB, Range = −1.943 dB 6.794 dB) compared to the visual paradigm (mean = −0.023 dB, STD = 0.655 dB, Range = −6.954 dB 5.212 dB) not only over the frontal but over the parietooccpital channels, too.

In case of the alpha frequency band we found that the power was significantly lower ($p < 0.001$) during the visual paradigm (mean = −0.278 dB, STD = 1.159 dB, Range = −6.664 dB 0 dB), than in the audiovisual one (mean = 0.012 dB, STD = 0.140 dB, Range = −1.386 dB 1.041 dB) over the occipital channels, 350 ms to 170 ms before the answer.

We observed no significant difference in the beta power between the visual and the audiovisual paradigm.

The power of the gamma band was significantly higher ($p = 0.005$) during the audiovisual paradigm (mean = 0.093 dB, STD = 0.417 dB, Range = −0.496 dB 4.472 dB) than in the visual one (mean = 0.08 dB, STD = 0.36 dB, Range = −0.842 dB 3.491 dB), over the parietal channels, starting from 0 ms until 500 ms after the given answer.

Retrieval phase. For the graphical interpretation of our time-frequency results in the retrieval phase see Fig. 2.

The Mann-Whitney test revealed that the power of the theta band was significantly higher ($p < 0.001$) in the audiovisual paradigm (mean = 0.066 dB, STD = 0.383 dB, Range = −1.871 dB 3.718 dB) than in the visual paradigm (mean = −0.02 dB, STD = 0.276 dB, Range = −3.549 dB 2.006 dB) over the temporal and frontal channels, 500 ms to 0 ms before the answer.

In case of the power of the alpha frequency band we found that it was significantly lower ($p < 0.001$) during the visual paradigm (mean = −0.253 dB, STD = 1.058 dB, Range = −8.308 dB 0 dB) than in the audiovisual paradigm (mean = −0.036 dB, STD = 0.222 dB, Range = −2.324 dB 0.971 dB) over the parietooccipital channels, from 500 ms before the answer.

The power of the beta frequency band was significantly higher ($p < 0.001$) during the audiovisual paradigm (mean = 0.027 dB, STD = 0.276 dB, Range = −3.61 dB 2.994 dB) than in the visual paradigm (mean = −0.093 dB, STD = 0.47 dB, Range = −5.524 dB 1.11 dB), over the occipital and parietooccipital channels, from 500 ms before the answer.

The power of the gamma band was significantly higher ($p < 0.001$) during the audiovisual paradigm (mean = 0.026 dB, STD = 0.27 dB, Range = −3.205 dB 4.133 dB) compared to the visual paradigm

Condition	Frequency band	Time bounds	Cortical region	Power in visual paradigm				p-value	Power in audiovisual paradigm			
				mean	std	min	max		mean	std	min	max
Acquisition	Theta	−400ms −170ms	Frontal	−0,042	0,459	−3,698	2,012	<0.001	0,118	0,500	0,000	2,814
Acquisition	Theta	0 ms 400 ms	Frontal Parietooccipital	−0,023	0,655	−6,954	5,212	<0.001	0,078	0,494	−1,943	6,794
Acquisition	Alpha	−350ms −170ms	Occipital	−0,278	1,159	−6,644	0,000	<0.001	0,012	0,140	−1,386	1,041
Acquisition	Gamma	0 ms 500 ms	Parietal	0,080	0,360	−0,842	3,491	0.005	0,093	0,417	−0,496	4,472
Retrieval	Theta	−500 ms 0 ms	Temporal Frontal	−0,020	0,276	−3,549	2,006	<0.001	0,066	0,383	−1,871	3,718
Retrieval	Alpha	−500 ms 0 ms	Parietooccipital	−0,253	1,058	−8,308	0,000	<0.001	−0,036	0,222	−2,324	0,971
Retrieval	Beta	−500 ms 0 ms	Occipital Parietooccipital	−0,093	0,470	−5,524	1,110	<0.001	0,027	0,276	−3,610	2,994
Retrieval	Gamma	−500 ms 0 ms	Frontal + Parietooccipital	−0,041	0,302	−4,662	2,088	<0.001	0,026	0,270	−3,205	4,133
Generalization	Theta	−500 ms 0 ms	Frontal + Parietooccipital	−0,107	0,677	−8,810	2,529	<0.001	0,009	0,356	−3,022	3,157
Generalization	Alpha	−500 ms 0 ms	Occipital + Parietooccipital	−0,245	1,065	−8,110	0,381	<0.001	−0,033	0,409	−4,785	3,102
Generalization	Beta	−500 ms 0 ms	Parietooccipital	−0,066	0,438	−6,089	3,068	<0.001	0,017	0,347	−5,557	3,933
Generalization	Gamma	−500 ms 0 ms	Frontal + Parietooccipital	−0,038	0,376	−5,521	3,490	<0.001	0,026	0,346	−4,803	4,537

Table 1. Table of the statistics of the most important differences between the visual and audiovisual time-frequency results. We provide a summarizing table of the descriptive statistic of the normalized powers in different frequency band and time-window identified in the interactive surface provided in the Supplementary Data 1. The p-value between the visual and audiovisual task was calculated with Mann-Whitney test.

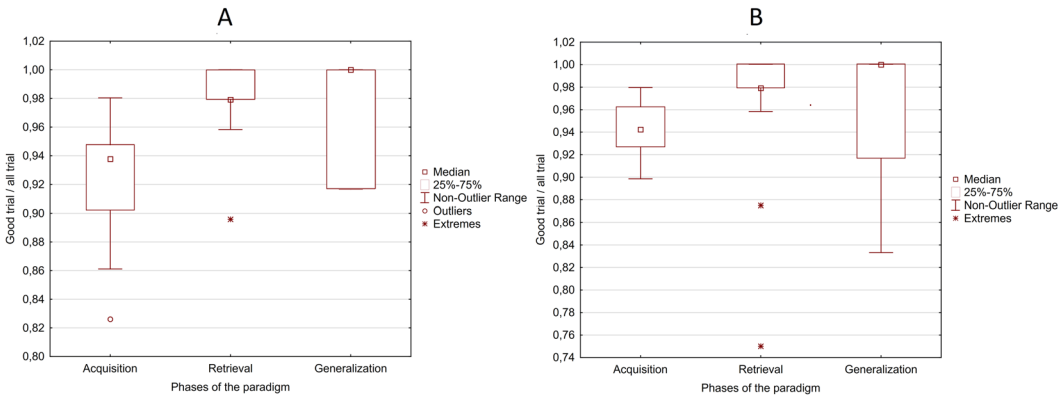

Figure 6. Box plots of the correct trial ratios in each phase of the paradigm during visual (**A**) and Audio-visual (**B**) acquired equivalence learning test.

(mean = −0.041 dB, STD = 0.302 dB, Range = −4.662 dB 2.088 dB), over the frontal and parietooccipital channels, starting from 500 ms before the answer.

Generalization phase. For the graphical interpretation of our time-frequency results in the generalization phase see Fig. 3.

The Mann-Whitney test revealed that the power of the theta band was significantly higher ($p < 0.001$) during the audiovisual paradigm (mean = 0.009 dB, STD = 0.356 dB, Range = −3.022 dB 3.157 dB) than in the visual one (mean = −0.127 dB, STD = 0.677 dB, Range = −8.810 dB 2.529 dB) over the frontal and parietooccipital channels, from 500 ms before the answer.

The power of the alpha frequency band was significantly lower ($p < 0.001$) during the visual paradigm (mean = −0.245 dB, STD = 1.065 dB, Range = −8.11 dB 0.381 dB), compared to the audiovisual paradigm (mean = −0.033 dB, STD = 0.409 dB, Range = −4.785 dB 3.102 dB) over the occipital and parietooccipital channels, from 500 ms before the answer.

The power of the beta frequency band was significantly higher ($p < 0.001$) during the audiovisual paradigm (mean = 0.017 dB, STD = 0.347 dB, Range = −5.557 dB 3.102 dB) compared to the visual paradigm (mean = −0.066 dB, STD = 0.438 dB, Range = −6.089 dB 3.068 dB), over the parietooccipital channels, starting from 500 ms before the answer.

The power of the gamma band was significantly higher in the audiovisual paradigm (mean = 0.026 dB, STD = 0.346 dB, Range = −4.803 dB 4.537 dB) than in the visual paradigm (mean = −0.038 dB, STD = 0.376 dB, Range = −5.521 dB 3.49 dB), over the frontal and parietooccipital channels, starting from 500 ms before the answer.

Correlation between TF-power and psychophysical performance. To reveal the significant TF-power that correlated with the psychophysical performance, we calculated the correlation between the mean power of different frequency bands and performance in the different phases of the paradigm (Acquisition – before and after the given answer – Retrieval, Generalization). See detailed description of the calculations in the Materials and Methods section. In this section we summarize the significant differences in the regions in different frequency bands during the different phases of the paradigm. In the topographical figures we present the significant correlation coefficients found in different phases of the paradigm (Fig. 5).

Visual associative learning paradigm. We found a positive correlation between the power of the higher frequency oscillations (beta, gamma) during the acquisition phase over the parietal and temporal channels before and after the answer.

In the alpha band, we found positive correlations between the power over the temporal channels before and after the answer and performance.

In the theta band power, we found a positive correlation between the performance and power before the answer over the temporal channels. However, we found that the power of theta band over the parietal channels after the answer was negatively correlated with performance.

During the retrieval phase of the visual-associative learning paradigm, we found that power of the gamma band over the temporal channels positively correlated with performance. Concerning the lower frequency bands, their power over the parietooccipital channels positively correlated with performance.

In case of the generalization phase, we observed positive correlation between the psychophysical performance and the power of beta band over the frontal channels.

In case of the alpha band, we observed positive correlation over the frontal channels, and in case of the theta band we found positive correlation over the frontotemporal and parietal channels.

Audiovisual associative learning paradigm. In the acquisition phase of the audiovisual paradigm we found no significant correlation between the power of the higher frequency band (beta, gamma) and the psychophysical performance.

We observed positive correlation between the power of the alpha band before the answer over the frontal and frontotemporal channels and performance. After the answer we found, that the power of the alpha band positively correlated over the frontal channels, and negatively correlated over the parietooccpital channels.

We observed negative correlation over the frontal channels and positive correlation over the temporoparietal channels between performance and the power of the theta band before the answer. After the answer we found, that the power of the theta band negatively correlated over the parietooccipital channels with performance.

In the retrieval phase of the audiovisual paradigm we found, that the power of the theta band over the parietal channels positively correlated with the psychophysical performance. We did not find any significant correlations between the power of other frequency bands and the psychophysical performance.

In the generalization phase we found, that the power of the alpha band over the parietooccipital negatively correlated with performance. We also found that the power of the theta band over the parietotemporal channels positively correlated with performance.

Cross-frequency coupling in the visual and Audio-visual associative learning paradigms. During the acquisition phase of the paradigm, we found a significant decrease in cross-frequency theta-beta coupling compared to baseline-activity both in the case of the visual and the audiovisual paradigm before the given answer. After the given answer, we found significant SI-elevation compared to baseline activity over the occipital-parietooccipital channels (Iz, PO8), which was higher during the audiovisual paradigm.

Regarding the alpha-beta coupling, we found a significant increase of the SI-values before the answer over the whole scalp in the case of the audiovisual paradigm, and over the left frontal-frontotemporal (FP1, AF3, AF7, F1, F3, F5, F7, FC1, FC3, FC5) and parietooccipital-occipital (PO4, O2) channels. Comparing the visual and the audiovisual paradigm, before the given answer in the acquisition phase, we found that the SI-values were significantly higher over the temporal (T7, T8, TP8, C6) and frontotemporal (FC6, F6) channels during the audiovisual paradigm.

After the answer, we found that alpha-beta coupling was significantly higher compared to the baseline activity both in the visual and the audiovisual paradigm, predominantly over the parietooccipital-occipital (PO4, PO8, O2, Oz) channels, which was higher during the audiovisual paradigm.

During the retrieval phase of the paradigm, we observed significant theta-beta coupling decrease over the whole scalp during both the visual and audiovisual paradigm. Comparing the visual and the audiovisual paradigm, we found that the SI-decrease was higher over the right parietooccipital (P8, P6) channels during the visual paradigm.

For the alpha-beta coupling, we observed a significant decrease of the SI-values compared to baseline activity over the right temporal, frontotemporal and parietoocciptal channels during the visual paradigm. We observed significant alpha-beta cross-frequency coupling increase over the whole scalp during the audiovisual paradigm. Comparing the visual and the audiovisual paradigm, we found that the SI-values were higher over the right temporal-frontotemporal (T8, C6, FT8, F8) and parietooccipital-occipital (Iz, P9) channels during the audiovisual paradigm.

During the generalization phase, we found significant theta-beta coupling over the parietooccipital-occipital channels (PO8, PO4, P2, P4, P6, P8) during the visual paradigm. We found that the theta-beta coupling was significantly higher compared to baseline activity over the whole scalp during the audiovisual paradigm. Comparing

the visual and audiovisual theta-beta coupling strength, we found that the SI-values were significantly higher over the frontotemporal (C4, F8, F6) and occipital (Iz, Oz, POz) channels during the audiovisual paradigm.

In the case of the alpha-beta coupling, we found the same pattern of SI-value increase that was observed in the theta-beta coupling during the generalization phase.

Discussion

The present study analyzed the EEG correlates in a visually-guided and an Audio-visually (bimodal or multisensory) guided acquired -equivalence learning tasks. To our knowledge, this is the first study to address the comparison of the cortical power spectra and their changes in a unimodal visual and a multisensory associative learning task. The major finding of the study is that the cortical activity depends critically on the phase of the paradigm, and some changes in cortical powers are characteristic to unimodal visual and multisensory Audio-visual tasks. In general, during the audiovisual paradigm, the power changes of the event-related low and high-oscillations were higher compared to the visual paradigm, but the psychophysical performance of the acquisition phase only correlated with the power of different frequency bands during the visual paradigm. On the other hand, while the power changes of the event-related oscillations were higher during the audiovisual paradigm, the performance did not depend on the power of different oscillations, and the strength of the cross-frequency coupling was higher. Furthermore, the performance of the acquisition phase seems to be more connected to the strength of the alpha-beta coupling during the audiovisual paradigm. We are convinced that the cortical power differences in the two paradigms cannot be the result of having previously completed the first task (precondition), hence the order of the two paradigms (visual and Audio-visual) varied randomly across subjects.

The role of multimodal cues in associative learning has been widely investigated (for review see[40]). The psychological studies provided evidence, that multisensory working memory improves recall for cross-modal objects compared to modality-specific objects[41,42], working memory capacity is higher for cross-modal objects under certain circumstances[43] and visual and auditory information can interfere with each other[44]. While former studies revealed mainly cortical areas are involved in associative learning[45,46], only few electrophysiological studies showed the functional basis of the multisensory integration[47], and to our knowledge, our study is the first that describes the role of different oscillations in multisensory integration during learning.

The performance of the investigated population in the psychophysical test (acquisition error ratio, retrieval error ratio, generalization error ratio) was in the same range as that of the earlier investigated healthy controls of neurological and psychiatric patients[2,4,6,48]. Based on this we are strongly positive that the electrophysiological results showed here are representative.

One of the common findings both in the visual and the Audio-visual paradigm is the increased theta band activity in the parietooccipital, frontal midline, and prefrontal areas during the acquisition and retrieval phases. Frontal midline theta activity has been widely investigated (for review, see[49]), and its contribution seems to be obvious to internally-guided cognitive tasks that require no external responses[50–52]. A more general interpretation of the increased theta power in the frontal cortex could be the coordinated reactivation of information represented in visual areas. This was also found in single-unit recordings in primate V4[53] as well as LFP-synchronisation between the prefrontal cortex and V4[54]. Regarding our findings, we hypothesize that the initial acquisition phase of the task requires more repeated reactivation of the cortical areas where the stimulus is processed. We also assume (based on the power-performance correlation we observed) that the better the associations are encoded, the more enhanced theta activity can be observed in the frontal midline areas.

The earlier findings of human electrophysiological studies indicated the role of the alpha band in visual[55,56] as well as Audio-visual processing[57]. Moreover, Hanslmayr and his colleagues[58] found that the performance in processing stimuli is more likely to be linked to decreased power in the alpha band. Another function that has been attributed to alpha activity is a mechanism of sensory suppression, thus functional gating of information in the task-irrelevant brain areas[59,60]. Indeed, our findings suggest that the initial parts of the trials (0–50 ms) are coupled to decreased alpha power, which were then followed by an increase of it in the visual (occipital) and Audio-visual (parietooccipital) cortical areas. These together suggest that after a rapid processing of the cue image and sound, the threshold of the visual/Audio-visual cortical areas for external stimuli becomes higher, allowing the information to be encoded (or retrieved) internally.

In the case of the beta frequency range, there is a growing evidence that enhanced beta oscillations appear in patients with Parkinson disease (PD)[61]. A number of investigations found that a power increase of the beta frequency band correlates with the severity of parkinsonian motor symptoms such as akinesia and rigidity[62,63]. As a result, beta oscillations are currently investigated as a potential biomarker tracking the effectiveness of deep brain stimulation treatment of PD patients[64]. Furthermore, deep brain stimulation of the subthalamic nucleus at beta frequencies worsens motor symptoms in PD patients[65]. One of the main functions of the basal ganglia is to contribute to associative learning by the trial-and-error method[66,67]. It is well-known that in PD (along with other deficits in which basal ganglia are affected) this learning mechanism is reduced[33,34]. Having seen in our results that a robust decrease of beta-power occurred in all phases (acquisition, retrieval and generalization phases) of both the visual and Audio-visual learning tasks, one may consider that this cortical power density decrease in the beta band is a necessary cortical outcome of the normal action of the basal ganglia in visual and Audio-visual associative learning

The gamma frequency band plays an important role in memory processes[68] as well as other cognitive processes, such as word learning, reading, and expectancy[36,37]. We observed a power increase during the acquisition phase of the task in the frontal cortex and in associative cortical areas connected to the modality of the presented stimuli (i.e. the occipital cortex in the visual task, the parietotemporal areas in the Audio-visual task). Thus, we hypothesize that the acquisition phase of the learning paradigm needs strong cortical contribution. The power differences between the acquisition phase of the visual and Audio-visual learning paradigm suggest stronger cortical contribution to the multisensory learning task. On the other hand, this increase in the gamma power was not

detectable in the retrieval and the generalization phases of the paradigm. The explanation for this could be that the already-learned acquisitions were already transmitted to the hippocampus and the application of the earlier acquisitions does not need strong cortical activation in the gamma band. There is also evidence that a decrease in the gamma power of the local field potential correlates with performance and attention by selectively gating sensory inputs[69,70] We assume that the decrease of the gamma power we found during the task over the cortical areas where the stimulus was processed (i.e. occipital areas in the visual and parietotemporal in the Audio-visual task) could be beneficial in memory encoding and retrieval by filtering irrelevant external stimuli.

Calculating the synchronization indices, we found increased coupling between theta and alpha/beta in each phase of both the visual and the Audio-visual task, which are in accordance with earlier studies that emphasize the role of theta-gamma/beta coupling in memory processes[40,41] as well as the alpha gamma/beta coupling in visual perception[42,43]. We also found that this synchronization was significantly stronger during each phase of the Audio-visual task than in the visual paradigm. Furthermore, during the retrieval and generalization phases, we found that the synchronization between theta-beta and alpha-beta was significantly stronger in the audiovisual task. We argue that the audiovisual paradigm required stronger synchronized cortical contribution in all phases of the task because of the cross-modal integration of the visual and auditory stimuli. Furthermore, as the power of the cortical oscillations increased more during the visual task compared to the Audio-visual task, this indicates that the multimodal (audiovisual) associations require less, but more synchronized activation of the cortex.

Optimal performance in the acquisition phase of the learning paradigms appears to depend mainly on the integrity of the basal ganglia, whereas performance in the test phase (both retrieval and generalization) has been linked to the integrity of the hippocampal region[2,71,72]. It is also known that both fundamentally-involved structures, the basal ganglia and the hippocampi, are involved in attention processes (for a reviews, see[73]). At the behavioral level, multisensory integration could be dependent on the level of attention and is not an automatic, unconscious process[74]. A multisensory task seems to be more complex and probably needs more attention from the participants. However, our psychophysical results show no significant differences between the performances in the visual and the multisensory tasks. In summary, although the role of attention cannot be excluded in the psychophysical learning test, the same level of performance in the unimodal visual and multimodal (Audio-visual) learning paradigms contradicts the assumption that attention contributes significantly to the differences in cortical activation patterns.

We can conclude that the changes in the power of the different frequency-band oscillations were more critical during the visual paradigm. On the other hand, the encoding and the retrieval part of the bimodal, Audio-visual task required more strongly synchronized cortical activity than those of the visual one. The two former statements are probably due to the fact that in the case of the multisensory associations the investigated memory processes (encoding, retrieval, and generalization) require less prominent, but more synchronized cortical activation, while the unimodal associations require more prominent and less synchronized cortical activity during the same memory processes. These findings further emphasize the effect of multimodal integration during associative learning and memory processes.

Materials and Methods

The EEG data of 23 adult healthy young adults were recorded (12 females, 11 males, mean age: 26 years, range = 18–32). The participants were free of any ophthalmological or neurological conditions, and they were tested for parachromatism with the PseudoIsochromatic Plate Color Vision Test. The participants were recruited on a voluntary basis. The potential subjects were informed about the background and goals of the study, as well as about the procedures involved. It was also emphasized that, given the lack of compensation or any direct benefit, the participants were free to quit at any time without any consequence (no one did so). Those who decided to volunteer signed an informed consent form. The study protocol conformed to the tenets of the Declaration of Helsinki in all respects, and was approved by the Medical Ethics Committee of the University of Szeged, Hungary (Number: 50/2015-SZTE). The datasets generated and analyzed during the present study and the Matlab codes, that were used in the analytical process connected to this study are available in the Supplementary Data 2.

Visual associative learning test. The testing software (described in earlier studies and originally written for iOS[2]) was adapted to Windows. It was coded in Assembly for Windows and translated into Hungarian, with the written permission of the copyright holder. The paradigm was also slightly modified to reduce the probability of completing its acquisition phase by mere guessing (see below). The tests were run on a PC. The stimuli were displayed on a standard 17- inch CRT monitor (refresh rate 100 Hz) in a quiet room separated by a one-way mirror from the recording room. Participants sat at a 114 cm distance from the monitor. One participant was tested at a time and no time limitation was set. The test was structured as follows: in each trial of the task, the participants saw a face and a pair of fish of different color, and had to learn through trial and error which fish was connected with which face (Fig. 1). There were four faces (A1, A2, B1, B2) and four possible fish (X1, X2, Y1, Y2), referred to as antecedents and consequents, respectively. In the initial, acquisition stages, the participants were expected to learn that when A1 or A2 appears, the correct answer was to choose fish X1 over fish Y1; given face B1 or B2, the correct answer was to choose fish Y1 over fish X1. If the associations were successfully learned, participants also learned that face A1 and A2 were equivalent with respect to the associated fish (faces B1 and B2 likewise). Next, participants learned a new set of pairs: given face A1, they had to choose fish X2 over Y2, and given face B1, fish Y2 over X2. This was the end of the acquisition phase. To this point, the computer provided feedback about the correctness of the choices, and six of the possible eight fish-face combinations were taught to the participants. In the following phases (retrieval and generalization), no feedback was provided. Beside the already-acquired six pairs (tested in the retrieval phase) the hitherto not shown two pairs were also presented, which were predictable based on the learned rules (tested in the generalization phase). Having learned, that faces A1 and A2 are equivalent, participants were expected to generalize from learning that if A1 goes with X2, A2 also goes with X2; the

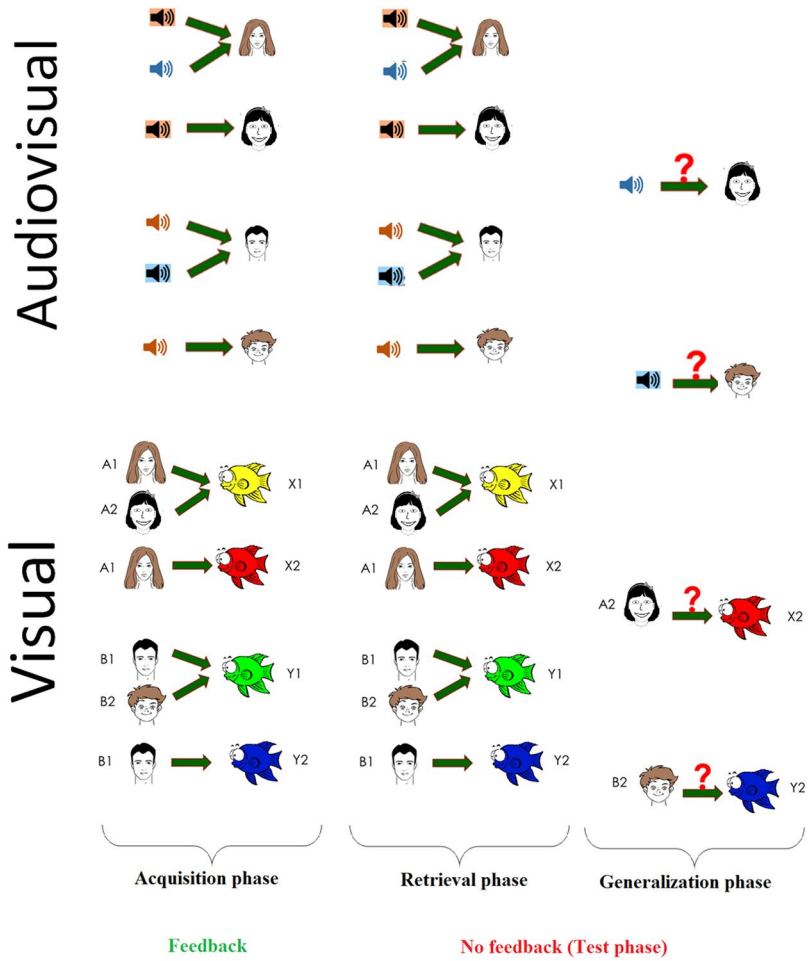

Figure 7. Graphic overview of the unimodal visual (lower panel) and the bimodal Audio-visual (upper panel) acquired equivalence paradigms.

same holds for B2 (equivalent to B1) and Y2 (equivalent to B1). During the acquisition stages, new associations were introduced one by one, mixed with trials of previously-learned associations. The subjects had to achieve a certain number of consecutive correct answers after the presentation of each new association (4 after the presentation of the first association, and 4, 6, 8, 10, 12 with the introduction of each new association, respectively) to be allowed to proceed. In order to minimize the repetition effect in the acquisition phase, the last, 12-answer trial of the acquisition phase were set to be the part of the retrieval phase. This resulted in an elevated number of the required consecutive correct trials compared to the original paradigm, which made getting through the acquisition phase by mere guessing less probable. Similarly, in the test phase there were 48 trials (12 trials of new and 36 trials of previously-learned associations), as opposed to the 16 trials of the original paradigm.

Audio-visual associative learning test. We developed the Audio-visual (multisensory or bimodal) guided acquired equivalence learning test. The structure of the paradigm was the same as of the visual associative learning test, with the difference that the four antecedents were four sounds (A1, A2, B1, B2) and the consequents were the same four faces as in the visual associative learning paradigm. The main task of the participants was to determine from trial to trial which of the two given faces corresponds to the sound heard at the beginning of the trial. The sounds of the paradigm were a female voice saying "Hello", the sound of a guitar, the sound of a motorcycle, and the sound of a cat. Each sound lasted less than 1 sec. The category rule implemented in the four faces (i.e. sex, age, hair color) was the same as in the visual paradigm, so similarity across the sounds was not important, but the similarity across the four faces was the same as in case of the visual paradigm. During the acquisition phase, six of the possible eight sound-face combinations were learned. During the test phase, no feedback was provided anymore, but beside the already-acquired six pairs (learned in the retrieval phase), the hitherto not shown last two pairs were also presented (generalization phase). For visual representation of the two task, see Fig. 7.

Data acquisition. Sixty-four channel EEG recordings were performed using a Biosemi ActiveTwo AD-box with 64 active electrodes. Actiview software was used to set up the parameters and record the EEG-data (Biosemi B.V., The Netherlands). The sampling rate was 2048 Hz. Electrode offsets were all kept within normal and acceptable ranges. Raw signals were recorded on the computer that controlled the psychophysical learning task. The

stimulating software generated trigger signals to indicate the beginning of each trial. These trigger signals were recorded on an additional (sixty-fifth) channel. In order to obtain the baseline activity, one-minute-long resting state activities were recorded before and after testing the visual and Audio-visual associative learning test. The order of the two tests (visual and Audio-visual associative learning test) varied randomly across volunteers.

Preprocessing. The raw EEG data was first high-pass filtered (the filtering method used a 2 Hz highpass, two-way, least-squares FIR procedure, as implemented in the eegfilt.m script included in the eeglab package)), and then re-referenced to the average of the channels. All trials were visually inspected, and those containing EMG or other artefacts not related to blinks were manually removed. Independent components analysis was computed using the EEGLab toolbox for Matlab[75], and components containing blink/oculomotor artefacts or other artefacts that could be clearly distinguished from brain-driven EEG signals were subtracted from the data. The trials were defined as 500 ms before and after the given answer. In order to minimize the repetition effect in the acquisition phase, the last 12-answer trial of the acquisition phase was set to be the part of the retrieval phase. The subtracted trials did not exceed 1% of all trials. The mean trials of the phases of the paradigm was 54, 50 and 12, in the acquisition, retrieval and generalization phase, respectively. Additionally, noisy channels were interpolated using EEGLab toolbox. Then we used Laplacian fitting to improve the spatial resolution of the recording[76]. After the preprocessing steps, the data was resampled to 256 Hz, to minimize the computational time. This is the reason that in the present study the results of the time-frequency analysis are given in 10 ms-bins.

Data analysis. All data analysis was performed using Matlab (MATLAB and Statistics Toolbox Release 2018a, The MathWorks, Inc., Natick, Massachusetts, United States.) and Statistica software (Dell Statistica for Windows v13).

Analysis of the performances in the psychophysical learning tasks. The psychophysical data were analysed in three groups: data from the acquisition phase, data from the retrieval parts of the test phase (i.e. when the participant was presented an already-learned association), and data from the generalization part of the test phase (i.e. previously-not-learned associations). The number of correct and wrong responses were calculated in all phases, as well as the ratio of these to the total number of trials during the respective phase.

Time-frequency analysis. Time-frequency analysis was performed using a Continous Morlet wavelet convolution (CMW) via FFT algorithm[77]. Firstly, FFT was first performed on one selected channel of the raw data. Then complex Morlet wavelets were created for each frequency (1–70 Hz) on which FFT was also executed. The cycles of the wavelets increased logarithmically as the frequency varied in a linear manner. After that, we calculated the dot product of the given channel's FFTs and the FFTs of the complex Morlet wavelets at each individual frequency, which yielded 70 complex numbers. Thereafter, the inverse Fast Fourier transform of the results of the dot product showed the alterations of the power in the time domain as follows:

$$K_x = IFFT(fft(C) \cdot fft(W_x))$$

where the K is the time-series of the given channel, wavelet-filtered to frequency x, C is the time series of all trials of different phases, and W is the complex Morlet wavelet in a given frequency x. In order to avoid the edge-artifacts of the Morlet wavelet convolution, the raw data was multiplied five times before the convolution, yielding a two-series-long buffer zone at the beginning and the end of the time-series, which was cut out after the time-frequency analysis. After that, the channel's data was cut into different phases of the paradigm (baseline, acquisition, retrieval, generalization). The trials were defined as the 500 ms before and after the given answer. As the baseline activity was longer than the compared periods (i.e. the signal belonging to a given condition), the baseline activity was bootstrap-resampled to match the given condition by cutting one-second-long periods randomly from the baseline activity (1–1 minute before and after the first and the last trigger-signal, respectively). The bootstrapping method was the same as described in[78].The data set for the purposed null-hypothesis (global band) was generated by iteratively calculating the mean difference of the randomized permutation of the power values of a particular channel in a given frequency band in two different phases of the paradigm (Baseline-Acquisition, Baseline-Retrieval, Baseline-Generalization). The Z-scores for each channel were then calculated between the distributions derived from the global band and the mean difference of the power values in a given frequency band between the analysed phase and the baseline activity. Z-scores were corrected by the minimum and maximum point of the null hypothesis distribution (also known as cluster-mass correction[77,79]).

Group-level analysis of the CMW was carried out in the same way as in the individual analysis described above, with the difference that the random permutation was performed across the mean power values of the subjects and not across the power value of each individual trial. The visualized methodological procedures of the above-described permutation-based test can be seen in one of our earlier publications through an individual example[80]. In the interactive surface provided in the Supplementary Material (Supplementary Data 1) only significant Z-scores calculated the above mentioned way are provided. As the data was resampled to 256 Hz, the time-bins in the Supplementary Data are 10 ms.

We identified the time-windows in which we found significant difference between the visual and the audio-visual paradigm, using the interactive surface provided in the Supplementary Material (Supplementary Data 1). After we identified the significant time-windows and the corresponding channels in each frequency band and condition, we additionally tested if the individual normalized powers of the different frequency bands in the selected channels and time-points are significantly different in the visual and the audiovisual paradigm by using Mann-Whitney test. The individual normalized powers were obtained by normalizing each individual time-frequency power in each condition and on each channel to the mean power of the baseline activity in the same channel and same frequency using decibel-normalization. Furthermore, to see the significant differences in

the time-domain in the selected channels, we performed permutation-test between the normalized power time series of the visual and audiovisual test.

Calculation of event-related cross-frequency coupling. Event-related synchronization index (SI) was calculated in order to examine whether the power of the high-frequency oscillations are coupled to the phase of the low-frequency oscillations on the same channel. The calculation method was almost the same as described by Cohen[81]. We will give a detailed description of the calculation of the SI in one phase of the paradigm in one channel's data referred as raw analytic signal. In the first step, the higher-frequency power time series were extracted from the concatenated trials. This was done by the combination of band-pass filtering and Hilbert transformation. First, we used a narrow band pass to filter the analytic signal to each frequency of beta and gamma band (15–70 Hz). The filtering method used a 4 Hz-width, two-way, least-squares FIR procedure (as implemented in the eegfilt.m script included in the eeglab package). Then we performed Hilbert transformation on the narrow bandpass-filtered epochs. The power time-series was extracted as the squared magnitude of z(t), the analytic signal obtained from the Hilbert transform (power time series: $p(t) = real[z(t)]2 + imag[z(t)]2$).

Then we band-pass filtered the raw analytic signal to each frequency of the low-frequency range (2–20 Hz, with 4 Hz-width). The phase of the band-pass filtered low- and high-frequency power time series were obtained from the Hilbert transform of the two time-series, respectively.

The synchronization between the phases of the two power time series can be calculated using the synchronization index (SI) as follows:

$$SI = \left| \frac{1}{n} \times \sum_{t=1}^{n} e^{i(\varphi_{lt} - \varphi_{ut})} \right|^2$$

where n is the number of time points, φ_{ut} is the phase value of the fluctuations in the higher-frequency power time series at time point t, and φ_{lt} is the phase value of the lower-frequency band time series at the same time point. The SI varied between 0 and 1. At SI 0 the phases are completely desynchronized, and at SI 1 the phases are perfectly synchronized.

Significant changes of the cross-frequency coupling at a population level were calculated by comparing the mean synchronization index in a given modulating - and modulated frequency range of the baseline activity and the given phase of the paradigm. The mean SI-values in each phase of the paradigm were then compared using permutation-based statistics, and the resulting Z-scores were corrected by the minimum and maximum point of the null hypothesis distribution (also known as cluster-mass correction[77,79]). See Supplementary Figs 1 and 2 for the graphical interpretation of the calculation of the SI values and their statistical comparison.

Correlation between performance in the psychophysical test and the power density changes. Correlation between individual performance and power density changes in a given channel and frequency band was also calculated in each phase of the paradigm. Performance was defined as the ratio of the correct (good) trials to all trials, and the individual power changes were defined as the individual Z-scores between the baseline activity's power density and the given phase's power density in a given channel in a given frequency band. The Pearson correlation coefficient was calculated using the *'corr'* function of Matlab. Statistical analysis was performed by calculating the t-score for each correlation coefficient as follows:

$$t_{ch,fr} = r_{ch,fr} * \sqrt{\frac{n-2}{1 - r_{ch,fr}^2}}$$

where r is the correlation coefficient in channel (ch) and frequency (fr) band, n is the number of samples (in this case it was 18), and t is the calculated t value in a given channel and frequency band. T-values whose absolute values were smaller than 2.583 (which is the critical t-value if the degree of freedom is 16 and the significance level is 0.01) were set to 0. The corrected t-values in different frequency bands in each phase of the paradigm were plotted to a topographical map using the '*topoplot*' function of EEGLab.

References

1. Hall, G., Ray, E. & Bonardi, C. Acquired equivalence between cues trained with a common antecedent. *Journal of Experimental Psychology: Animal Behavior Processes* **19**, 391 (1993).
2. Myers, C. E. *et al*. Dissociating hippocampal versus basal ganglia contributions to learning and transfer. *Journal of Cognitive Neuroscience* **15**, 185–193 (2003).
3. Vadhan, N. P. *et al*. Stimulus–response learning in long-term cocaine users: Acquired equivalence and probabilistic category learning. *Drug & Alcohol Dependence* **93**, 155–162 (2008).
4. Bódi, N., Csibri, É., Myers, C. E., Gluck, M. A. & Kéri, S. Associative learning, acquired equivalence, and flexible generalization of knowledge in mild Alzheimer disease. *Cognitive and Behavioral Neurology* **22**, 89–94 (2009).
5. Kéri, S., Nagy, O., Kelemen, O., Myers, C. E. & Gluck, M. A. Dissociation between medial temporal lobe and basal ganglia memory systems in schizophrenia. *Schizophrenia research* **77**, 321–328 (2005).
6. Öze, A. *et al*. Acquired equivalence and related memory processes in migraine without aura. *Cephalalgia* **37**, 532–540 (2017).
7. Shohamy, D. & Wagner, A. D. Integrating memories in the human brain: hippocampal-midbrain encoding of overlapping events. *Neuron* **60**, 378–389 (2008).
8. Nyberg, L., Habib, R., McIntosh, A. R. & Tulving, E. Reactivation of encoding-related brain activity during memory retrieval. *Proceedings of the National Academy of Sciences* **97**, 11120–11124 (2000).
9. Nyberg, L. *et al*. Reactivation of motor brain areas during explicit memory for actions. *Neuroimage* **14**, 521–528 (2001).
10. Rösler, F., Heil, M. & Hennighausen, E. Distinct cortical activation patterns during long-term memory retrieval of verbal, spatial, and color information. *Journal of Cognitive Neuroscience* **7**, 51–65 (1995).
11. Slotnick, S. D. Memory for color reactivates color processing region. *NeuroReport* **20**, 1568–1571 (2009).

12. Hebb, D. O. The Organization of Behavior: A Neuropsychological Theory (1949).
13. Donamayor, N., Marco-Pallarés, J., Heldmann, M., Schoenfeld, M. A. & Münte, T. F. Temporal dynamics of reward processing revealed by magnetoencephalography. *Human brain mapping* **32**, 2228–2240 (2011).
14. Cohen, M. X., Elger, C. E. & Ranganath, C. Reward expectation modulates feedback-related negativity and EEG spectra. *Neuroimage* **35**, 968–978 (2007).
15. Gruber, T., Keil, A. & Müller, M. M. Modulation of induced gamma band responses and phase synchrony in a paired associate learning task in the human EEG. *Neuroscience letters* **316**, 29–32 (2001).
16. Gruber, T., Müller, M. M. & Keil, A. Modulation of induced gamma band responses in a perceptual learning task in the human EEG. *Journal of cognitive neuroscience* **14**, 732–744 (2002).
17. Hsieh, L.-T. & Ranganath, C. Frontal midline theta oscillations during working memory maintenance and episodic encoding and retrieval. *Neuroimage* **85**, 721–729 (2014).
18. Jensen, O. & Tesche, C. D. Frontal theta activity in humans increases with memory load in a working memory task. *European journal of Neuroscience* **15**, 1395–1399 (2002).
19. Onton, J., Delorme, A. & Makeig, S. Frontal midline EEG dynamics during working memory. *Neuroimage* **27**, 341–356 (2005).
20. Schack, B., Vath, N., Petsche, H., Geissler, H.-G. & Möller, E. Phase-coupling of theta–gamma EEG rhythms during short-term memory processing. *International Journal of Psychophysiology* **44**, 143–163 (2002).
21. Roux, F. & Uhlhaas, P. J. Working memory and neural oscillations: alpha–gamma versus theta–gamma codes for distinct WM information? *Trends in cognitive sciences* **18**, 16–25 (2014).
22. Bates, S. L. & Wolbers, T. How cognitive aging affects multisensory integration of navigational cues. *Neurobiology of aging* **35**, 2761–2769 (2014).
23. Nagy, A., Eördegh, G., Paróczy, Z., Márkus, Z. & Benedek, G. Multisensory integration in the basal ganglia. *European Journal of Neuroscience* **24**, 917–924 (2006).
24. Ravassard, P. *et al*. Multisensory control of hippocampal spatiotemporal selectivity. *Science* **340**, 1342–1346 (2013).
25. Nagy, A., Paróczy, Z., Norita, M. & Benedek, G. Multisensory responses and receptive field properties of neurons in the substantia nigra and in the caudate nucleus. *European Journal of Neuroscience* **22**, 419–424 (2005).
26. Sarter, N. B. J. I. j. o. i. e. Multimodal information presentation: Design guidance and research challenges. **36**, 439–445 (2006).
27. Oviatt, S. & Cohen, P. J. C. o. t. A. Perceptual user interfaces: multimodal interfaces that process what comes naturally. **43**, 45–53 (2000).
28. Newman, E. A. & Hartline, P. H. Integration of visual and infrared information in bimodal neurons in the rattlesnake optic tectum. *Science* **213**, 789–791 (1981).
29. Peck, C. K. Visual-auditory integration in cat superior colliculus: implications for neuronal control of the orienting response. *Prog Brain Res* **112**, 167–177 (1996).
30. Chudler, E. H., Sugiyama, K. & Dong, W. K. Multisensory convergence and integration in the neostriatum and globus pallidus of the rat. *Brain Res* **674**, 33–45 (1995).
31. Olcese, U., Iurilli, G. & Medini, P. Cellular and synaptic architecture of multisensory integration in the mouse neocortex. *Neuron* **79**, 579–593, https://doi.org/10.1016/j.neuron.2013.06.010 (2013).
32. Wallace, M. T., Meredith, M. A. & Stein, B. E. Multisensory integration in the superior colliculus of the alert cat. *J Neurophysiol* **80**, 1006–1010, https://doi.org/10.1152/jn.1998.80.2.1006 (1998).
33. Nagy, A., Eordegh, G., Paroczy, Z., Markus, Z. & Benedek, G. Multisensory integration in the basal ganglia. *Eur J Neurosci* **24**, 917–924, https://doi.org/10.1111/j.1460-9568.2006.04942.x (2006).
34. Reig, R. & Silberberg, G. Multisensory integration in the mouse striatum. *Neuron* **83**, 1200–1212, https://doi.org/10.1016/j.neuron.2014.07.033 (2014).
35. Minciacchi, D., Tassinari, G. & Antonini, A. Visual and somatosensory integration in the anterior ectosylvian cortex of the cat. *Brain Res* **410**, 21–31 (1987).
36. Lee, H., Stirnberg, R., Stocker, T. & Axmacher, N. Audiovisual integration supports face-name associative memory formation. *Cogn Neurosci* **8**, 177–192, https://doi.org/10.1080/17588928.2017.1327426 (2017).
37. Lanz, F., Moret, V., Rouiller, E. M. & Loquet, G. Multisensory Integration in Non-Human Primates during a Sensory-Motor Task. *Front Hum Neurosci* **7**, 799, https://doi.org/10.3389/fnhum.2013.00799 (2013).
38. Godfroy-Cooper, M., Sandor, P. M., Miller, J. D. & Welch, R. B. The interaction of vision and audition in two-dimensional space. *Front Neurosci* **9**, 311, https://doi.org/10.3389/fnins.2015.00311 (2015).
39. Puszta, A. *et al*. Cortical power-density changes of different frequency bands during a visually guided associative learning test: a human EEG-study. *Frontiers in human neuroscience* **12**, 188 (2018).
40. Quak, M., London, R. E. & Talsma, D. A multisensory perspective of working memory. *Frontiers in human neuroscience* **9**, 197 (2015).
41. Goolkasian, P. & Foos, P. W. Bimodal format effects in working memory. *The American journal of psychology*, 61–78 (2005).
42. Delogu, F., Raffone, A. & Belardinelli, M. O. Semantic encoding in working memory: Is there a (multi) modality effect? *Memory* **17**, 655–663 (2009).
43. Fougnie, D. & Marois, R. What limits working memory capacity? Evidence for modality-specific sources to the simultaneous storage of visual and auditory arrays. *Journal of Experimental Psychology: Learning, Memory, and Cognition* **37**, 1329 (2011).
44. Morey, C. C. & Cowan, N. When do visual and verbal memories conflict? The importance of working-memory load and retrieval. *Journal of Experimental Psychology: Learning, Memory, and Cognition* **31**, 703 (2005).
45. Calvert, G. A., Campbell, R. & Brammer, M. J. Evidence from functional magnetic resonance imaging of crossmodal binding in the human heteromodal cortex. *Current biology* **10**, 649–657 (2000).
46. Beauchamp, M. S., Lee, K. E., Argall, B. D. & Martin, A. Integration of auditory and visual information about objects in superior temporal sulcus. *Neuron* **41**, 809–823 (2004).
47. Giard, M. H. & Peronnet, F. Auditory-visual integration during multimodal object recognition in humans: a behavioral and electrophysiological study. *Journal of cognitive neuroscience* **11**, 473–490 (1999).
48. Myers, C. E. *et al*. Learning and generalization deficits in patients with memory impairments due to anterior communicating artery aneurysm rupture or hypoxic brain injury. *Neuropsychology* **22**, 681 (2008).
49. Hsieh, L. T. & Ranganath, C. Frontal midline theta oscillations during working memory maintenance and episodic encoding and retrieval. *Neuroimage* **85**(Pt 2), 721–729, https://doi.org/10.1016/j.neuroimage.2013.08.003 (2014).
50. Hsieh, L. T., Ekstrom, A. D. & Ranganath, C. Neural oscillations associated with item and temporal order maintenance in working memory. *J Neurosci* **31**, 10803–10810, https://doi.org/10.1523/JNEUROSCI.0828-11.2011 (2011).
51. Gevins, A., Smith, M. E., McEvoy, L. & Yu, D. High-resolution EEG mapping of cortical activation related to working memory: effects of task difficulty, type of processing, and practice. *Cereb Cortex* **7**, 374–385 (1997).
52. Roberts, B. M., Hsieh, L. T. & Ranganath, C. Oscillatory activity during maintenance of spatial and temporal information in working memory. *Neuropsychologia* **51**, 349–357, https://doi.org/10.1016/j.neuropsychologia.2012.10.009 (2013).
53. Liebe, S., Hoerzer, G. M., Logothetis, N. K. & Rainer, G. Theta coupling between V4 and prefrontal cortex predicts visual short-term memory performance. *Nature neuroscience* **15**, 456 (2012).
54. Lee, H., Simpson, G. V., Logothetis, N. K. & Rainer, G. Phase locking of single neuron activity to theta oscillations during working memory in monkey extrastriate visual cortex. *Neuron* **45**, 147–156 (2005).
55. Worden, M. S., Foxe, J. J., Wang, N. & Simpson, G. V. Anticipatory biasing of visuospatial attention indexed by retinotopically specific-band electroencephalography increases over occipital cortex. *J Neurosci* **20**, 1–6 (2000).

56. Ergenoglu, T. *et al*. Alpha rhythm of the EEG modulates visual detection performance in humans. *Cognitive Brain Research* **20**, 376–383 (2004).
57. Schaefer, R. S., Vlek, R. J. & Desain, P. Music perception and imagery in EEG: Alpha band effects of task and stimulus. *International Journal of Psychophysiology* **82**, 254–259 (2011).
58. Hanslmayr, S. *et al*. Prestimulus oscillations predict visual perception performance between and within subjects. *Neuroimage* **37**, 1465–1473 (2007).
59. Foxe, J. J. & Snyder, A. C. The role of alpha-band brain oscillations as a sensory suppression mechanism during selective attention. *Frontiers in psychology* **2**, 154 (2011).
60. Michels, L., Moazami-Goudarzi, M., Jeanmonod, D. & Sarnthein, J. EEG alpha distinguishes between cuneal and precuneal activation in working memory. *Neuroimage* **40**, 1296–1310 (2008).
61. Beck, M. H. *et al*. Short- and long-term dopamine depletion causes enhanced beta oscillations in the cortico-basal ganglia loop of parkinsonian rats. *Experimental neurology* **286**, 124–136, https://doi.org/10.1016/j.expneurol.2016.10.005 (2016).
62. Stein, E. & Bar-Gad, I. beta oscillations in the cortico-basal ganglia loop during parkinsonism. *Experimental neurology* **245**, 52–59, https://doi.org/10.1016/j.expneurol.2012.07.023 (2013).
63. Timmermann, L. & Fink, G. R. Pathological network activity in Parkinson's disease: from neural activity and connectivity to causality? *Brain: a journal of neurology* **134**, 332–334, https://doi.org/10.1093/brain/awq381 (2011).
64. Little, S. *et al*. Controlling Parkinson's disease with adaptive deep brain stimulation. *Journal of visualized experiments: JoVE*, https://doi.org/10.3791/51403 (2014).
65. Chen, C. C. *et al*. Stimulation of the subthalamic region at 20 Hz slows the development of grip force in Parkinson's disease. *Experimental neurology* **231**, 91–96, https://doi.org/10.1016/j.expneurol.2011.05.018 (2011).
66. Doya, K. Complementary roles of basal ganglia and cerebellum in learning and motor control. *Current opinion in neurobiology* **10**, 732–739 (2000).
67. Graybiel, A. M. The basal ganglia: learning new tricks and loving it. *Current opinion in neurobiology* **15**, 638–644 (2005).
68. Howard, M. W. *et al*. Gamma oscillations correlate with working memory load in humans. *Cerebral cortex* **13**, 1369–1374 (2003).
69. Ossandón, T. *et al*. Transient Suppression of Broadband Gamma Power in the Default-Mode Network Is Correlated with Task Complexity and Subject Performance. *The Journal of Neuroscience* **31**, 14521–14530, https://doi.org/10.1523/jneurosci.2483-11.2011 (2011).
70. Chalk, M. *et al*. Attention Reduces Stimulus-Driven Gamma Frequency Oscillations and Spike Field Coherence in V1. *Neuron* **66**, 114–125, https://doi.org/10.1016/j.neuron.2010.03.013 (2010).
71. Myers, C. E. *et al*. Dissociating hippocampal versus basal ganglia contributions to learning and transfer. *J Cogn Neurosci* **15**, 185–193, https://doi.org/10.1162/089892903321208123 (2003).
72. Moustafa, A. A., Myers, C. E. & Gluck, M. A. A neurocomputational model of classical conditioning phenomena: a putative role for the hippocampal region in associative learning. *Brain Res* **1276**, 180–195, https://doi.org/10.1016/j.brainres.2009.04.020 (2009).
73. Smith, Y., Surmeier, D. J., Redgrave, P. & Kimura, M. Thalamic contributions to basal ganglia-related behavioral switching and reinforcement. *Journal of Neuroscience* **31**, 16102–16106 (2011).
74. Koelewijn, T., Bronkhorst, A. & Theeuwes, J. Attention and the multiple stages of multisensory integration: A review of audiovisual studies. *Acta Psychol (Amst)* **134**, 372–384, https://doi.org/10.1016/j.actpsy.2010.03.010 (2010).
75. Delorme, A. & Makeig, S. EEGLAB: an open source toolbox for analysis of single-trial EEG dynamics including independent component analysis. *Journal of neuroscience methods* **134**, 9–21 (2004).
76. Perrin, F., Pernier, J., Bertrand, O. & Echallier, J. Spherical splines for scalp potential and current density mapping. *Electroencephalography and clinical neurophysiology* **72**, 184–187 (1989).
77. Cohen, M. X. *Analyzing neural time series data: theory and practice*. (MIT press, 2014).
78. Parks, N. A., Gannon, M. A., Long, S. M. & Young, M. E. Bootstrap signal-to-noise confidence intervals: an objective method for subject exclusion and quality control in ERP studies. *Frontiers in human neuroscience* **10**, 50 (2016).
79. Ing, A. & Schwarzbauer, C. Cluster size statistic and cluster mass statistic: Two novel methods for identifying changes in functional connectivity between groups or conditions. *PloS one* **9**, e98697 (2014).
80. Puszta, A. *et al*. Cortical Power-Density Changes of Different Frequency Bands in Visually Guided Associative Learning: A Human EEG-Study. *Frontiers in human neuroscience* **12**, 188, https://doi.org/10.3389/fnhum.2018.00188 (2018).
81. Cohen, M. X. Assessing transient cross-frequency coupling in EEG data. *Journal of neuroscience methods* **168**, 494–499 (2008).

Acknowledgements

The authors thank to Nóra Cserháti for her help during data collection and all the participants for engaging in the research. This work was supported by Hungarian Brain Research Program Grant KTIA_13_NAP-A-I/15 and SZTE ÁOK-KKA Grant No: 2019/270-62-2.

Author Contributions

A.Pu., B.B., E.G. and A.N. designed the study. A.Pu., D.Ny., Zs.G., X.K., B.B. performed the assessment and documented the findings; A.Pu. analyzed the data; A.Pu., A.Pe. and A.N. organized the study and wrote the manuscript.

Additional Information

Supplementary information accompanies this paper at https://doi.org/10.1038/s41598-019-45978-3.

Competing Interests: The authors declare no competing interests.

Publisher's note: Springer Nature remains neutral with regard to jurisdictional claims in published maps and institutional affiliations.

II

Puszta, A., Katona, X., Bodosi, B., Pertich, Á., Nyujtó, D., Braunitzer, G., & Nagy, A. (2018). Cortical power-density changes of different frequency bands during a visually guided associative learning test: a human EEG-study. *Frontiers in human neuroscience, 12,* 188.

frontiers in Human Neuroscience

ORIGINAL RESEARCH
published: 08 May 2018
doi: 10.3389/fnhum.2018.00188

Cortical Power-Density Changes of Different Frequency Bands in Visually Guided Associative Learning: A Human EEG-Study

*András Puszta[1], Xénia Katona[1], Balázs Bodosi[1], Ákos Pertich[1], Diána Nyujtó[1], Gábor Braunitzer[2] and Attila Nagy[1]**

[1]Sensorimotor Lab, Department of Physiology, Faculty of Medicine, University of Szeged, Szeged, Hungary, [2]Laboratory for Perception & Cognition and Clinical Neuroscience (LPCCN), National Institute of Psychiatry and Addictions at Nyírő Gyula Hospital, Budapest, Hungary

The computer-based Rutgers Acquired Equivalence test (RAET) is a widely used paradigm to test the function of subcortical structures in visual associative learning. The test consists of an acquisition (pair learning) and a test (rule transfer) phase, associated with the function of the basal ganglia and the hippocampi, respectively. Obviously, such a complex task also requires cortical involvement. To investigate the activity of different cortical areas during this test, 64-channel EEG recordings were recorded in 24 healthy volunteers. Fast-Fourier and Morlet wavelet convolution analyses were performed on the recordings. The most robust power changes were observed in the theta (4–7 Hz) and gamma (>30 Hz) frequency bands, in which significant power elevation was observed in the vast majority of the subjects, over the parieto-occipital and temporo-parietal areas during the acquisition phase. The involvement of the frontal areas in the acquisition phase was remarkably weaker. No remarkable cortical power elevations were found in the test phase. In fact, the power of the alpha and beta bands was significantly decreased over the parietooccipital areas. We conclude that the initial acquisition of the image pairs requires strong cortical involvement, but once the pairs have been learned, neither retrieval nor generalization requires strong cortical contribution.

Keywords: EEG, acquired equivalence, associative learning, FFT, time-frequency analysis

OPEN ACCESS

Edited by:
Camillo Porcaro, Istituto di Scienze e Tecnologie della Cognizione (ISTC)—CNR, Italy

Reviewed by:
Antonio Ivano Triggiani, University of Foggia, Italy
Quanying Liu, California Institute of Technology, United States
Giovanni Pellegrino, IRCCS Fondazione Ospedale San Camillo, Italy

****Correspondence:***
Attila Nagy
nagy.attila.1@med.u-szeged.hu

Received: *06 November 2017*
Accepted: *18 April 2018*
Published: *08 May 2018*

Citation:
Puszta A, Katona X, Bodosi B, Pertich À, Nyujtó D, Braunitzer G and Nagy A (2018) Cortical Power-Density Changes of Different Frequency Bands in Visually Guided Associative Learning: A Human EEG-Study. Front. Hum. Neurosci. 12:188. doi: 10.3389/fnhum.2018.00188

INTRODUCTION

Associative learning is a basic cognitive function, through which discrete and often strongly different ideas and percepts are linked together. This type of learning is responsible for classical conditioning (Ito et al., 2008), as well as weather-prediction (Gluck et al., 2002), latent inhibition (Weiss and Brown, 1974) and sensory preconditioning (Rescorla, 1980). Visual equivalence learning is a special kind of associative learning, which can be tested with the Rutgers Acquired Equivalence Test (RAET, Myers et al., 2003). The RAET can be divided into two main phases. The first one of these is the acquisition phase where the subjects learn to associate two different visual stimuli. The participants' task throughout the whole test is to indicate their choice by pressing one of two

Abbreviations: CMW, Complex Morlet Wavelet convolution; FFT, Fast Fourier Transform; RAET, Rutgers acquired equivalence test.

marked keyboard buttons. During the acquisition phase, the computer provides feedback about the correctness of the responses. When this phase is over, the test phase follows. In this phase, both the previously learned stimulus pairs (retrieval) and hitherto not seen but predictable associations (generalization or transfer) are presented. The subjects get no feedback about the correctness of their responses in the test phase (**Figure 1**).

Optimal performance in the acquisition phase appears to depend mainly on the integrity of the basal ganglia, whereas the test phase performance (both retrieval and generalization) has been linked to the integrity of the hippocampal region (Myers et al., 2003; Moustafa et al., 2009). Clinical studies corroborate this. Patients with Alzheimer's and schizophrenia, characterized by hippocampal functional deficit (Seab et al., 1988; Altshuler et al., 1998) showed intact acquisition but poor retrieval and generalization as compared to healthy controls (Bódi et al., 2009; Weiler et al., 2009). On the other hand, patients with Parkinson's, affecting primarily the basal ganglia (Montgomery, 2009), performed poorly in the acquisition phase. However, if they managed to pass it, their retrieval and transfer performance was comparable to controls (Myers et al., 2003; Ventre-Dominey et al., 2016). In a recent study of ours, we demonstrated altered performance in migraine in both the acquisition and test phases of RAET, pointing to suboptimal functioning of the basal ganglia in migraine (Öze et al., 2017).

As previous investigations emphasized the role of the hippocampus and the basal ganglia during the test, (Moustafa et al., 2010) information is lacking about the cortical areas involved in RAET in healthy humans. Earlier studies indicated that increased gamma band phase coherence over parieto-occipital areas is important during associative learning (Miltner et al., 1999; Gruber et al., 2001), and that frontal midline theta power elevation is related to working memory maintenance and retrieval (Hsieh and Ranganath, 2014; Kardos et al., 2014). In a test where the subjects had to learn categories, the contribution of the prefrontal associative cortex was demonstrated (Helie et al., 2015), but hitherto the cortical contribution to acquired equivalence learning has not been studied.

In this study, we sought to investigate what cortical areas are activated during the individual phases of RAET by means of multichannel EEG recordings in healthy human subjects. We hypothesized that activation would be seen in the associative cortices (i.e., the prefrontal and parieto-temporo-occipital regions) that serve as the cortical input to the cognitive loops of the basal ganglia (Shepherd, 2003). Specifically, we hypothesized that different activation patterns would be seen in the different phases of the paradigm, as what we know so far is that the different phases are related to different subcortical structures, which suggests different cortical input sources.

MATERIALS AND METHODS

Participants

EEG data of 30 healthy young adults were recorded. The data of six participants were excluded because of bad signal quality. Thus, we present the results of 24 participants (14 females, 10 males, mean age: 26 $\pm$ 5.28 years). The participants were free of any ophthalmological or neurological conditions. The participants were recruited on a voluntary basis from our university. The potential subjects were informed about the background and goals of the study, as well as about the procedures involved. It was also emphasized that given the lack of compensation or any direct benefit, the participants were free to quit at any time and without any consequence (no one did so). This study was carried out in accordance with the recommendations of the Guideline for non-invasive investigations involving healthy human volunteers, of the Medical Ethics Committee of the University of Szeged, with written informed consent from all subjects and also in accordance with the Declaration of Helsinki. The protocol was approved by the Medical Ethics Committee of the University of Szeged Hungary. The datasets generated and analyzed during the current study are available from the corresponding author on request.

The Instrument

The testing software (described in Myers et al., 2003 and originally written for iOS) was adapted to Windows and translated into Hungarian in Assembly for Windows, with the written permission of the copyright holder. The paradigm was also slightly modified to make getting through its acquisition phase by mere guessing less probable (see below). The tests were run on a PC. The stimuli were displayed on a standard 17″ CRT monitor (refresh rate 60 Hz) in a quiet room separated from the recording room by a semi-transparent mirror. Participants sat at a 114-cm distance from the monitor. One participant was tested at a time and no time limit was set. The test was structured as follows: On each trial of the task, participants saw a face and a pair of fish (where each member of the pair had different color), and had to learn through trial and error which fish was associated with which face (**Figure 1**).

There were four faces (A1, A2, B1, B2) and four possible fish (X1, X2, Y1, Y2), referred to as antecedents and consequents, respectively. In the initial (acquisition) stages, the participants were expected to learn that when A1 or A2 appeared, the correct answer was to choose fish X1 over fish Y1; given face B1 or B2, the correct answer was to choose fish Y1 over fish X1. In that context, if the associations are successfully learned, participants also learn that face A1 and A2 are equivalent with respect to the associated fish (faces B1 and B2 likewise). Next, participants learned a new set of pairs: given face A1, they had to choose fish X2 over Y2, and given face B1, fish Y2 over X2. This was the end of the acquisition phase. Until this point, the computer had provided feedback about the correctness of the choices, and six of the possible eight fish-face combinations had been taught to the participants. In the following phase (the test phase), no feedback was provided anymore, but beside the already acquired six pairs (retrieval testing) the hitherto not shown last two pairs were also shown (generalization testing). Having learned that faces A1 and A2 are equivalent, participants may generalize from learning that if

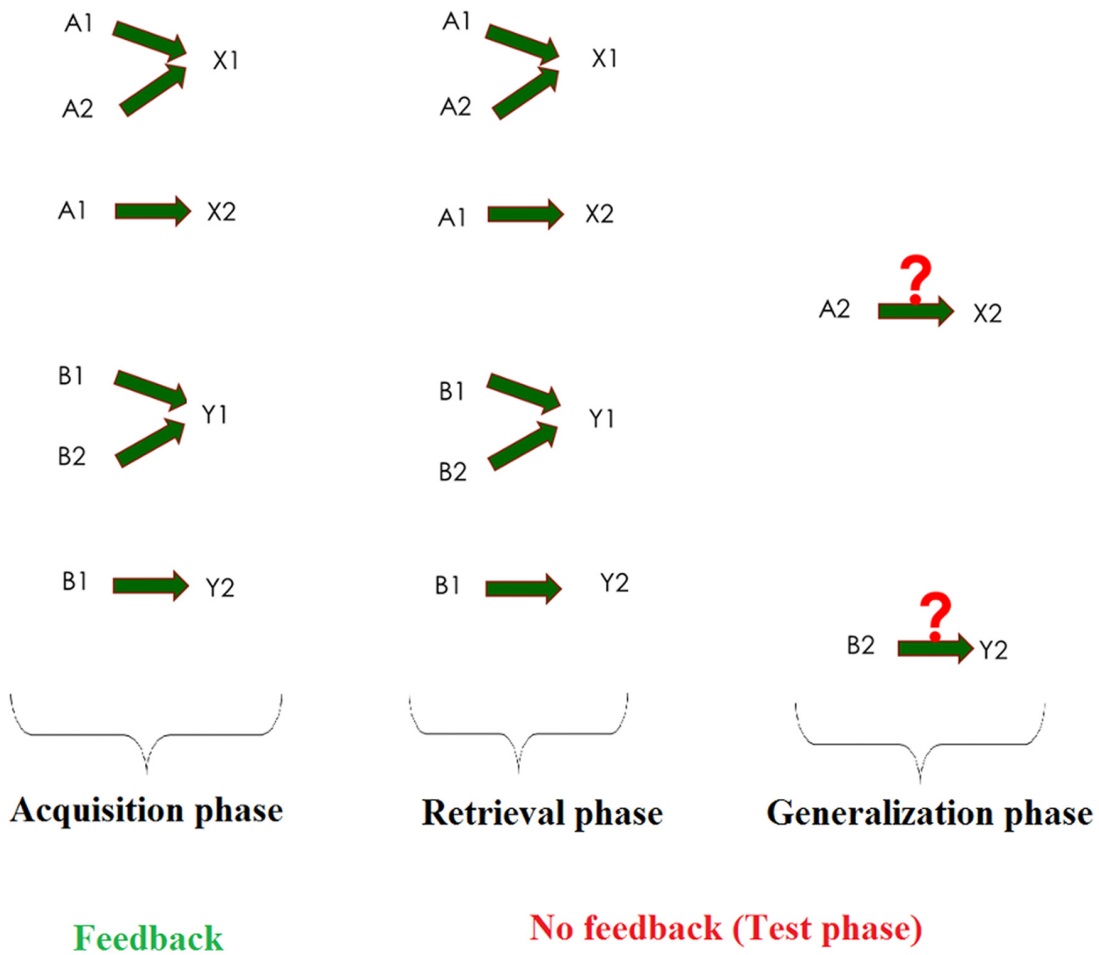

FIGURE 1 | Summary of the acquired equivalence task. The task consists of three phases: acquisition, retrieval and generalization. In the acquisition phase, the subject has to learn three image pairs (one fish and one face make a pair) out of four pairs, one by one, through trial-and-error learning with feedback. Then, in the test phases, the subject will get no feedback, and, beyond the already learned three pairs (retrieval), a new, previously not taught but predictable pair is also presented (generalization).

A1 goes with X2, A2 also goes with X2; the same holds true for B2 (equivalent to B1) and Y2 (associated with B1). While the formal description may make the impression that the task is a difficult one, in fact, healthy children (Goyos, 2000) and also mentally retarded individuals (de Rose et al., 1988; Dube et al., 1989) reliably make this kind of generalization. During the acquisition stages, new associations were introduced one by one, mixed with trials of previously learned associations. To be allowed to proceed, the subjects had to reach a predefined number of consecutive correct responses after the presentation of each new association (four after the presentation of the first association, and 4, 6, 8, 10, 12 with the introduction of each new association, respectively). This meant an elevated number of the required consecutive correct responses compared to the original paradigm, which made getting through the acquisition phase by mere guessing less probable. Similarly, in the test phase there were 48 trials (12 trials of new and 36 trials of previously learned associations), as opposed to the 16 trials of the original paradigm.

Data Acquisition

Sixty-four channel EEG recordings were made. Data were acquired in Actiview, via the ActiveTwo AD-box with 64 active electrodes (Biosemi B.V., Netherlands). The signal of each electrode was referenced to the algebraic sum of the electric signals recorded by five scalp electrodes given by the manufacturer (FPz, T7, Cz, T8, Oz). The sampling rate was 2048 Hz. The impedance of the electrodes was consistently below 5 kΩ. Raw signals were recorded on the stimulating computer. The stimulating software generated trigger signals (TTL pulses) to indicate the beginning of each trial. These trigger signals were recorded on an additional (65th) channel. To obtain baseline activity, 1-min-long resting state activities were recorded before and after stimulus presentation.

Data Analysis

The psychophysical data were analyzed in three groups: data from the acquisition phase, data from the retrieval part of the test phase (i.e., when the participant was presented with already learned associations) and data from the generalization part of the test phase (i.e., when the participant was presented with previously not learned associations). The number of correct and wrong responses were calculated in all phases, as well as the ratio of these to the total number of trials during the respective phase (**Figure 2**). The number of trials necessary for the completion of the acquisition phase was also recorded.

Preprocessing

After visual inspection to confirm that the signal-to-noise ratio was acceptable, the raw EEG data were first exported to a .mat file using Spike2 (CED). This was followed by high-pass filtering (>2 Hz, FIR filter). The signal of each channel was referenced to the average signal of all channels. All trials were visually inspected and those containing EMG or other artifacts not related to blinks were manually removed. The removal of blink/oculomotor artifacts was based on independent components analysis performed in the Eeglab toolbox for Matlab (Delorme and Makeig, 2004). The Eeglab toolbox was also used to interpolate noisy channels. Then we used Laplacian to improve the spatial resolution of the recording (Perrin et al., 1989). Finally, the trials were sorted by the phases of the psychophysical paradigm (acquisition, retrieval and generalization), based on the trigger signals and on the event file generated by the stimulating software.

Fast Fourier Transformation

The majority of the trials were somewhat longer than 1 s. To avoid mismatch on summation, the first second of each trial (2048 data points) was analyzed. If the trial was shorter than 1 s (data points <2048), the trial was not analyzed to avoid zero-padding artifacts during the Fast Fourier Transform (FFT). The baseline periods (1 min) were divided into 1-s-long (2048 data points) epochs. After these pre-processing steps, FFT was performed on all trials in each phase, and for every channel. To give an example, in the acquisition phase the power spectra were whitened and normalized to baseline as follows:

$$N_{fr} = 100 + 100 * \left(\prod_{i=1}^{n} PA_{fr_i} - \prod_{i=1}^{n} PB_{fr_i} \right) \Big/ \prod_{i=1}^{n} PB_{fr_i}$$

where N is the normalized power density of a given fr frequency band for a given channel, PA is the whitened power density in the acquisition phase's given i trial within the same channel and same fr frequency, and PB is the whitened power density during baseline activity. Note that both for PB and PA, the letter n indicates the number of trials within the phase that was compared to the baseline (in this case the acquisition phase). As the baseline activity was longer than the compared periods (i.e., the signal belonging to a given phase), the baseline activity was cropped to match the given phase by cutting 1-s-long periods randomly.

After the FFT, the nonparametric permutation test was utilized to compare power spectra among the different phases of the behavioral task, in the following frequency bands: delta (1–4 Hz), theta (4–8 Hz), alpha (9–14 Hz), beta (15–31 Hz) and gamma (32–70 Hz). The following comparisons were made: baseline-acquisition phase, baseline-retrieval phase and baseline-generalization phase, learning phase-retrieval phase, learning phase–generalization phase, retrieval phase–generalization phase. Statistically significant differences were tested based on nonparametric permutation testing and correction for multiple comparisons at the minimum-maximum point of the null-hypothesis distribution.

The data set for the global band was generated by iteratively calculating the mean difference of randomized permutation of the power values of a particular channel in a given frequency band in two different phases of the paradigm. The Z-scores for each channel were then calculated between the distributions derived from the global band and the mean difference of the power values in a given frequency band between the two different analyzed phases. Z-scores were corrected by the minimum and maximum point of the null hypothesis distribution, also known as cluster mass statistics (Ing and Schwarzbauer, 2014). Group-level analysis of the FFT was carried out in the same way as in the individual analysis described above, with the difference that the random permutation was performed across the mean power values of the subjects and not across the power value of each individual trial.

For the FFT topographical plots, we used the "*topoplot*" function of EEGlab (Delorme and Makeig, 2004).

Morlet Wavelet Convolution

Time-frequency analysis was performed using continuous Morlet Wavelet Convolution (CMW) via FFT algorithm (Cohen, 2014). The convolution was decomposed into different steps. First, we performed FFT on one selected channel of the raw data. Then, we created complex Morlet wavelets for each frequency (1–70 Hz) on which we executed the FFT. After that, we calculated the dot product of the given channel's FFTs and the FFTs of the complex Morlet wavelets at each individual frequency, which yielded 70 complex numbers. An inverse FFT of the dot product results was utilized to show power alterations in the time domain as follows:

$$K_x = IFFT\left(fft(C) \cdot fft(W_x)\right)$$

where the K is the time-series of the given channel, wavelet-filtered to x-frequency, C is the time series of all trials of different phases, and W is the complex Morlet wavelet at a given $\times$ frequency. To avoid the edge-artifacts of the Morlet wavelet convolution, the raw data was multiplied five times before the convolution, yielding a two-series-long buffer zone at the beginning and the end of the time-series, which were cut out after the time-frequency analysis. After that, the data were cut according to the different phases of the paradigm (baseline, acquisition, retrieval, generalization). The data set for the global band was generated by iteratively calculating the mean difference of randomized permutation of the power values of a particular channel in a given frequency band in two different phases of the paradigm. The Z-scores for each channel were then calculated between the distributions derived from the global

band and the mean difference of the power values in a given frequency band between the two different analyzed phases. *Z*-scores were corrected by the minimum and maximum point of the null hypothesis distribution. See individual time-frequency plots in Supplementary Figure S1. Group-level analysis of the CMW was carried out in the same way as in the individual analysis described above, with the difference that the random permutation was performed across the mean power values of the subjects and not across the power value of each individual trial. These procedures are shown in detail in the Supplementary Material (Supplementary Figure S2).

Correlation Between Performance in the Psychophysical Test and Power Density Changes

Correlation between individual performance and power density changes in a given channel and frequency band was also calculated in each phase of the paradigm. Performance was defined as the ratio of the successful trials to all trials. Individual power changes were expressed as the individual *Z*-scores between the baseline activity's power density and the given phase's power density in a given channel in a given frequency band. Pearson correlation coefficients were calculated using the "*corr*" function of Matlab. The *t*-score for each correlation coefficient was calculated as follows:

$$t_{ch,fr} = r_{ch,fr} * \sqrt{\frac{n-2}{1-r_{ch,fr}^2}}$$

where r is the correlation coefficient in channel ch and fr frequency band, n is the number of samples (in this case it was 24), and the t is the calculated t-value in given channel and frequency band. T-values whose absolute value were smaller than 2.819 (which is the critical t-value if the degree of freedom is 22 and the significance level is 0.01) were set to 0. The corrected t-values in different frequency bands in each phase of the paradigm were plotted to a topographical map using EEGLab "*topoplot*" function.

Data Visualization

The electrophysiological results are presented below for each phase of the paradigm (Acquisition, Retrieval and Generalization) and for the four different frequency bands (theta (4–8 Hz), alpha (9–14 Hz), beta 15–31 Hz), and gamma (32–70 Hz). The results of FFT and CMW are shown at the population level, where each phase of the paradigm (acquisition, retrieval and generalization) are compared to the baseline activity. As our research is more exploratory than hypothesis-driven we will not discuss the statistical *p*-values in detail, but we do discuss the significant *z*-score maps of the group-level statistic of the FFT and CMW. Time-frequency plots of the channels where the FFT results showed significant changes are presented for each phase of the paradigm. Examples for individual time-frequency plots can be found in the Supplementary Material (Supplementary Figure S1). The correlation between performance in the psychophysical test and cortical power changes (rho values) for each frequency band are plotted in topographical figures. See corresponding **Figures 3–6** for electrophysiological results in each frequency band.

RESULTS

The data of 24 participants were analyzed. The participants accomplished the acquisition phase in a mean of 55 trials (SD ± 6.93, Range: 44–73). The mean number of failed trials in the acquisition phase was 4.43 (SD ± 2.67, Range: 0–32), in the retrieval phase 4.69 (SD ± 5.96, Range: 0–24), and 2.87 in the generalization phase (SD ± 4.18, Range: 0–12). The means of the error ratios in the different phases were the following: in the acquisition phase 0.08 (SD ± 0.036; Range: 0–0.14), in the retrieval phase: 0.15 (SD ± 0.17, Range: 0–0.65), and in the generalization phase 0.31 (SD ± 0.38, Range: 0–1) (**Figure 2**).

Acquisition Phase

Power Density Changes

Theta Band (4–8 Hz)

The group-level analysis revealed significant power-elevation in parietooccipital-occipital areas as well as in the frontal areas.

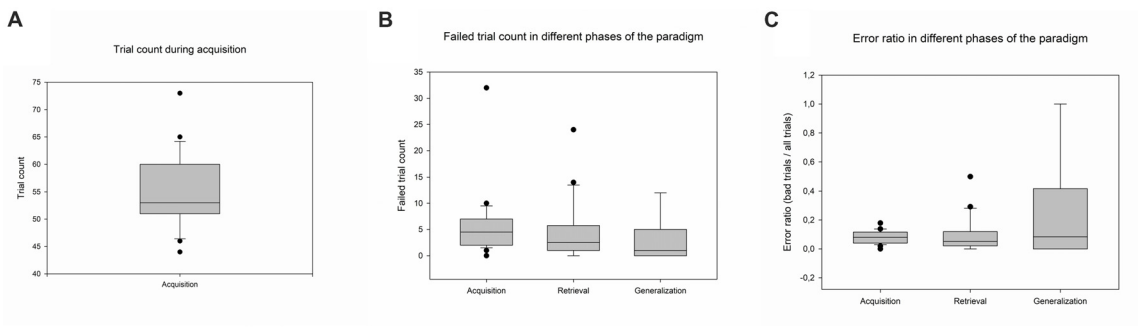

FIGURE 2 | Psychophysical results. Panel **(A)** denotes the number of trials in the acquisition phase. Panel **(B)** shows the number of failed trials in different phases of the paradigm, and Panel **(C)** shows the error ratio during all three phases of the paradigm. The lower margin of the boxes indicates the 25th percentile, the line within the boxes marks the median, and the upper margin of the box indicates the 75th percentile. Whiskers (error bars) above and below the box indicate the 90th and 10th percentiles.

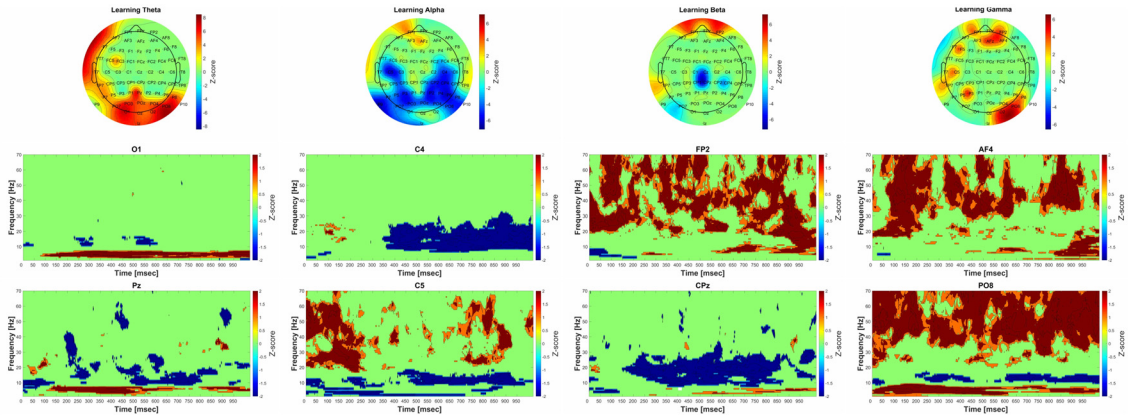

FIGURE 3 | Significant group-level changes in the power of the different frequency bands during acquisition. The power of the investigated four frequency bands (theta, alpha, beta, gamma) during acquisition were compared to the baseline activity using nonparametric permutation test with correction for multiple comparisons at the minimum-maximum point of the null-hypothesis distribution. The upper part of the figure shows the Fast Fourier Transform (FFT) results of the 64 channel EEG recordings in topographic representation in different frequency band during acquisition, while the lower part of the figure corresponds to the group-level time-frequency results in different channels (O1, C4, FP2, AF4, Pz C5, CPz, PO8, respectively). The color scales beside the upper three panels indicate the *z*-score values, obtained by calculating cluster-mass statistics in individual power changes between acquisition and baseline activity. The red color indicates significant power-increase and the blue color represents significant power-decrease compared to baseline. The *z*-scores threshold was set to 1.645 (which is equal to the 0.05 *p*-value).

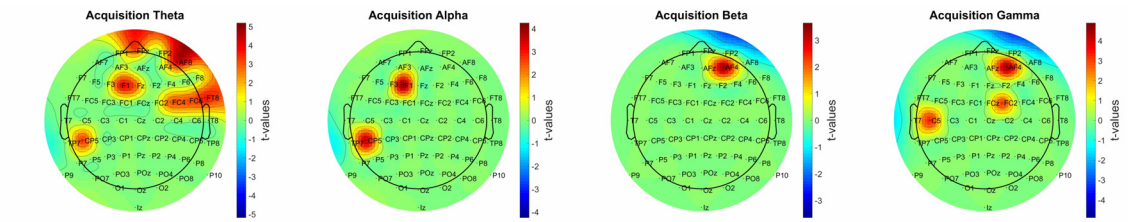

FIGURE 4 | Significant power-performance correlation during acquisition in different frequency bands. The corrected *t*-values in different frequency bands were plotted to a topographical map using EEGLab "*topoplot*" function.

The time-frequency results indicate that the power elevation in the occipital and parietooccipital areas started earlier (around 75 ms after the beginning of the trial), than over the frontal areas (around 550 ms after the beginning of the trial).

Alpha Band (9–14 Hz)

A significant decrease in power could be observed during acquisition compared to baseline over the parietal, parietooccipital and temporal areas. The time-frequency results show that the power decrement was phasically present over the parietooccipital areas, and over the temporal-central areas it started around 300 ms after the beginning of the trial.

Beta Band (15–30 Hz)

A significant decrement of power was found during acquisition compared to baseline over the central areas. A significant increase of power was also found over frontal areas. The Morlet wavelet convolution showed that the frontal power increase occurred phasically, and the power decrease—along with the changes in the alpha frequency band—started around 300 ms after the beginning of the trial.

Gamma Band: (31–70 Hz)

The group-level analysis revealed significant power-elevation over the frontal, parietooccipital, and temporal areas. The results of the time-frequency analysis indicate that the power increase over the parietooccipital areas began immediately after the beginning of the trial and 50 ms later over the frontal areas.

Power-Performance Correlation

Significant correlation was found over the frontal and temporal areas in all frequency bands (**Figure 4**). The most prominent changes occurred in the theta and gamma frequency bands, while in the beta frequency band the correlation was limited to channel AF4.

Retrieval Phase

Power Density Changes

Theta Band (4–8 Hz)

The group-level analysis revealed significant power elevation over the parietooccipital and occipital and frontal areas. The time-frequency results indicate that the power elevation

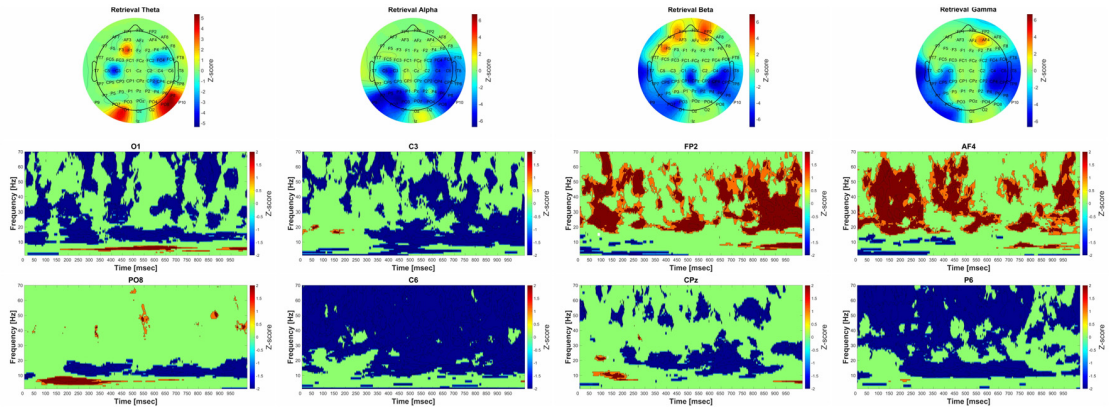

FIGURE 5 | Significant group-level changes in the power of the different frequency bands during retrieval. The power of the investigated four frequency bands (theta, alpha, beta, gamma) during retrieval were compared to the baseline activity using nonparametric permutation test with correction for multiple comparisons at the minimum-maximum point of the null-hypothesis distribution. The upper part of the figure shows the FFT results of the 64 channel EEG recordings in topographic representation in different frequency band during retrieval, while the lower part of the figure corresponds to the group-level time-frequency results in different channels (O1, C3, FP2, AF4, PO8 C6, CPz, P6, respectively). The color scales beside the upper three panels indicate the *z*-score values, obtained by calculating cluster-mass statistics in individual power changes between retrieval and baseline activity. The red color indicates significant power-increase and the blue color represents significant power-decrease compared to baseline. The *z*-scores threshold was set to 1.645 (which is equal to the 0.05 *p*-value).

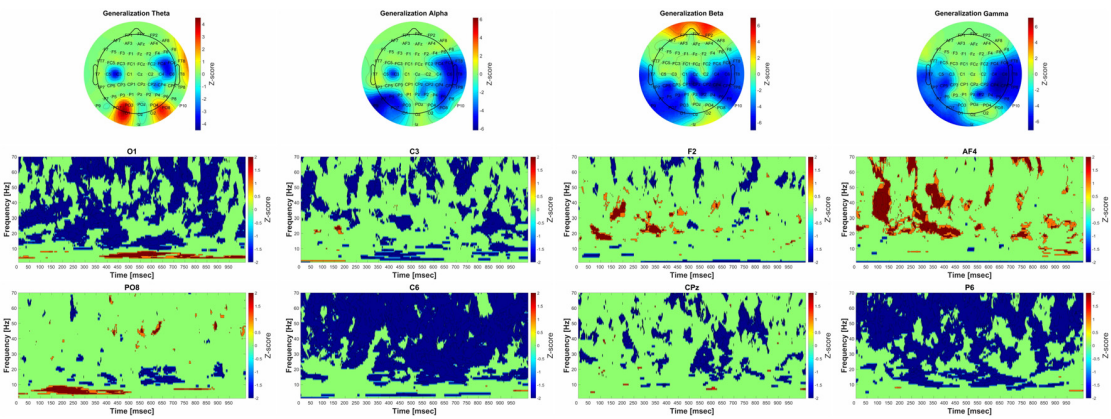

FIGURE 6 | Significant group-level changes in the power of the different frequency bands during generalization. The power of the investigated four frequency bands (theta, alpha, beta, gamma) during generalization were compared to the baseline activity using nonparametric permutation test with correction for multiple comparisons at the minimum-maximum point of the null-hypothesis distribution. The upper part of the figure shows the FFT results of the 64 channel EEG recordings in topographic representation in different frequency band during generalization, while the lower part of the figure corresponds to the group-level time-frequency results in different channels (O1, C3, F2, AF4, PO8 C6, CPz, P6, respectively). The color scales beside the upper three panels indicate the *z*-score values, obtained by calculating cluster-mass statistics in individual power changes between generalization and baseline activity. The red color indicates significant power-increase and the blue color represents significant power-decrease compared to baseline. The *z*-scores threshold was set to 1.645 (which is equal to the 0.05 *p*-value).

over the occipital and parietooccipital areas started earlier (around 75 ms after the beginning of the trial) than over the frontal areas (around 700 ms after the beginning of the trial).

Alpha Band (9–14 Hz)

Significant power decrease could be observed compared to baseline over the parietal, parietooccipital and temporal areas. The results of the time-frequency analysis show that the power decrement was phasically present over the parietooccipital areas, while over the temporal-central areas it started around 300 ms after the beginning of the trial.

Beta Band (15–30 Hz)

There was a significant power decrease over the parietooccipital, temporal and central areas during retrieval phase compared to baseline. Significant power increase was also found over the frontal areas. CMW showed that the frontal power increase occurred phasically, and the power decrease—similarly to the changes in the alpha frequency band—started around 300 ms after the beginning of the trial.

Gamma Band: (31–70 Hz)

The group-level analysis revealed significant power decrease over the parietooccipital and temporal areas. Significant

power increase was also found over the frontal areas. The time-frequency analysis revealed that the power changes occurred over the parietooccipital areas immediately after the stimulus onset, while over the frontal areas they began 50 ms after the beginning of the trial.

Power-Performance Correlation

The correlation between the performance and the power changes was not significant in either frequency band or channel.

Generalization Phase

Power Density Changes

Theta Band (4–8 Hz)

The group-level analysis revealed significant power elevation over the parietooccipital and occipital areas, and power decrease over the temporal areas. The time-frequency analysis showed that the power elevation over the occipital and parietooccipital areas started earlier (around 75 ms after the beginning of the trial) than the central-temporal power decrease (around 300 ms after the beginning of the trial).

Alpha Band (9–14 Hz)

Significant power decrease could be observed compared to baseline over the parietal, parietooccipital and temporal areas. The time-frequency results show that the power decrement was phasically present over the parietooccipital areas, and over the temporal-central areas it started around 300 ms after the beginning of the trial.

Beta Band (15–30 Hz)

A significant power decrease compared to baseline was observed over the parietooccipital, temporal and central areas. Significant power increase was found over the frontal areas. CMW showed that the frontal power increase occurred phasically, and the power decrease—along with the changes in alpha frequency band—started around 300 ms after the beginning of the trial.

Gamma Band: (31–70 Hz)

The group-level analysis revealed significant power decrease over the parietooccipital and temporal areas. The results of the time-frequency analysis indicate that the power changes occurred over the parietooccipital areas immediately after stimulus onset, while over the frontal areas they started 50 ms after the beginning of the trial.

Power-Performance Correlation

No significant correlations were found in either frequency band or channel.

DISCUSSION

In the present study we analyzed the psychophysical performance and EEG data of 24 healthy young volunteers in a visual associative learning test. As for the behavioral performance in the psychophysical paradigm, the results were comparable to the findings of other studies using the same paradigm in adult healthy volunteers (Öze et al., 2017). Behavioral performance in this paradigm was widely investigated in healthy volunteers and patients with psychiatric and neurological disorders (Myers et al., 2008; Vadhan et al., 2008; Meeter et al., 2009; Simon and Gluck, 2013; Kostek et al., 2014). However, to our knowledge, no study so far has attempted to investigate cortical activity associated with behavioral performance.

Despite the considerable individual variability in the changes of the power spectra, characteristic patterns of power change could be identified over different cortical areas as related to the different phases of the paradigm at the population level. Correct and missed trials could not be compared, though, because of the low number of missed trials. Subtraction of the EEG signal recorded during the missed trials from all trials left the activation patterns virtually unchanged, so we decided to analyze and present both types of trials together.

In the acquisition phase, markedly increased population-level activity could be observed over the parieto-temporo-occipital areas, and somewhat weaker increase over the frontal associative areas in the theta (4–7 Hz) and the gamma frequency bands (over 30 Hz). Such a strong power increase was not found in the retrieval and generalization phases of the task. In those phases, power decrement was the dominant tendency over the same areas. That tendency was obvious not only in the alpha and beta frequency bands, but also in the gamma frequency band.

The detailed mathematical analysis showed the most robust power increment in the gamma frequency band (>30 Hz) in the parietal, parietooccipital and temporoparietal channels during the acquisition phase in most of the participants. These channels correspond to the associative cortical areas, which were mainly suppressed during the retrieval and generalization phases. The most noteworthy finding of this study is the strong difference in the power density changes between the acquisition and the test phases (i.e., retrieval and the generalization) in the gamma band. Furthermore, the frontal and prefrontal associative cortices showed activity increment in the gamma band in the acquisition phase too, and weak power elevation was found in the test phase. The strong increment in the power of the gamma band over the parieto-temporo occipital associative cortex suggests a critical role of this region in the studied task. These cortical structures, together with the connected basal ganglia (Postuma and Dagher, 2006) could be necessary for this kind of equivalence learning (Middleton and Strick, 2000; Yin and Knowlton, 2006). Nos such increment was detectable in the gamma band in the retrieval and the generalization phases. The explanation of this could be that the successfully learned associations had already been transmitted to the hippocampus, and the utilization of these does not require strong cortical contribution. Hamamé et al. (2014), applying a visual naming model in humans, found robust activity increment in the high gamma frequency band in the left hippocampus, 500 ms post-stimulus. Although the model tests long-term memory retrieval rather than associative retrieval, their findings correlate well with psychophysical (Gluck et al., 2003; Myers et al., 2003) and electrophysiological studies in primates regarding associative retrieval (Brincat and Miller, 2015). As high gamma activity can be regarded as an indicator of multi-unit spiking activity (Le Van Quyen et al., 2010), we assume that acquired equivalence learning requires cortical activation,

whereas retrieval and generalization do not. In a similar test, where the task was category learning, marked contribution of the prefrontal associative cortex was demonstrated in the acquisition phase (Helie et al., 2015). Our results show not only increased power over the frontal areas but also a strong correlation between the performance and the gamma power changes during acquisition, which points to the frontal areas' prominent role in memory encoding and rule based learning (Gruber et al., 2002; Hester et al., 2007). While we found similar power increment over the frontal areas during acquisition, it was less pronounced than that found in the cited studies. The reason for this difference may be the lower difficulty of the task we applied.

Power decrements were found in most of the participants in the alpha and beta frequency bands. These decrements occurred over the central and more characteristically over the parieto-temporo-occipital areas, similarly to what was found in other studies with different visual paradigms (Hanslmayr et al., 2005; Romei et al., 2008; Klimesch, 2012). Concerning the lowest frequencies (delta and theta bands), their role in cognitive tasks is still a matter of debate (Hanslmayr et al., 2016). The power spectrum analysis in our study revealed significant power elevation over the parietooccipital and occipital, as well as over the frontal areas. The enhanced frontal midline and parietooccipital power of the theta band during working memory encoding and retrieval is a well-known phenomenon in learning tasks (Klimesch et al., 1997; Weiss et al., 2000; Sauseng et al., 2010) and in attentional processes (Fellrath et al., 2016). Indeed, in our study we found that the frontal-midline theta power alterations are in strong correlation with task performance during acquisition, but not during the second part (retrieval and generalization) of the paradigm. This could indicate that the early part of the paradigm (acquisition) required a high level of attention, while the later parts (retrieval and generalization) did not.

In summary, the most robust cortical power changes were observed in the higher frequency bands (gamma, over 30 Hz) in the acquisition phase of the applied paradigm over the parieto-temporo-occipital associative cortex. The frontal associative areas were less involved. On the other hand, such power changes were not obvious in the retrieval and generalization phases. These findings indicate that the activation of the associative cortical areas is necessary for acquisition, but retrieval and generalization are relatively independent of cortical activation. In other words, basal ganglia-mediated learning in the given context depends on the cortical input, but once the equivalence has been acquired, the hippocampi can apply the learned and memorized information without significant cortical contribution.

AUTHOR CONTRIBUTIONS

AP, AN and GB designed the study and prepared the main manuscript text. AP, XK, ÁP and DN registered the EEG. AP analyzed the data and prepared the figures and supplementary figures. AP and BB prepared the stimuli (artwork) and programed the stimulus presentation software. All authors reviewed the manuscript.

FUNDING

This work was supported by Hungarian Brain Research Program Grant No. KTIA_13_NAP-A-I/15.

ACKNOWLEDGMENTS

The authors would like to express their gratitude to Catherine E. Myers at Rutgers University for her generousity in allowing us to re-code and use the RAET test in Hungarian.

SUPPLEMENTARY MATERIAL

The Supplementary Material for this article can be found online at: https://www.frontiersin.org/articles/10.3389/fnhum.2018.00188/full#supplementary-material

REFERENCES

Altshuler, L. L., Bartzokis, G., Grieder, T., Curran, J., and Mintz, J. (1998). Amygdala enlargement in bipolar disorder and hippocampal reduction in schizophrenia: an MRI study demonstrating neuroanatomic specificity. *Arch. Gen. Psychiatry* 55, 663–664.

Bódi, N., Csibri, E., Myers, C. E., Gluck, M. A., and Kéri, S. (2009). Associative learning, acquired equivalence and flexible generalization of knowledge in mild Alzheimer disease. *Cogn. Behav. Neurol.* 22, 89–94. doi: 10.1097/WNN.0b013e318192ccf0

Brincat, S. L., and Miller, E. K. (2015). Frequency-specific hippocampal-prefrontal interactions during associative learning. *Nat. Neurosci.* 18, 576–581. doi: 10.1038/nn.3954

Cohen, M. X. (2014). *Analyzing Neural Time Series Data: Theory and Practice.* Cambridge, MA: MIT Press.

de Rose, J. C., McIlvane, W. J., Dube, W. V., and Stoddard, L. (1988). Stimulus class formation and functional equivalence in moderately retarded individuals' conditional discrimination. *Behav. Process.* 17, 167–175. doi: 10.1016/0376-6357(88)90033-2

Delorme, A., and Makeig, S. (2004). EEGLAB: an open source toolbox for analysis of single-trial EEG dynamics including independent component analysis. *J. Neurosci. Methods* 134, 9–21. doi: 10.1016/j.jneumeth.2003.10.009

Dube, W. V., McIlvane, W. J., Maguire, R. W., Mackay, H. A., and Stoddard, L. T. (1989). Stimulus class formation and stimulus—reinforcer relations. *J. Exp. Anal. Behav.* 51, 65–76. doi: 10.1901/jeab.1989.51-65

Fellrath, J., Mottaz, A., Schnider, A., Guggisberg, A. G., and Ptak, R. (2016). Theta-band functional connectivity in the dorsal fronto-parietal network predicts goal-directed attention. *Neuropsychologia* 92, 20–30. doi: 10.1016/j.neuropsychologia.2016.07.012

Gluck, M. A., Meeter, M., and Myers, C. E. (2003). Computational models of the hippocampal region: linking incremental learning and episodic memory. *Trends Cogn. Sci.* 7, 269–276. doi: 10.1016/s1364-6613(03)00105-0

Gluck, M. A., Shohamy, D., and Myers, C. (2002). How do people solve the "weather prediction" task? individual variability in strategies for probabilistic category learning. *Learn. Mem.* 9, 408–418. doi: 10.1101/lm.45202

Goyos, C. (2000). Equivalence class formation via common reinforcers among preschool children. *Psychol. Rec.* 50, 629–654. doi: 10.1007/bf03395375

Gruber, T., Keil, A., and Müller, M. M. (2001). Modulation of induced γ band responses and phase synchrony in a paired associate learning task in the human EEG. *Neurosci. Lett.* 316, 29–32. doi: 10.1016/s0304-3940(01)02361-8

Gruber, T., Müller, M. M., and Keil, A. (2002). Modulation of induced γ band responses in a perceptual learning task in the human EEG. *J. Cogn. Neurosci.* 14, 732–744. doi: 10.1162/08989290260138636

Hamamé, C. M., Alario, F. X., Llorens, A., Liégeois-Chauvel, C., and Trébuchon-Da Fonseca, A. (2014). High frequency gamma activity in the left hippocampus predicts visual object naming performance. *Brain Lang.* 135, 104–114. doi: 10.1016/j.bandl.2014.05.007

Hanslmayr, S., Klimesch, W., Sauseng, P., Gruber, W., Doppelmayr, M., Freunberger, R., et al. (2005). Visual discrimination performance is related to decreased α amplitude but increased phase locking. *Neurosci. Lett.* 375, 64–68. doi: 10.1016/j.neulet.2004.10.092

Hanslmayr, S., Staresina, B. P., and Bowman, H. (2016). Oscillations and episodic memory: Addressing the synchronization/desynchronization conundrum. *Trends Neurosci.* 39, 16–25. doi: 10.1016/j.tins.2015.11.004

Helie, S., Ell, S. W., and Ashby, F. G. (2015). Learning robust cortico-cortical associations with the basal ganglia: an integrative review. *Cortex* 64, 123–135. doi: 10.1016/j.cortex.2014.10.011

Hester, R., Barre, N., Murphy, K., Silk, T. J., and Mattingley, J. B. (2007). Human medial frontal cortex activity predicts learning from errors. *Cereb. Cortex* 18, 1933–1940. doi: 10.1093/cercor/bhm219

Hsieh, L.-T., and Ranganath, C. (2014). Frontal midline theta oscillations during working memory maintenance and episodic encoding and retrieval. *Neuroimage* 85, 721–729. doi: 10.1016/j.neuroimage.2013.08.003

Ing, A., and Schwarzbauer, C. (2014). Cluster size statistic and cluster mass statistic: two novel methods for identifying changes in functional connectivity between groups or conditions. *PLoS One* 9:e98697. doi: 10.1371/journal.pone.0098697

Ito, R., Robbins, T. W., Pennartz, C. M., and Everitt, B. J. (2008). Functional interaction between the hippocampus and nucleus accumbens shell is necessary for the acquisition of appetitive spatial context conditioning. *J. Neurosci.* 28, 6950–6959. doi: 10.1523/JNEUROSCI.1615-08.2008

Kardos, Z., Tóth, B., Boha, R., File, B., and Molnár, M. (2014). Age-related changes of frontal-midline theta is predictive of efficient memory maintenance. *Neuroscience* 273, 152–162. doi: 10.1016/j.neuroscience.2014.04.071

Klimesch, W. (2012). α-band oscillations, attention, and controlled access to stored information. *Trends Cogn. Sci.* 16, 606–617. doi: 10.1016/j.tics.2012.10.007

Klimesch, W., Doppelmayr, M., Schimke, H., and Ripper, B. (1997). Theta synchronization and α desynchronization in a memory task. *Psychophysiology* 34, 169–176. doi: 10.1111/j.1469-8986.1997.tb02128.x

Kostek, J. A., Beck, K. D., Gilbertson, M. W., Orr, S. P., Pang, K. C., Servatius, R. J., et al. (2014). Acquired equivalence in US veterans with symptoms of posttraumatic stress: reexperiencing symptoms are associated with greater generalization. *J. Trauma. Stress* 27, 717–720. doi: 10.1002/jts.21974

Le Van Quyen, M., Staba, R., Bragin, A., Dickson, C., Valderrama, M., Fried, I., et al. (2010). Large-scale microelectrode recordings of high-frequency γ oscillations in human cortex during sleep. *J. Neurosci.* 30, 7770–7782. doi: 10.1523/JNEUROSCI.5049-09.2010

Meeter, M., Shohamy, D., and Myers, C. E. (2009). Acquired equivalence changes stimulus representations. *J. Exp. Anal. Behav.* 91, 127–141. doi: 10.1901/jeab.2009.91-127

Middleton, F. A., and Strick, P. L. (2000). Basal ganglia and cerebellar loops: motor and cognitive circuits. *Brain Res. Rev.* 31, 236–250. doi: 10.1016/s0165-0173(99)00040-5

Miltner, W. H., Braun, C., Arnold, M., Witte, H., and Taub, E. (1999). Coherence of γ-band EEG activity as a basis for associative learning. *Nature* 397, 434–436. doi: 10.1038/17126

Montgomery, E. B. Jr. (2009). Basal ganglia pathophysiology in Parkinson's disease. *Ann. Neurol.* 65, 618; author reply 618–619. doi: 10.1002/ana.21649

Moustafa, A. A., Keri, S., Herzallah, M. M., Myers, C. E., and Gluck, M. A. (2010). A neural model of hippocampal-striatal interactions in associative learning and transfer generalization in various neurological and psychiatric patients. *Brain Cogn.* 74, 132–144. doi: 10.1016/j.bandc.2010.07.013

Moustafa, A. A., Myers, C. E., and Gluck, M. A. (2009). A neurocomputational model of classical conditioning phenomena: a putative role for the hippocampal region in associative learning. *Brain Res.* 1276, 180–195. doi: 10.1016/j.brainres.2009.04.020

Myers, C. E., Hopkins, R. O., DeLuca, J., Moore, N. B., Wolansky, L. J., Sumner, J. M., et al. (2008). Learning and generalization deficits in patients with memory impairments due to anterior communicating artery aneurysm rupture or hypoxic brain injury. *Neuropsychology* 22, 681–686. doi: 10.1037/0894-4105.22.5.681

Myers, C. E., Shohamy, D., Gluck, M. A., Grossman, S., Kluger, A., Ferris, S., et al. (2003). Dissociating hippocampal versus basal ganglia contributions to learning and transfer. *J. Cogn. Neurosci.* 15, 185–193. doi: 10.1162/089892903321208123

Öze, A., Nagy, A., Benedek, G., Bodosi, B., Kéri, S., Pálinkás, É., et al. (2017). Acquired equivalence and related memory processes in migraine without aura. *Cephalalgia* 37, 532–540. doi: 10.1177/0333102416651286

Perrin, F., Pernier, J., Bertrand, O., and Echallier, J. (1989). Spherical splines for scalp potential and current density mapping. *Electroencephalogr. Clin. Neurophysiol.* 72, 184–187. doi: 10.1016/0013-4694(89)90180-6

Postuma, R. B., and Dagher, A. (2006). Basal ganglia functional connectivity based on a meta-analysis of 126 positron emission tomography and functional magnetic resonance imaging publications. *Cereb. Cortex* 16, 1508–1521. doi: 10.1093/cercor/bhj088

Rescorla, R. A. (1980). Simultaneous and successive associations in sensory preconditioning. *J. Exp. Psychol. Anim. Behav. Process.* 6, 207–216. doi: 10.1037/0097-7403.6.3.207

Romei, V., Rihs, T., Brodbeck, V., and Thut, G. (2008). Resting electroencephalogram α-power over posterior sites indexes baseline visual cortex excitability. *Neuroreport* 19, 203–208. doi: 10.1097/WNR.0b013e3282f454c4

Sauseng, P., Griesmayr, B., Freunberger, R., and Klimesch, W. (2010). Control mechanisms in working memory: a possible function of EEG theta oscillations. *Neurosci. Biobehav. Rev.* 34, 1015–1022. doi: 10.1016/j.neubiorev.2009.12.006

Seab, J. P., Jagust, W. J., Wong, S. T., Roos, M. S., Reed, B. R., and Budinger, T. F. (1988). Quantitative NMR measurements of hippocampal atrophy in Alzheimer's disease. *Magn. Reson. Med.* 8, 200–208. doi: 10.1002/mrm.1910080210

Shepherd, G. M. (2003). *The Synaptic Organization of the Brain*. New York, NY: Oxford University Press.

Simon, J. R., and Gluck, M. A. (2013). Adult age differences in learning and generalization of feedback-based associations. *Psychol. Aging* 28, 937–947. doi: 10.1037/a0033844

Vadhan, N. P., Myers, C. E., Rubin, E., Shohamy, D., Foltin, R. W., and Gluck, M. A. (2008). Stimulus-response learning in long-term cocaine users: acquired equivalence and probabilistic category learning. *Drug Alcohol Depend.* 93, 155–162. doi: 10.1016/j.drugalcdep.2007.09.013

Ventre-Dominey, J., Mollion, H., Thobois, S., and Broussolle, E. (2016). Distinct effects of dopamine vs. STN stimulation therapies in associative learning and retention in Parkinson disease. *Behav. Brain Res.* 302, 131–141. doi: 10.1016/j.bbr.2016.01.010

Weiler, J. A., Bellebaum, C., Brüne, M., Juckel, G., and Daum, I. (2009). Impairment of probabilistic reward-based learning in schizophrenia. *Neuropsychology* 23, 571–580. doi: 10.1037/a0016166

Weiss, K. R., and Brown, B. L. (1974). Latent inhibition: a review and a new hypothesis. *Acta Neurobiol. Exp.* 34, 301–316.

Weiss, S., Müller, H. M., and Rappelsberger, P. (2000). Theta synchronization predicts efficient memory encoding of concrete and abstract nouns. *Neuroreport* 11, 2357–2361. doi: 10.1097/00001756-200008030-00005

Yin, H. H., and Knowlton, B. J. (2006). The role of the basal ganglia in habit formation. *Nat. Rev. Neurosci.* 7, 464–476. doi: 10.1038/nrn1919

Conflict of Interest Statement: The authors declare that the research was conducted in the absence of any commercial or financial relationships that could be construed as a potential conflict of interest.